1-1-2013

Effect of Physiological Oxygen Levels On Osteogenic Differentiation of Adipose-Derived Stem Cells

Suchit Sahai
University of South Carolina

Effect of Physiological Oxygen Levels on Osteogenic Differentiation of Adipose-derived Stem Cells

by

Suchit Sahai

Bachelor of Technology
ICFAI Institute of Science and Technology, 2007

Submitted in Partial Fulfillment of the Requirements

For the Degree of Doctor of Philosophy in

Biomedical Engineering

College of Engineering and Computing

University of South Carolina

2013

Accepted by:

Dr. James Blanchette, Advisor

Dr. Esmaiel Jabbari, Committee Member

Dr. Peisheng Xu, Committee Member

Dr. Melissa Moss, Committee Member

Dr. Shekhar Patel, Committee Member

Lacy Ford, Vice Provost and Dean of Graduate Studies

DEDICATION

I dedicate my research work to my parents, Mrs. Radha Sahai and Mr. Rajiv Sahai, my brother-in-law, Aditya, sister Suniti, my nephew Maadhav, Ashwani uncle and his family for their unfaltering faith in me, their blessings and their love- I owe this success to you. I still remember the "phone call" advise Aditya gave me that changed my life.

ACKNOWLEDGEMENTS

I would like to thank to my PhD advisor, Dr. James Blanchette (Jay) for supporting me during these past four and a half years. Jay is a great advisor, humorous, energetic and enthusiastic. His open door policy, unique ways to discuss research topics and valuable insights helped me to dig deeper into science. He'll be my role model as a scientist, advisor, and teacher. I also have to thank the members of my PhD committee, Dr. Moss, Dr. Jabbari, Dr. Patel, Dr. Xu for their class lectures and helpful advices. A good support system is important to surviving and staying sane in grad school. Matt, Pritesh, Romone, Amanda, Brandon, Rachel and Aiden formed the core of my research time in the Blanchette group. Matt is a person I could always ask for advice or opinions and go for a drink after a long day at work.

My Tauji, Taiji & Saurabh have always believed in me, and I hope to always stand up to their expectations all my life. My Grandfather late Dr. S. Sahai, though we could never talk science that he did at Sorbonne University, but his writings on life lessons are forever. My Childhood friends – Jayant, Radhika, Gitsy, Tango, Mayank, Karan, College friends- Abid, Punit, Ron, Nipun, Utsav, AGASTS- Amal, Grishma, Aditi, Sharvari, Tanu, Chai Addicts- Shraddha, Pallavi, Krutica and Sradha. Each one of you is mad, thanks for the crazy times. Katy and Samaneh, many good times shared together in grad school, hiking, cooking out or weekends at 5-points. Finally, the Indian student organization (ISO family) who made it home away from home. Thanks to ALL again for making Life easy.

ABSTRACT

Regenerative medicine presents exciting strategies for healing critical-size bone defects through the implantation of cells and biocompatible scaffolds. Most in vitro studies are performed in atmospheric oxygen conditions (~20%), which do not accurately mimic the CSD microenvironment. Due to damage to the vasculature at CSDs, oxygen levels fall into the hypoxic range (<5%), which can impact viability, proliferation and differentiation of the cells employed for bone regeneration. Understanding the cellular responses to hypoxia has grown primarily from study of individual molecular factors. The master regulator of adaptive responses to low oxygen availability is the nuclear factor, hypoxia-inducible factor-1. HIF-1 is a heterodimeric protein, stable below 6% O_2 condition in the nucleus and has been shown to play a role in angiogenic-osteogenic coupling. We have developed a responsive, fluorescent, hypoxia detection system and determined whether HIF activity can be tracked in both 2-D and 3-D cultures. Adipose-derived stem cells (ASCs) were selected due to their broad utilization in tissue engineering strategies and characterized the influence of HIF signaling on its phenotype. The work done identified that of hypoxia impaired osteogenic differentiation of ASCs in both 2-D and 3-D cultures and HIF-1 did not mediate this effect. Ischemic preconditioning (IPC) strategy and varied protocols used represents a clinically feasible manipulation of cell preparation to help the survival of implanted ASCs and accelerate osteogenic differentiation at physiological oxygen levels.

TABLE OF CONTENTS

DEDICATION ii

ACKNOWLEDGEMENTS iii

ABSTRACT iv

LIST OF TABLES vii

LIST OF FIGURES viii

LIST OF ABBREVIATIONS ix

CHAPTER 1 INTRODUCTION 1

1.1 EFFECT OF LOW OXYGEN ON STEM CELLS 1

1.2 MECHANISM OF CELL RESPONSE 5

1.3 EFFECT OF OXYGEN ON OSTEOGENIC DIFFERENTIATION 13

CHAPTER 2 OBJECTIVES AND EXPERIMENTAL DESIGN 21

CHAPTER 3 TRACKING HYPOXIC SIGNALING IN ENCAPSULATED STEM CELLS 24

3.1 INTRODUCTION 24

3.2 MATERIALS AND METHODS 28

3.3 RESULTS 33

3.4 DISCUSSION 39

CHAPTER 4: OSTEOGENIC DIFFERENTIATION OF ADIPOSE-DERIVED STEM CELLS IS HIF-1 INDEPENDENT 43

4.1 INTRODUCTION 43

4.2 Materials and Methods 45

4.3 Results 51

4.4 Discussion 61

Chapter 5: Varied Ischemic Preconditioning Protocols to Enhance Engraftment and Differentiation of Adipose Derived Stem Cells 64

5.1 Introduction 64

5.2 Materials and Methods 66

5.3 Results 72

5.4 Discussion 79

Chapter 6 Scientific Contributions of this study 82

References 84

LIST OF TABLES

Table 1 Studies examining effect of oxygen on osteogenesis of stem cells 18

Table 5.1 Comparison of apoptotic markers at 1% oxygen.....77

Table 5.2 Comparison of apoptotic markers at 2% oxygen.....77

Table 5.3 Comparison of apoptotic markers at 4% oxygen.....77

LIST OF FIGURES

Figure 1.1 Stem cell microenvironment....2

Figure 1.2 Mechanism of cell response to hypoxia 10

Figure 2.1 Experimental Design 1 21

Figure 2.2 Experimental Design 2 22

Figure 2.3 Experimental Design 3 23

Figure 3.1 Immunostaining for HIF-1α 34

Figure 3.2 Hypoxia marker progressions in 2-D and 3-D 36

Figure 3.3 Quantification of cells positive for marker signal 37

Figure 3.4 Western Blot of HIF-1α and β-actin....38

Figure 4.1 Effect of HIF-1 on ALP Activity in 2-D and 3-D 52

Figure 4.2 Effect of HIF-1 on mineral deposition in 2-D and 3-D 54

Figure 4.3 Effect of HIF-1 on the expression of ON & OPN in 2-D....56

Figure 4.4 Effect of HIF-1 on the expression of ON & OPN in 3-D....57

Figure 4.5 Effect of HIF-1 on VEGF release in 2-D and 3-D 59

Figure 4.6 Effect of HIF-1 on the viability in 2-D and 2-D....60

Figure 5.1 Overview of IPC....68

Figure 5.2 Flow Cytometric analysis to examine the effect of IPC on stemness 72

Figure 5.3 Expression of apoptotic markers in the absence of HIF-1 73

Figure 5.4 Expression of apoptotic markers in the presence of HIF-1 74

Figure 5.5 Effect of IPC on the expression of osteogenic markers 78

List of Abbreviations

2-D ..... Two-Dimensional

3-D ..... Three-Dimensional

ALP ..... Alkaline Phosphatase

ANOVA ..... Analysis Of Variation

ASCs ..... Adipose-derived Stem Cells

BMP ..... Bone Morphogenetic Protein

BMSCs ..... Bone-marrow Mesenchymal Cells

BSA ..... Bovine Serum Albumin

CSDs ..... Critical-Size Bone Defects

DNA ..... Deoxyribonucleic acid

ECM ..... Extracellular Matrix

ESCs ..... Embryonic Stem Cells

FBS ..... Fetal Bovine Serum

FITC ..... fluorescein isothiocyanate

HBSS ..... Hanks Balanced Salt Solution

HIF ..... Hypoxia Inducible Factor

hMSCs ..... human Mesenchymal Stem Cells

HRE ..... Hypoxia-Responsive Elements

IF ..... Immunoflourescence

IPC ..... Ischemic Preconditioning

mRNA ..... messenger Ribonucleic Acid

OC .....Osteocalcin

ODD .....Oxygen Dependent Domain

ON ..... Osteonectin

OPN .....Osteopontin

P .....Passage

p.....Probability

P/S .....Penicillin/Streptomycin

PNPP .....p-nitrophenyl phosphate

pVHL .....von Hippel-Lindau tumor suppressor gene

SDS-PAGE ..... Sodium Dodecyl Sulfate Polyacrylamide Gel Electrophoresis

VEGF ..... Vascular Endothelial Growth Factor

CHAPTER 1

INTRODUCTION

1.1 EFFECT OF LOW OXYGEN ON STEM CELLS

1.1.1 Stem Cells and their Microenvironment

Stem cells produce all tissues in the body through proliferation and differentiation in response to cues from their microenvironment. Because of their plasticity, they are particularly sensitive to their immediate environments. *In vivo* they are thought to reside in specific niches, which maintain their pluripotent or multipotent capabilities. Consequently, differentiation along specific lineages is thought to coincide with their migration out of their specific niche into an environment that provides appropriate differentiation cues [Watt 2000].

As the field of tissue engineering has matured, new technology has been employed to regulate the application of mechanical as well as biological factors to developing tissue constructs. However, one developmentally important stimulus that is still rarely accounted for during *in vitro* culture is the oxygen tension. Low oxygen or hypoxia plays a substantial and critical role in many essential physiological and developmental pathways.

Human embryonic stem cells that are derived from the inner cell mass of early stage blastocytes adapt to grow in this low oxygen environment until about the 11th week when the cytotrophoblasts traverse the arterial walls and the local partial pressure

of oxygen increases from 2.3% to 7.8% O_2 [Rodesch 1992]. The oxygen distribution within the bone marrow has been studied almost exclusively in the context of hematopoietic stem cells (HSCs) and to a much lesser extent in the context of mesenchymal stem cells (MSCs). Early direct measurement revealed that bone marrow in general is hypoxic, where some regions are as low as 1–2% O_2 [Cipolleschi 1993, Kofoed 1985]. Results from recent *in vivo* studies, however, provided direct experimental evidence that long-term repopulating HSCs in the mouse reside in a hypoxic environment and hypoxia may in fact be an essential part of the microenvironment that maintains them in an undifferentiated state [Parmar 2007]. These measurements were further supported by modeling analysis of *in vivo* oxygen distribution in bone marrow indicating that HSCs exist within an extremely hypoxic region within bone marrow [Chow 2001].

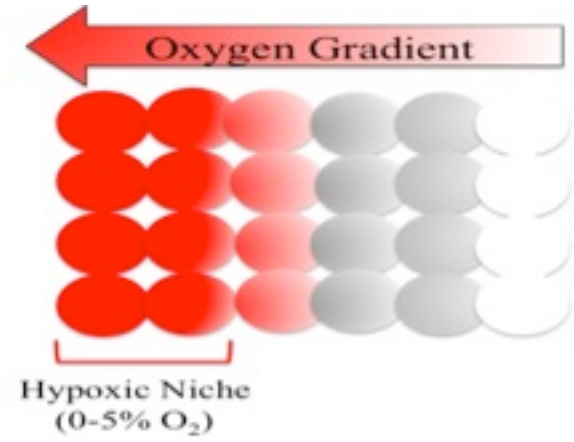

Figure 1.1: Stem cell microenvironment.

In addition to bone marrow MSCs, adipose tissue has been identified as a source of multipotent cells that have the capacity to differentiate towards the adipogenic, chondrogenic, myogenic and osteogenic lineages [Gronthos 2001, Zuk 2002, Cho 2005, Knippenberg 2005, Lin 2005, Peterson 2005, Guilak 2006]. Adipose-derived stem cells

(ASCs) can be readily obtained from tissue harvested through liposuction or through abdominoplasty procedures. Despite the high degree of vascularity of adipose tissue relative to bone marrow, *in vivo* measurements of oxygen concentrations in mouse adipose tissues have shown the oxygen concentration to be in the vicinity of 3%, and so hypoxic cultures may still be beneficial to ASC *in vitro* proliferation and differentiation characteristics [Matsumoto 2005, Wang 2005, Zachar 2011]. Thus, physiologically relevant stem cell responses should be expected to occur as oxygen levels shift within this range.

1.1.2 Effect of Oxygen on Proliferation and Differentiation of Stem Cells

Low O_2 environments have long been used by embryologists to culture embryos and the blastocytes produced under low O_2 have significantly more inner cell mass compared with those generated under higher O_2 [Nakao 1990, Thompson 1990, Harvey 2004]. The benefits have been demonstrated for rabbit, mouse, sheep, cow, and human embryos [Thompson 1990, Umaoka 1992, Li 1993, Catt 2000]. Culture conditions utilizing a physiological oxygen tension of 5% instead of 20% were also found to improve the establishment of mouse ESCs line by reducing oxidative stress [Wang 2006]. An oxygen tension of 2% resulted in enhanced human ESC clonal recovery and reduced chromosomal abnormalities without inducing hESCs to adopt a more differentiated phenotype [Forsyth 2006]. Low oxygen tension studies have been carried out with bone marrow MSCs from a variety of mammalian species. In general, MSCs exhibited greater colony-forming potential while proliferating at a higher rate and for an extended duration. [Lennon 2001, Grayson 2006, Ren 2006, Buravkova 2007, Fehrer 2007, Grayson 2007,

Martin-Rendon 2007]. Fewer investigations have been carried out concerning the effects of hypoxia on ASCs. Different conditions using oxygen concentration in the range of 1-5% increased the growth rate of stem cells [Lee and Kemp 2005, Wang 2005, Malladi 2006, Xu 2007, Lee 2009, Fink 2011, Rasmussen 2011].

Local oxygen concentrations can also direct cellular differentiation. In 1961, Bassett and Hermann demonstrated that cells isolated from embryonic chick tibial cortexes differentiate *in vitro* toward bone when maintained under high (35%) oxygen concentrations and toward cartilage when maintained under low oxygen (5%) concentrations [Bassett 1961]. A number of investigations have recently been confirmed these early observations of oxygen-directed differentiation of cartilage and bone [Murphy 2001, Domm 2002, Saini 2004, Mizuno 2005, Utting 2006, Mizuno 2005, Chen 2006, D'ippolito 2006, Hirao 2006]. Hypoxia inhibited the differentiation of primary rat osteoblasts and human bone marrow MSCs to an osteogenic phenotype [D'Ippolito 2006, Utting 2006]. In contrast, low oxygen conditions have been demonstrated to induce chondrogenic differentiation when expanded human chondrocytes were pelleted or embedded in alginate [Domm 2002, Malda 2004, Murphy 2004]. Studies have shown the strong influence of hypoxia on the differentiation potential of ASCs [Wang 2005, Betre 2006, Lee and Kemp 2006, Malladi 2006, Xu 2006, Khan 2007]. Lee and Kemp showed that hypoxia affected the potential of human ASCs to differentiate along muscle and osteogenic lineages [Lee and Kemp 2006]. The effect of hypoxia on the differentiation potential of ASCs was also reported for murine cells. It was found that murine ASCs exhibited decreased chondrogenic and osteogenic potential when differentiated at 2% O_2 compared with normoxic conditions [Malladi 2006]. The following reviews include

examples of hypoxia both encouraging and discouraging differentiation of various types of stem cells and influencing the specific lineage of differentiation [Malda 2007, Lin 2008, Ma 2009, Abdollahi 2010]. Hence, much effort has to expend to elucidate the mechanisms via which cells sense oxygen levels and transduce the signal to elicit a response.

1.2 Mechanism of Cell Response

Hypoxia Inducible Factors (HIF) family of proteins has been convincingly demonstrated to mediate majority of the cellular responses under low oxygen environment [Semenza and Wang 1992, Weiner 1996, Maltepe 1997, Iyer 1998, Wenger 2000, Goda 2003]. HIF is a αβ heterodimeric transcription factor. The HIF family comprises three α subunits: HIF-1α, HIF-2α and HIF-3α that are regulated by cellular oxygen levels. The HIF-1β subunit (also known as the aryl hydrocarbon receptor nuclear translocator, ARNT) is constitutively expressed in the nucleus in an oxygen-independent manner [Wang 1993]. Among the HIF family, HIF-1 is very well characterized and has been shown to play a role in regulating more than 200 genes [Loboda, 2012, Haase 2013]. HIF-2α shares 48% amino acid homology and has similar structure and functional domains with HIF-1α. Consequently, it is regulated via the same hydroxylase mechanisms described for HIF-1α and, although not all the downstream target genes of HIF-2α been identified, it is believed that it has distinct functions from HIF-1α *in vivo* [Fedele 2002, Hu 2006, Rankin 2007, Ratcliff 2007, Loboda 2010]. HIF-3α is the more distantly related isoform and, in certain splicing arrangements, encodes a polypeptide that

antagonizes hypoxia-responsive element dependent gene expression. [Wenger 2000, Maynard 2007, Augstein 2011].

1.2.1 HIF-1: Mediator of Hypoxic Response

HIF-1 was identified and isolated by Semenza and Wang, due to its binding an enhancer region in the 3'-flanking region of the EPO gene in response to hypoxia [Semenza and Wang 1992]. It has since been shown that HIF-1 also binds the enhancer region of VEGF (in its 5'-flanking region), GLUT-1, GLUT-3, GAPDH and a plethora of other genes during hypoxic stress [Semenza 1999]. HIF-1 protein is upregulated during hypoxia and when hypoxia is simulated by culturing cells in the presence of cobalt chloride to replace the iron in the heme proteins, and knocking out the gene for the HIF-1α subunit prevents cells from responding to hypoxic stress. These data indicate that HIF-1 plays a central role in the mechanism for eliciting cellular responses to hypoxia.

1.2.2 Mechanism of Cellular Hypoxia Response: HIF-1

Further examination of 256-base-pair region of the erythropoietin gene, the study delineated the essential 50-nucleotide enhancer sequence, eventually termed the hypoxia-responsive element (HRE), and identified a nuclear factor which exhibited hypoxia-dependent binding to the HRE [Semenza 1992]. Presence of a functional HRE resulted in a seven-fold increase in erythropoietin production in response to hypoxia (1% oxygen). Maxwell, et al., soon showed that HRE elicited hypoxia-responsive transcription in a number of other cell types and species as well [Maxwell 1993]. Human

fetal lung fibroblasts, human skin fibroblasts, human monocyte/macrophage cells, monkey renal fibroblasts, pig retinal epithelial cells, rat aortic endothelial cells, Chinese hamster lung fibroblasts, Chinese hamster ovary cells, mouse renal adenocarcinomas, and mouse erythroleukemias were transiently transfected with a plasmid containing the HRE enhancer fused to a broadly active promoter and the α1-globin gene as a reporter [Maxwell 1993]. In 1% oxygen, 11 of the 12 tested lines demonstrated a 3 to 11-fold induction of α1-globin production, similar to the original observations in hepatomas. This implied that the same hypoxia-responsive nuclear factor responsible for HRE binding and erythropoietin upregulation must be present in a range of cell types and may represent a widespread mechanism for response to hypoxia.

Following studies by Wang and Semenza showed that HIF-1 DNA binding occurred in response to hypoxia in a number of mammalian cells types not expressing the erythropoietin gene and that the sequence of the enhancer binding region was conserved [Wang 1993]. HIF-1 ubiquity was further shown when Weiner, et al., demonstrated HIF-1 expression in all human and mouse organs tested, including brain, kidney, liver, heart, placenta, pancreas, and skeletal muscle [Weiner 1996]. Additionally, they showed an *in vivo* upregulation of HIF-1 in rats chambered in 7% oxygen. But beyond triggering pathways designed to directly increase tissue oxygenation, HIF-1 activity was found to be vital in essential physiological and developmental pathways. Embryogenesis, for example, is inhibited in embryonic stem cells that are unable to produce HIF-1, even under normal, physiological oxygen conditions [Maltepe 1997, Iyer 1998]. HIF-1 is also essential for cell cycle arrest in hypoxic cells [Goda 2003]. The combined conclusion of these studies implies the broad influence of hypoxia on cell fate.

1.2.3 Structure of HIF-1

HIF-1 is a heterodimeric protein composed of α and β subunits. Both subunits have been identified as basic-helix-loop-helix-PER-ARNT-SIM proteins (bHLH/PAS) [Wang 1995, Kewely 2004]. Factors in this family must dimerize to become functional and are defined by three major domains: (1) A bHLH domain near the N-terminus responsible for non-specific dimerization with the basic region being the site of DNA binding [Murre 1989, Ferré-D'Amaré 1993). (2) A PAS homology domain (named for three early homologous Drosophila and human proteins in which the sequence was found, periodic circadian protein (PER), aryl hydrocarbon receptor nuclear translocator protein (ARNT), and single-minded protein (SIM)) which establishes dimerization partner specificity and target gene specificity [Pongratz 1998]. (3) A transactive domain which interacts with transcriptional coactivators to help initiate transcription [Kewely 2004]. Wang et al., identified HIF-1α as a novel 120 kDa bHLH/PAS polypeptide while HIF-1β was identified as the previously known ARNT [Wang 1995]. While the β unit is known to interact with a number of other bHLH/PAS proteins, HIF-1 α dimerizes almost exclusively with HIF-1β. In hepatoma cells, levels of both HIF-1α and HIF-1β RNA and protein were dramatically increased upon exposure to 1% oxygen. RNA levels peaked at 1-2 hours of continuous hypoxia while protein levels peaked between 4 and 8 hours. Levels of both diminished to basal values within minutes after cells were returned to 20% oxygen. Additionally, HIF-1α was found to contain large clusters of proline, glutamic acid, serine or threonine (PEST) residues, which are implicated in protein instability and degradation [Wang 1995].

1.2.4 Regulation of HIF-1

Activation of HIF-1 is oxygen-dependent and is regulated by stability of the HIF-1α protein subunit. Both HIF-1α and HIF-1β mRNAs are constitutively expressed intracellularly, but HIF-1α protein levels are nearly undetectable in normoxic cells, even when HIF-1α is overexpressed. In hypoxic cells, high levels HIF-1α are observed, but HIF-1β levels are unaffected. Both DNA binding of HIF-1 and levels of HIF-1α rapidly decrease upon reintroduction of normoxia [Haung 1996, Nguyen 2013, Prabhakar 2013]. The regulation of HIF-1 is represented schematically in Figure 1.2.

Ratcliffe et al. identified a region between amino acids 530 and 652 in HIF-1α that conferred oxygen-dependent repression when transferred to a reporter gene system and suggested that the mechanism of regulation may be mediated by proteolytic degredation [Ratcliffe 1998]. It was shown that in the presence of oxygen, the product of the von Hippel-Lindau tumor suppressor gene (pVHL), in complex with several other proteins, interacts directly with this region of HIF-1α (termed the oxygen-dependent degradation domain (ODD)), marking the protein for proteosomal degradation by the E3-ubiquitin ligase pathway [Ohh 2000]. Furthermore, a conserved family of prolyl-4-hydroxylases were found to post-translantionally modify HIF-1 by hydroxylating specific residues [Bruick 2001, Epstein 2001]. Most notably, HIF prolyl 4-hydroxylase 2 (P4H2) is responsible for hydroxylating two key proline residues (Pro564 and Pro402) in the HIF-1α ODD required for binding of pVHL [Ivan 2001, Masson 2001, Berra 2003]. Activity of the HIF prolyl-hydroxylase family of enzymes is dependent on Fe(II) and 2-oxogluterate as cofactors and dioxygen as a cosubstrate.

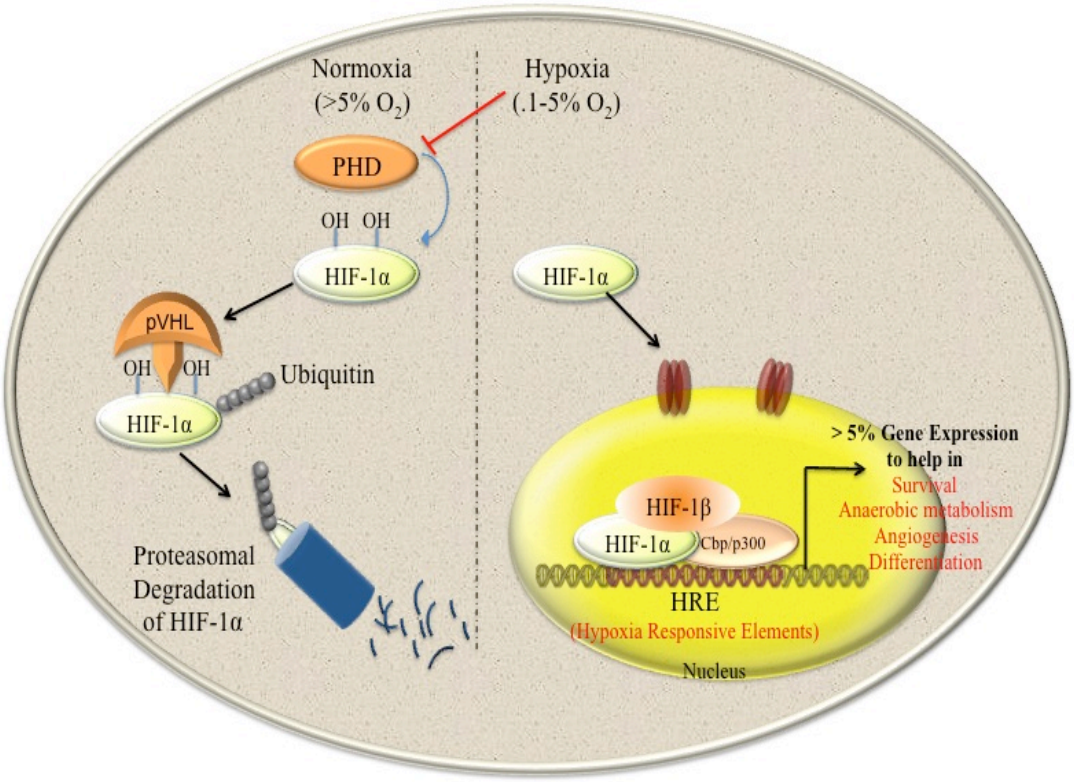

Figure 1.2: Mechanism of cell response in hypoxia.

In low oxygen conditions, the hydroxylase is not active, HIF-1α is not modified, the pVHL complex fails to bind, and HIF-1α is not degraded. Additionally, P4H2 mRNA is oxygen-inducible [Epstein, 2001]. Thus this enzyme appears to be the key oxygen sensor responsible for setting basal normoxic HIF-1 levels. A secondary regulatory mechanism was found to work in a similar manner. Under hypoxic conditions, the C-terminal domain of HIF-1α is able to interact with coactivators, such as p300/CBP, to initiate transcription of target genes [Ema 1999]. In normoxic conditions, a key asparagine residue (Asp201) is hydroxylated, preventing binding of p300/CBP and suppressing HIF-1 activity [Lando 2002]. The factor responsible for asparagine hydroxylation, deemed factor inhibiting HIF-1 (FIH-1), functions similarly to P4H2, and likewise shows iron and oxygen dependence [Lando 2002]. Thus two primary

mechanisms, both dependent on post-translational protein modification, exist for oxygen-dependent regulation of HIF-1α.

In summary, HIF-1α is constitutively expressed, but in normoxia the protein levels are kept low by rapid ubiquitination and proteosomal degradation. Activity of any remaining basal HIF-1α is suppressed by the failure of the p300 co-activator to bind. In hypoxic conditions, oxygen dependency of both hydroxylases prevents HIF-1α modification and subsequently inhibits degradation and allows for binding of co-activators and dimerization.

1.2.5 Kinetics of HIF-1 Response

Hydroxylated HIF-1α is rapidly degraded in vivo, with a half-life of approximately 5 minutes [Huang 1998]. Though the HIF-1α protein is very unstable in normoxia, HIF-1α mRNA is constitutively expressed and the protein is constantly produced. Additionally, P4H2, the enzyme primarily responsible for hydroxylating HIF-1α, has an activity dependent upon dioxygen with a K_m (Michaelis constant) just above the concentration of dissolved O_2 in air. This high value ensures that even a small decrease in oxygen is likely to have a significant effect on P4H2 activity and makes oxygen concentration the limiting determiner of HIF-1α stability [Hirsila 2003]. Thus HIF-1 can be both a highly sensitive and rapidly responsive initiator of hypoxia response. Even though low oxygen activity of HIF-1 is dependent upon *de novo* production of HIF-1α, this can occur rapidly because HIF-1α mRNA is constantly produced [Semenza 1992]. Studying hepatoma cells exposed to 1% oxygen for 0-4 hours, Wang and Semenza found that HIF-1 activity was first detectable within 15 minutes, with 8% maximal

activity at 30 minutes, 50% maximal activity between 1 and 2 hours, and maximal activity at 4 hours [Wang 1993]. After rapid re-exposure to 20% oxygen, HIF-1 activity was reduced to 34% within 5 minutes and was eliminated by 15 minutes. The group also showed that binding of stabilized HIF-1 to DNA occurred rapidly, with 77% binding within 1 minute and 100% binding within 5 minutes.

1.2.6 Gradation of HIF-1 Response

The sensitivity of P4H2 to changes in oxygen concentration also imparts a graded responsiveness of HIF-1 to O_2. Jiang et al. exposed HeLa cells to oxygen concentrations ranging from 0 to 20% and measured levels of the HIF-1 subunit proteins and HIF-1 DNA binding [Jiang 1996]. As expected, the HIF-1α subunit was dramatically responsive to oxygen concentration. Between 20 and 6% oxygen, HIF-1α levels and DNA binding modestly increased as oxygen concentration decreased. However, below 6% oxygen both HIF-1α and HIF-1 DNA binding increased exponentially to reach maximal values at 0.5% oxygen. Half-maximal responses were observed between 1.5 and 2% oxygen. Thus, the majority of HIF-1 activity takes place over a physiologically relevant range of oxygen 0-5%, with the largest response at hypoxic levels 0.5-1.5%.

Bracken et al., tested the graded response of HIF-1 in a similar set of experiments with a variety cell types: HEK293T, HeLa, COS-1, HepG2, CACO-2, and PC12 cells [Bracken 2006]. In every case, they also found an exponential increase in HIF-1α protein levels as oxygen was decreased from 5 to less than 1%. However, though HIF-1 activity, as measured by reporter protein production, was also maximal below 1% oxygen, the response did not always match HIF-1α protein levels. In addition to

differences in maximal reporter protein production levels between cells types, they noted two categories of response. Some cells gradually increased reporter protein production as oxygen decreased from 10 to less than 1%. Others required an oxygen concentration of less than 2% before exhibiting a dramatic increase in reporter protein production, which much more closely coincides with changes in HIF-1α levels. Therefore, having a system that can help in tracking HIF-1 activity, would be helpful for the tissue engineering community to link it to cell behavior or fate.

1.3 Effect of Oxygen on Osteogenic Differentiation

1.3.1 Clinical Relevance: Critical-size Bone Defects (CSDs)

CSDs are bone defects that do not heal by themselves, as they are large enough to preclude spontaneous healing. Critical-size bone defects can be either inherited, occur following trauma, surgical correction of hereditary defects, through infection, congenital anomalies but can also arise due to operative intervention such as cyst and tumor resections [Rodriguez-Merchan 2004, Hulth 1989]. In general, CSDs can be classified based on their morphological characteristics such as length, breadth and depth of injury. In addition to this the localization of the defect plays an important role in the treatment of the defect as it leads to decrease of mesenchymal progenitor cells. Apart from this the decreased vascularity leading to low oxygen concentration at the site plays a crucial role in the process of bone healing.

CSDs remain a clinically challenged problem in orthopedic surgery. Currently, an autograft bone surgery is the gold standard method to treat CSDs. But, the procedure requires a second surgical site, it is limited in quantity, and is restricted

regarding the integration of implanted bone and vascular structures with native tissue and longer rehabilitation time for patients in hospitals. To overcome these drawbacks, the need for an alternative has been recognized [Langer and Vacanti 1993]. The concept of the use of stem cells in therapeutic applications is an appealing one, as stem cells already have a natural role in tissue repair and regeneration [Green 1977, Laurencin 1999, Blau 2001, Spraddling 2001, Allison 2002, Kneser 2002, Presnell 2002, Preston 2003].

1.3.2 Bone Cells and Expression of Osteogenic Markers

Bone is a vascularised tissue that provides mechanical stability to the skeleton that is required for locomotion, load bearing and protection of the brain, spinal cord, heart and lungs. Furthermore it serves as a mineral reservoir for calcium and serves as an attachment ground for muscles, ligaments and tendons [Nakashima 2003]. There are two fundamentally different mechanisms of ossification. Firstly, direct ossification of embryonic connective tissue (intramembranous ossification) and secondly the replacement of hyaline cartilage by compact bone (endochondral ossification). Endochondral ossified bones, mainly large hollow bones such as femur, tibia or humerus, represent most of the adult bones. Bones, such as clavicula or the skull develop by intramembranous ossification [Bruick and McKnight 2002]. Both types of bone arise during embryonic development by a complex interaction of diffusion of nutrients, oxygen gradients and cellular apoptosis [Semenza 1999, Ivan 2001, Zhu 2001].

Bones are composed of different cell types; osteoprogenitor cells, osteoblasts, osteocytes, and osteoclasts. The osteoprogenitor cells located in periosteum, endosteum, and Haversian canals receive a stimulus to proliferate and differentiate into

osteoblasts before forming bone. Factors with the capacity to induce this differentiation towards osteoprogenitor cells and further towards osteoblasts include bone morphogenetic proteins (BMPs), transforming growth factor-β (TGF-β), fibroblast growth factor (FGF), insulin-derived growth factor (IGF), platelet-derived growth factor (PDGF), and interleukins. The primary function of osteoblasts is production and secretion of organic and inorganic bone ECM [Mackie 2003]. Osteoblasts are also not terminally differentiated cells. They have two fates: they become embedded in their own bone matrix and become osteocytes, or undergo apoptosis [Jilka 1998, Safadi 2003].

Osteoblasts contain active cytoskeletal proteins to maintain their structural integrity as well as facilitate motility and attachment to surfaces. Their contact interactions with neighboring osteoblasts and osteocytes at intercellular gap junctions are achieved by the extensions created by their plasma membranes. They lay down premineralized bone matrix, osteoid, and subsequently facilitate its mineralization. The osteoid matrix itself provides a favorable environment for crystallization. The mineralization process involves supersaturation of extracellular fluids at local zones and increased osteoblastic alkaline phophatase (ALP) activity, which raises local calcium and phosphate concentrations [Stains 2005, Iain 2001]. Notably, conditions of high bone turnover or rapid bone formation lead to increased ALP activity and increased circulatory ALP levels. Osteoblasts also produce osteocalcin, which binds calcium, further concentrating local calcium levels [Bielby 2004, Karner 2007].

The most abundant non-collagenous bone ECM protein is osteonectin. Osteonectin (ON) has multiple Ca^{2+} and collagen binding sites and has been shown to be a potential nucleator of Hap (Hydroxyapatite) [Young 1992, Maurer 1996]. The second

most abundant non-collagenous protein in bone matrix is osteocalcin, which is a vitamin-K dependent protein exhibiting Ca^{2+}/HAp affinity, and has also been suggested to play a role in osteoclast migration [Ducy 1996]. Osteopontin (OPN) is a multifunctional extracellular glycoprotein involved primarily in cell migration, and regulation of mineral deposition [de Oliveira 2004]. Among all the non-collagenous matrix proteins found in mineralized tissue, OPN is unique as it preferentially accumulates at mineralized tissue interfaces and at mineralized tissue/implant interfaces suggesting a role as an interfacial adhesion molecule, thereby maintaining overall structural integrity of bone and bone/implant systems [McKee 1996, Pietak 2006, Baht 2008]. ALP, OPN, OC and OPN are therefore the typical biomarkers used for osteoblast phenotypic behavior when tracking differentiation of a multipotent cell population.

1.3.3 Effect of Oxygen on Osteogenic Differentiation

Although it remains to be determined what true hypoxic conditions are, it is now widely accepted that 20% of oxygen as commonly used in cell culture is rather a state of artificial hyperoxia [Grayson 2007, Fehrer 2007, Malda 2007]. As discussed in previous sections, low oxygen tensions (non-atmospheric) are considered to be a more physiological milieu for stem cells and affects stem cell fate [Heppenstall 1975, Watt 2000, Warren 2001, Park 2002, Grayson 2006, Malladi 2006, Fehrer 2007, Potier 2007, Volkmer 2010]. Several studies have been summarized in Table 1, to provide a more detailed summary of the findings for the effects of *in vitro* hypoxia on the stem cells of interest. It has been reported that hypoxia (2% and 5% O_2) enhanced the *in vitro* and *in vivo* bone-forming potential of rat and human MSCs respectively [Lennon 2001, Grayson

2007]. But in another study hypoxia inhibited the *in vitro* osteogenic potential of MIAMI cells and induced down-regulation of osteoblastic genes in hMSCs *in vitro* [D'Ippolito 2006]. Several other articles have provided proof that osteogenic differentiation may be negatively affected by hypoxia [Park 2002, Salim 2004, Malladi 2006, Utting 2006, Potier 2007]. The majority of the studies have shown that hypoxia brings about a decrease in the expression level of key transcription factors and osteogenic marker genes, such as RUNX 2, OC, OPN and COL 1 [Park 2002, Salim 2004, Utting 2006]. However, it is very difficult to arrive at a consensus even after collating and analyzing the results of published studies. Differences in cell isolation methods, experimental parameters, growth factor concentrations, oxygen tensions, and specific evaluation techniques highlight the challenges in determining the role of oxygen in stem cell differentiation. Table 1 sums up the list of some studies examining the effect of hypoxia on osteogenic differentiation of stem cells.

At the site of fractured bone, a milieu of reduced oxygen triggers bone healing linking hypoxia to osteogenic differentiation of bone precursor cells [Ke 2006, Wang 2007, Giannoudis 2007, Riddle 2009, Araldi 2010]. It is thus evident that cells that are utilized to regenerate bone tissue will face hypoxic conditions, either when used in the setting of bone tissue engineering or whenever a fracture has occurred [Polykandriotis 2006, Kneser 2006].

Table 1: Studies examining effect of oxygen on osteogenic differentiation of stem cells.

Cell Type	Oxygen Tension	Osteogenic Differentiation (compared to 20% O2)	References
ASCs	2% O_2	Inhibited	Lee and Kemp 2006
ASCs	2% O_2	Inhibited	Malladi 2006
ASCs	1% and 5% O_2	Inhibited	He 2010
ASCs	5% O_2	Inhibited	Merceron 2010
ASCs	2% O_2	Upregulated	Valorani 2013
ASCs and BMSCs	1% and 5% O_2	Upregulated	Chung 2012
BMSCs	3% O_2	Inhibited	Fehrer 2007
BMSCs	2% O_2	Inhibited	Volkmer 2010
BMSCs	1% O_2	Inhibited	Yang 2011
BMSCs	2% O_2	Inhibited	Wang 2012
BMSCs	2% O_2	No Effect	Martin-Rendon 2007
BMSCs	2% O_2	Upregulated	Grayson 2006
BMSCs	2% O_2	Upregulated	Huang 2011
BMSCs	1% O_2	Upregulated	Hung 2011
BMSCs	5% O_2	Upregulated	Lennon 2011
BMSCs	2% O_2	Upregulated	Wagegg 2012
BMSCs	5% O_2	Upregulated	Zhou 2013
BMSCs	4% O_2	Upregulated/ Inhibited different markers	Potier 2007
human MIAMI cells	3% O_2	Inhibited	D'Ippolito 2006
MG63 cells	2% O_2	Inhibited	Park 2002

1.3.4 Role of HIF-1 Pathway in Bone Formation

Wan and colleagues conducted experiments in osteoblasts of mice that lacked pVHL and therefore had a constitutive HIF-1α activation and observed that these mice had an increased vascularity and produced more bone in response to distraction osteogenesis compared to mice that lacked HIF-1α that had an impaired angiogenesis and bone healing [Wan 2008]. Similarly Wang et al. showed that mice overexpressing HIF 1α in osteoblasts through the deletion of the *VHL* expressed high levels of VEGF and developed extremely dense, heavily vascularised long bones. In contrast they observed in mice lacking HIF-1α in osteoblasts an opposite skeletal phenotype; in either the long bones were substantially thinner and less vascularised. In mice that lacked both *VHL* and HIF-1α the phenotype of the long bone was intermediate between the mice lacking HIF-1α through the deletion of *VHL* and the mice overexpressing HIF-1α [Wang 2007]. Interestingly Wang et al. were able to show that upon HIF-1α knockdown the mice produced an elevated level of HIF-2α and as both HIF-1α and HIF-2α have overlapping function, HIF-2α might substitute partially for the loss of function of HIF-1α. This compensatory mechanism might also explain why HIF-1α knockdown mice were still able to develop functional bone [Wang 2007]. Taken together the results of Wang and Wan depicts HIF-1α pathway as a critical mediator of neoangiogenesis that is required for bone development and regeneration. Their studies collectively imply a possible therapeutic application of HIF-1 activators to improve bone repair.

1.3.5 Summary

Oxygen is not only a nutrient but also an important signaling molecule whose concentration can influence the fate of stem cells. The combination of 3-D scaffolds and cells used to in tissue engineering applications often have limitations of oxygen diffusion leading to gradient formation. Due to the link between local oxygen levels and cell behavior, these gradients can cause heterogeneous behavior of cells. Cell response to reduced oxygen tension is primarily regulated by HIF-1α. A number of techniques exist to measure the amount of HIF-1α in cells but many require that the cells be lysed or fixed. Also, HIF-1 activity does not always correlate with the amount of HIF-1 protein or mRNA that compromises techniques measuring such quantities that seek to predict expression of HIF-regulated genes. Therefore, it is important to have a system that can track HIF-1 activity in 2-D as well as in 3-D to help understand cell behavior.

CHAPTER 2

OBJECTIVES AND EXPERIMENTAL DESIGN

OBJECTIVE 1: The objective of this study is to evaluate a responsive, fluorescent, hypoxia detection system and determine whether HIF activity can be tracked at a cellular level in both 2D and 3D cultures.

Experimental Design 1: In order to test the hypoxia detection, adipose-derived stem cells (ASCs) are used, cultured in two-dimensional (2D) and 3D culture conditions and exposed to 20% or 1% oxygen environments for 96 h. The marker signal for HIF-1 is tracked at time point's 4hr, 8hr, 12hr, 24hr, 48hr, 72hr and 96hr. A parallel setup is prepared to track and quantify HIF-1 through other commonly used techniques such as Immunofluorescence and western blotting.

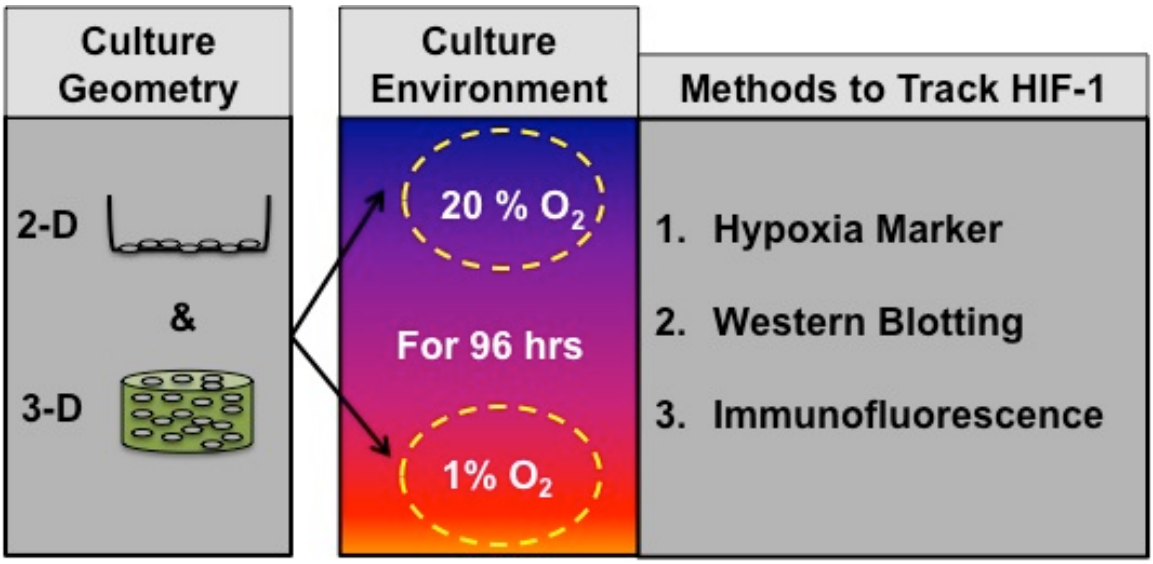

Figure 2.1: Experimental Design 1. To evaluate the hypoxia detection system.

OBJECTIVE 2: To examine the impact of hypoxia on osteogenesis of ASCs in both 2-D and 3-D culture condition and determine if HIF-1 represents a potential therapeutic target that would alter this effect.

Experimental Design 2: In order to examine the effect of hypoxia on osteogenesis, ASCs are cultured in two-dimensional (2D) and 3D culture conditions and exposed to 20%, 2% and 1% oxygen environments. 1% and 2% oxygen environments are modeled as the implantation environment in the study. The cells are directed towards osteogenic lineage using a differentiation media and processed for ALP activity (Days- 7, 14, 21, 28), Mineralization (Days- 14, 28) and protein detection (Osteonectin and Osteopontin- Day 28). In order to examine the role of HIF-1 in the process of osteogenic differentiation, a parallel setup is prepared with a HIF-1 inhibitor added to the osteogenic differentiation media.

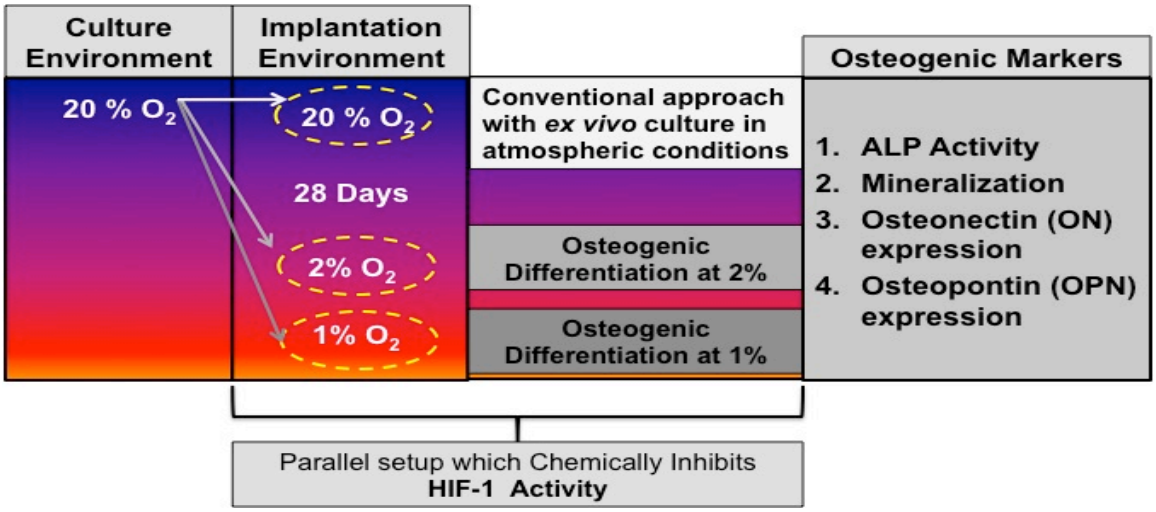

Figure 2.2: Experimental Design 2. To examine the effect of hypoxia and role of HIF-1 in osteogenic differentiation of ASCs.

OBJECTIVE 3: To examine the impact of varied ischemic preconditioning (IPC) protocols on ASCs phenotypic change, resistance to apoptosis and osteogenic differentiation.

Experimental Design 3: ASCs are cultured in 4%, 2% and 1% oxygen environments for 96 hours with and without the HIF-1 inhibitor. Every 24 hours, lysates are collected from each oxygen condition to examine the pro-apoptotic markers (HIF-1, pAKT, Bcl-2) and anti-apoptotic markers (Bax, active caspase-3). To examine the effect of hypoxia on phenotypic change, samples are collected at 96 hours to run flow cytometry to examine the presence stem cell antigen markers (CD 105, CD 45). To examine the effect of IPC on osteogenesis, 2% oxygen environment is modeled as the implantation site. 3 different IPC protocols are used step-up IPC (From 1% to 2%), standand IPC (from 2% to 2%) and step-down IPC (4% to 2%). ALP activity, mineralization and protein expression of ON and OPN are quantified to measure the degree of osteogenic differentiation.

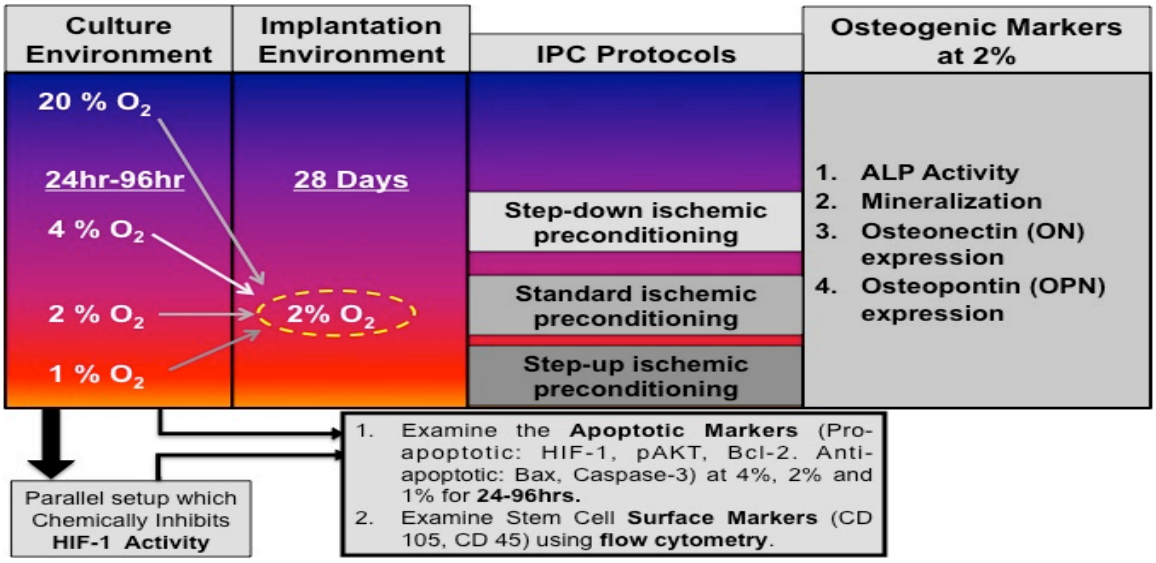

Figure 2.3: Experimental Design 3. To examine the effect of varied IPC protocols on stem cell phenotype, apoptotic marker expression and osteogenic differentiation of ASCs.

CHAPTER 3

TRACKING HYPOXIC SIGNALING IN ENCAPSULATED STEM CELLS

3.1 INTRODUCTION

Molecular oxygen serves as a metabolic substrate and signaling molecule for cells both *in vitro* and *in vivo*. Stems cells reside in a range of different microenvironments and the local oxygen concentration can help guide their differentiation. Ma et al., point out that mammalian embryogenesis and development take place at hypoxic conditions of 1.5-8% O_2 and 2.3-5.2% O_2, respectively [Ma 2009]. In the literature, oxygen concentrations less than 5% have been described as hypoxic conditions [Ren 2006, Fehrer 2007, Ma 2009]. Hypoxia can create a potentially lethal environment and limit cellular respiration and growth or, alternatively, enhance the production of specific extracellular matrix components and increase angiogenesis [Semenza 2000]. A hypoxic environment plays a substantial and critical role in many essential physiological and developmental pathways. It has been linked to maintenance, proliferation, survival and differentiation of various types of stem cells and influences the lineage commitment of multipotent cells [Malda 2007, Lin 2008, Ivanovic 2009, Abdollahi 2011].

Cell response to reduced oxygen tension is primarily regulated by hypoxia-inducible factors [Semenza 2002, Semenza 2010]. HIFs are transcription factors which belong to the bHLH-PAS (basic Helix-Loop-Helix-PER-ARNT-SIM) family. HIF-1 is a heterodimer composed of HIF-1α and HIF-1β. HIF-1β, also referred to as ARNT

(aryl hydrocarbon receptor nuclear translocator) is stable regardless of local oxygen tension, whereas, HIF-1α is only stable under hypoxic conditions. Under normoxia (high oxygen conditions), HIF-1α is rapidly degraded due to hydroxylation, which promotes ubiquitination and subsequent proteosomal degradation [Jiang 1996, Semenza 1998, Semenza 2002, Semenza 2010]. The amount of HIF-1α increases exponentially in cells as oxygen levels drop from 6% O_2 [Jiang 1996]. HIF-1 regulates transcription of genes which contain HREs in their promoters, introns and/or 3' enhancers. HIF-1 interacts with HREs leading to transcription of oxygen-regulated genes like VEGF, erythropoietin, iNOS, and glycolytic enzymes that enhance cellular adaptation to hypoxia [Sharp 2004, Hwang 2008, Wang 2007]. This oxygen-sensitive regulation of transcription allows cells to adapt to changing oxygen tensions or to survive in physiological environments where the oxygen level is always in the hypoxic range. It has been estimated that 5% or more of our genes are regulated by HIF-1. VEGF, basic fibroblast growth factor (bFGF), angiopoietin 2 (Ang-2) and platelet-derived growth factor (PDGF) are examples of angiogenic molecules whose expression is increased by HIF-1 activity [Forsythe 1996, Kelly 2003, Ceradin 2004, Manalo 2005, Simon 2008]. Hypoxia and HIF-1 are also implicated in the recruitment of circulating angiogenic cells, critical in vascular remodeling [Asahara 1999, Grant 2002, Kinnaird 2004, Kinnaird 2004]. Given the interest in driving vascularization of tissue engineering constructs, HIF-1 activity is an important event to monitor for cells in these scaffolds.

Most in vitro cell culture studies are conducted at atmospheric oxygen levels of approximately 20%, which far exceed the physiological levels. Since oxygen concentration is an important component of the stem cell "niche" which affects the

behavior of stem cells, it is important to account for it while interpreting experiments [Moore and Lemischka 2006]. The effect of oxygen on adipose-derived stem cells (ASCs) has been explored in a number of recent studies [Wang 2005, Lee 2006, Bhang 2011]. ASCs are multipotent, mesenchymal stem cells which can be isolated through lipoaspiration. ASCs have been used to differentiate into chondrogenic, osteogenic, endothelial, cardiomyogenic, myogenic, adipogenic and potentially neurogenic phenotypes with HIF-1 activity affecting many of these pathways [Zuk 2001, Wang 2005, Fraser 2006, Lee 2006, Schaffler 2007, Bunnell 2008, Bhang 2011, Liu 2011].

The design of a tissue engineering scaffold can also impact local oxygen levels for cells within the material. Hydrogels are an attractive choice as a scaffold material because their high water content facilitates transport of nutrients and waste products to and from the encapsulated cells. Poly(ethylene glycol) (PEG) hydrogels are broadly-utilized in the field of tissue engineering and can be easily functionalized to create custom microenvironments for encapsulated cells [Lin-Gibson 2004, Nuttelman 2004, Ford 2006, Hwang 2006, Benoit 2007, Buxton 2007, Salinas 2007, Stosich 2007, Weber 2008]. Oxygen supply to cells in 3-D constructs is more complex than in 2-D cultures as it is influenced by the chemistry of the scaffold material(s), scaffold dimensions, local oxygen tension, cell type, cell density as well as by the mechanisms of transport, i.e., diffusion or convection. Studies in 3-D culture revealed that the oxygen concentration decreases from the periphery toward the center of the scaffolds, which correlates with cell density and cell viability [Volkmer 2008, Radisic 2006]. The oxygen concentrations in the media and inside the scaffolds have been measured using oxygen-sensing dyes, oxygen microelectrodes, fluorescent probes and microparticles [Kellner

2002, Malda 2004, Cochran 2006, Revsbech 1983, Krihak 1996, Acosta 2009]. Mathematical modeling approaches have been developed accounting for scaffold geometry and local oxygen tension to predict oxygen gradients inside the scaffolds [Sengers 2007]. These techniques to measure or predict oxygen concentration offer a great deal of information to the tissue engineering community. However, it is also important to know how cells react to their local oxygen concentration to predict changes in phenotype.

Because of the importance of how cells respond to the local oxygen and the role of HIF-1 in stem cell behavior, we developed a responsive, fluorescent hypoxia marker based on a recombinant adenovirus [Skiles 2011]. The sequence of a red fluorescent protein (Ds Red DR) was placed under the control of a minimal promoter and HRE trimer. This virus is referred to as HRE Ds Red DR. Expression of the fluorescent protein should match the expression of other HIF-1-regulated genes. HIF-1 regulates expression of anti-apoptotic genes and secretion of numerous angiogenic factors. A system to track the onset of these events will assist tissue engineering efforts using a range of scaffold materials and culture in many different oxygen conditions. A number of techniques exist to measure the amount of HIF-1α in cells but many require that the cells be lysed or fixed. HIF-1 activity does not always correlate with the amount of HIF-1 protein or mRNA which compromises techniques measuring such quantities that seek to predict expression of HIF-regulated genes.

The objective of this study was to evaluate a responsive, fluorescent, hypoxia detection system and determine if HIF activity can be tracked at a cellular level in both 2-D and 3-D culture. ASCs were selected due to their broad utilization in tissue

engineering strategies and the influence of HIF signaling on ASC phenotype. The experiments outlined below were designed to examine the relationship between culture conditions and hypoxic signaling. A mechanism to continuously monitor HIF activity in encapsulated cells is a useful tool for the tissue engineering community.

3.2 Materials and Methods

3.2.1 Cell culture

Human ASCs isolated from human lipoaspirate tissue were purchased from Invitrogen at passage 1. Cells were cultured in proprietary MesenPRO RS^{TM} basal medium supplemented with MesenPRO RS^{TM} Growth Supplement, 1% penicillin/streptomycin (Mediatech, Manassas, VA) and 2 mM L-glutamine (MP Biomedicals, Irvine, CA, USA). Culture conditions for passaging were maintained at 95% air and 5% CO_2 at 37°C. For experiments, cells between passages 2 and 5 were used as recommended by the supplier.

3.2.2 Oxygen-controlled culture

Nitrogen-purged, programmable incubators were used to maintain constant oxygen levels for cellular studies (Napco Series 8000 WJ, Thermo Electron). Normoxic oxygen studies were maintained at 5% CO_2 and 20% oxygen and hypoxic studies were maintained at 5% CO_2 and 1% oxygen conditions. For 1% oxygen experiments, all media, buffered salt solutions, and fixatives to be used with cells were kept in vented tubes in the hypoxic incubator for 24 hours prior to use so as to equilibrate the solutions to the appropriate dissolved oxygen concentration. Previous studies in our

lab have shown this period to be sufficient to equilibrate the dissolved oxygen concentration [Skiles 2011]. All cell manipulation (media changes and imaging) was performed as quickly as possible to minimize exposure to atmospheric air. These procedures were kept under 10 minutes per day. Studies using a dissolved oxygen sensor tracked the change in dissolved oxygen levels in the media during this time and found that levels only increased from 0.3 mg/L (concentration equilibrated in 1% oxygen incubator) to 0.4 mg/L after 10 minutes outside of the incubator. The concentration had returned to 0.3 mg/L within 10 minutes of placement back in the incubator.

3.2.3 Infection of ASCs and tracking hypoxic signaling

The preparation of the virus was briefly described earlier and is detailed in previously published studies [Skiles 2011]. As observed in those previous studies, the virus exhibited 100% infection efficiency with ASCs. For marker studies, ASCs were seeded into a 12-well tissue culture treated plate with the HRE DsRed DR virus at a multiplicity of infection of 25. The plates were incubated overnight in static culture at 20% O_2 for the cells to attach to the surface and for the infection to take place. Both 2-D and 3-D samples were fluorescently imaged periodically over 96 hours using a Nikon Eclipse Ti microscope (Nikon, Tokyo, Japan) and the Nikon NIS-Elements imaging software with consistent exposure times and fluorescent lamp intensities. Multiple images (3-4 images for 2-D samples and 5-6 images for 3-D samples) from three independent studies were used to quantify the cells expressing positive marker signal.

3.2.4 Cell encapsulation for 3-D experiments

Poly(ethylene glycol) with an average molecular weight of 10,000 Da (Sigma-Aldrich, St. Louis, MO) was functionalized by addition of methacrylate end groups resulting in poly(ethylene glycol) dimethacrylate (PEGDM). ASCs were trypsinized, counted using a hemocytometer and spun down in a microcentrifuge tube prior to removal of the media. Cells were then re-suspended in a solution of 10 wt% PEGDM and 0.025 wt% 2-hydoxy-1-[4-(2-hydroxyethoxy)-phenyl-2-methyl-1-propanone (Irgacure 2959) (Ciba, Tarrytown, NY) which is a photoinitiator in Hank's balanced salt solution (HBSS) (Mediatech Inc, Manassas, VA). Each gel in these studies was designed to contain 400,000 dispersed ASCs so enough cells were added to the PEGDM to create a concentration of 10,000 cells/µl. After re-suspension of the cells, 40 µl of the PEGDM suspension was added to a 1 ml syringe and exposed to a 365 nm light source at an intensity of 7 mW cm^{-2} for 10 min under sterile conditions. The resulting gels are cylindrical discs measuring 5 mm in diameter and 2 mm in height. The gels were transferred to a 24 well plate, washed in HBSS and placed in 1.5 ml of media. The plates were cultured in the varied oxygen conditions on orbital shakers set to continuous rotation at 100 rpm. This encapsulation procedure has been shown previously to not have an adverse impact on viability for a range of cell types [Benoit 2007, Weber 2008].

3.2.5 Protein extraction and western blotting for HIF-1α

Total cell lysates were collected from the 2-D and 3-D samples with RIPA lysis buffer (Thermo Scientific, Rockford, IL) containing a protease and phosphatase inhibitor cocktail (Thermo Scientific, Rockford, IL), stirred on ice for 10 min and

sonicated for 15 min. The mixtures were then centrifuged at 14,000 rpm at 4°C for 15 min. The supernatants were collected and protein concentration was quantified using a Coomassie Plus Bradford Assay kit (Thermo Scientific, Rockford, IL) according to the manufacturers' instructions.

Western blotting was performed by SDS-PAGE with 50 µg of protein lysate loaded per lane of 4-20% gradient gels followed by transfer to PVDF membranes (Millipore, Billerica, MA). The membrane was first incubated in 5% dry milk, 1% bovine serum albumin (BSA) diluted in HBSS for 1 h at room temperature. The membrane was then washed twice for 10 min each in "wash 1" (0.1% Tween-20, 0.1% dry milk, 0.1% BSA in HBSS). The membrane was then incubated with rabbit anti-HIF-1α antibody (1:1000) (Santa Cruz Biotechnology, Santa Cruz, CA) and rabbit anti-b-actin antibody (1:1000) (Santa Cruz Biotechnology, Santa Cruz, CA) for 2 h at room temperature (RT). The membrane was then washed three times for 10 min each in "wash 1". Membranes were then incubated with peroxidase-conjugated, goat, anti-rabbit IgG (1:5000) (Rockland Immunochemicals, Gilbertsville, PA) for 2 h at RT. Membranes were then washed 3 times for 10 minutes each in "wash 2" (0.1% Tween-20 in HBSS). Protein detection was achieved by 5 min incubation in a chemiluminescence reagent, SuperSignal West Pico Substrate (Thermo Scientific, Rockford, IL). Bands were then detected using ChemiDoc™ XRS$^+$ System with Image Lab™ image acquisition and analysis software (Bio-Rad, Hercules. CA). With densitometry analysis, the expression of proteins was normalized to β-actin to account for % IOD (intensity optical density) fold difference of HIF-1α protein expression. All incubation steps and washes were performed on an orbital

shaker set to continuous rotation at 100 rpm. The statistics shown represent results obtained from three independent studies.

3.2.6 Immunostaining for HIF-1 activity

100,000 ASCs were plated in flat-bottom 96-well plates for 2-D experiments. The previously described, ASC-containing PEG gels were used for 3-D experiments. The samples were maintained in 1% and 20% O_2 for a period of 96 hours. To prepare the cells for staining, samples were fixed after 24h, 48h, 72h and 96h with 4% paraformaldehyde (Thermo Fisher, Waltham, MA) on ice for 30 min and washed twice with HBSS. Staining was performed every 24 hours during the 4 day period. Cells were permeabilized with 0.1% Triton X (EMD Chemicals, Gibbstown, NJ) for 30 min and then washed successively in 5% bovine serum albumin (EMD) and 5% normal donkey serum (EMD) for 1 h each. An overnight incubation at 4°C with polyclonal rabbit antibody to HIF-1α (1: 1000) (Santa Cruz Biotechnology, Santa Cruz, CA) was followed by two, 15 min washes in 1% BSA and a 1 h incubation in 5% normal donkey serum. A fluorescently-labeled, goat, anti-rabbit secondary antibody (1:1000) (Rockland Immunochemicals, Gilbertsville, PA) was added for an hour followed by final washes in 1% BSA in HBSS. Samples were fluorescently imaged with the instrumentation and software previously mentioned. Multiple images (3-4 images for 2-D samples and 5-6 images for 3-D samples) from three independent samples were analyzed to quantify the number of cells expressing HIF-1α.

3.2.7 Viability of ASCs

Live/Dead® staining kit (Invitrogen) was used to test the viability of the samples. Fluorescent dyes indicate esterase activity (observed as green signal in live cells) or loss of nuclear membrane integrity (observed as red signal in dead cells). The 2-D and 3-D samples were in culture conditions similar to the previous experiments and the staining was performed in accordance with the manufacturer's guidelines. Results are given as a percentage of viable cells based on analysis of three independent studies.

3.2.8 Statistical analysis

Statistical analysis was performed using Graphpad Prism 4.01 (GraphPad Software Inc., San Diego, CA). Experimental results were expressed as the mean ± standard deviation. All the collected data were analyzed by two-way ANOVA for comparisons and p-values < 0.05 were defined as statistically-significant differences.

3.3 RESULTS

3.3.1 HIF-1α immunostaining

The HIF-1α staining (green) was primarily focused in the cytoplasm of ASCs. In 2-D at 20% O_2, no staining was evident during the entire time course. A representative image after 96 hours of culture is shown in figure 3.1A. In 1% O_2, no signal was observed at 24 and 48 hours. 56±3% and 61±4% cells stained positive for HIF-1α at 72 and 96 hours respectively. Representative images are shown in figure 3.1 (B and C). In 3-D, no signal was observed at 24 and 48 hours at both 1% and 20% O_2. In 1% O_2, staining was observed at 72 and 96 hours with 13±2% and 25±4% cells staining

positive respectively. The representative image at 96 hours in 1% O_2 is shown in figure 3.1 (D1, D2 (overlay image)). Immunostaining was also observed at 20% O_2 in 3-D, with 9±2% and 11±3% cells stained positive for HIF-1α at 72 and 96 hours respectively as in shown in figure 3.1 (E1, E2 (overlay image)). These results are summarized in figure 3.1F.

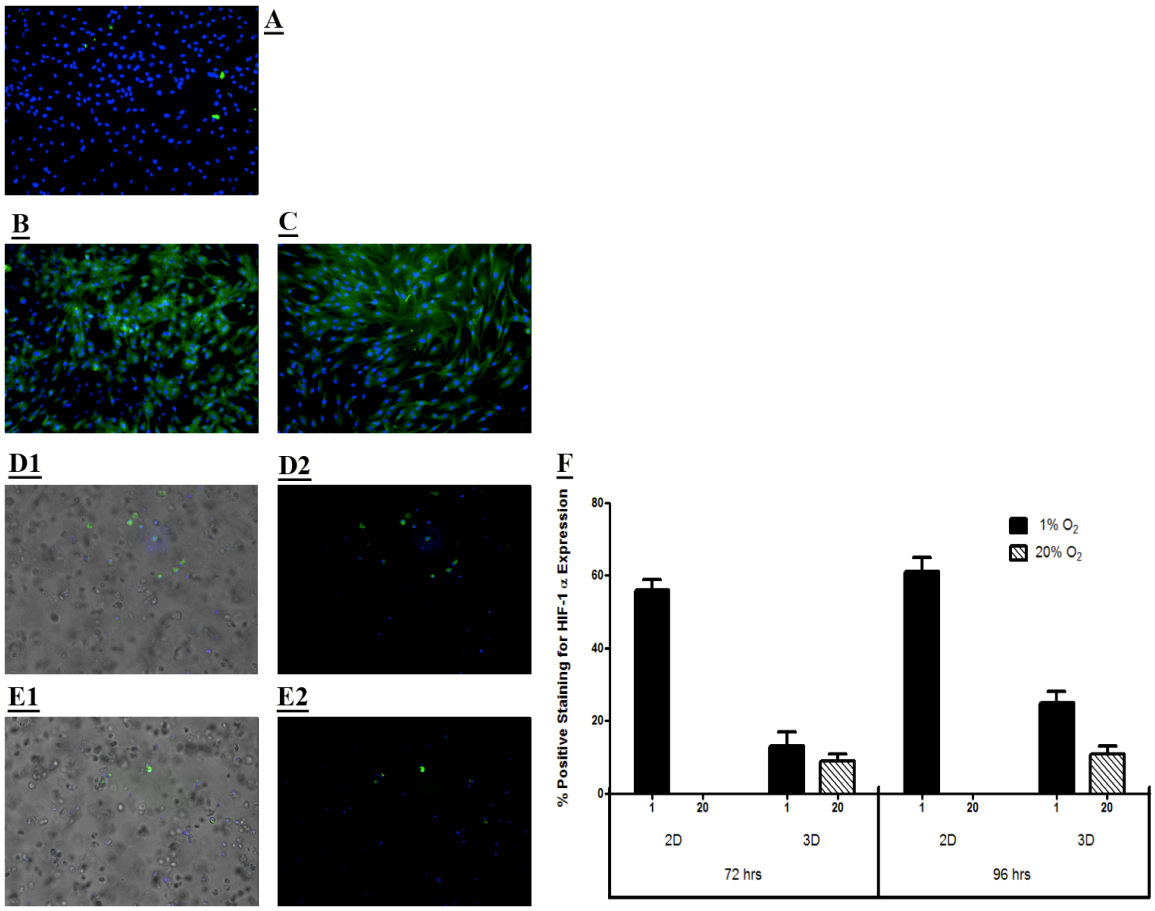

Figure 3.1: Immunostaining for HIF-1α. HIF-1α, if present, was stained green. As a counterstain, cell nuclei labeled with DAPI appear blue. (A) At 20% O_2, there was no significant staining at 96 h in 2D. (B,C) shows cells in 2D at 1% O_2 stained for HIF-1α at 72 and 96 h, respectively. (D, E) HIF-1α staining in 3D. (D1) Immunostaining in 1% at 96 h (D2 is an overlay image). (E1) is the representative image of staining at 20% O_2 at 96 h (E2 is an overlay image). Quantification of HIF-1α expressing cells (F) from each of the studies (A–E).

3.3.2 Hypoxia marker signaling

In 2-D at 20% O_2, there was no marker signal throughout the study period of 4 days. At 1% O_2, the onset of the signal was seen at 8 hours with 4±1% cells showing positive red fluorescence signal for HIF-1α activation. Signal progression increased with 11±3%, 17±4%, 26±3%, 54±2% and 59±3% of cells showing positive marker signal at 12, 24, 48, 72 and 96 hours respectively. A representative image for each time point is shown in Figure 3.2 (A1-A6). In 3-D at 1% O_2, we observed the onset of the marker signal at 4 hours with 5±1% cells expressing positive signal. The prevalence of the signal increased over time with 9±3%, 15±5%, 32±4%, 54±2%, 62±4% and 76±3% cells expressing positive marker signal at 8, 12, 24, 48, 72 and 96 hours respectively. Representative images for each time point are shown in Figure 3.2 (B1-B7). Marker signal was also observed in 3-D at 20% O_2. The onset of the signal was at 24 hours with 4±2% cells showing positive marker signal. The prevalence of the signal increased over time with 7±2%, 9±4% and 13±3% cells expressing positive marker signal at 48, 72 and 96 hours respectively (Figure 3.2: C1-C4). The above results are summarized in Figure 3.3.

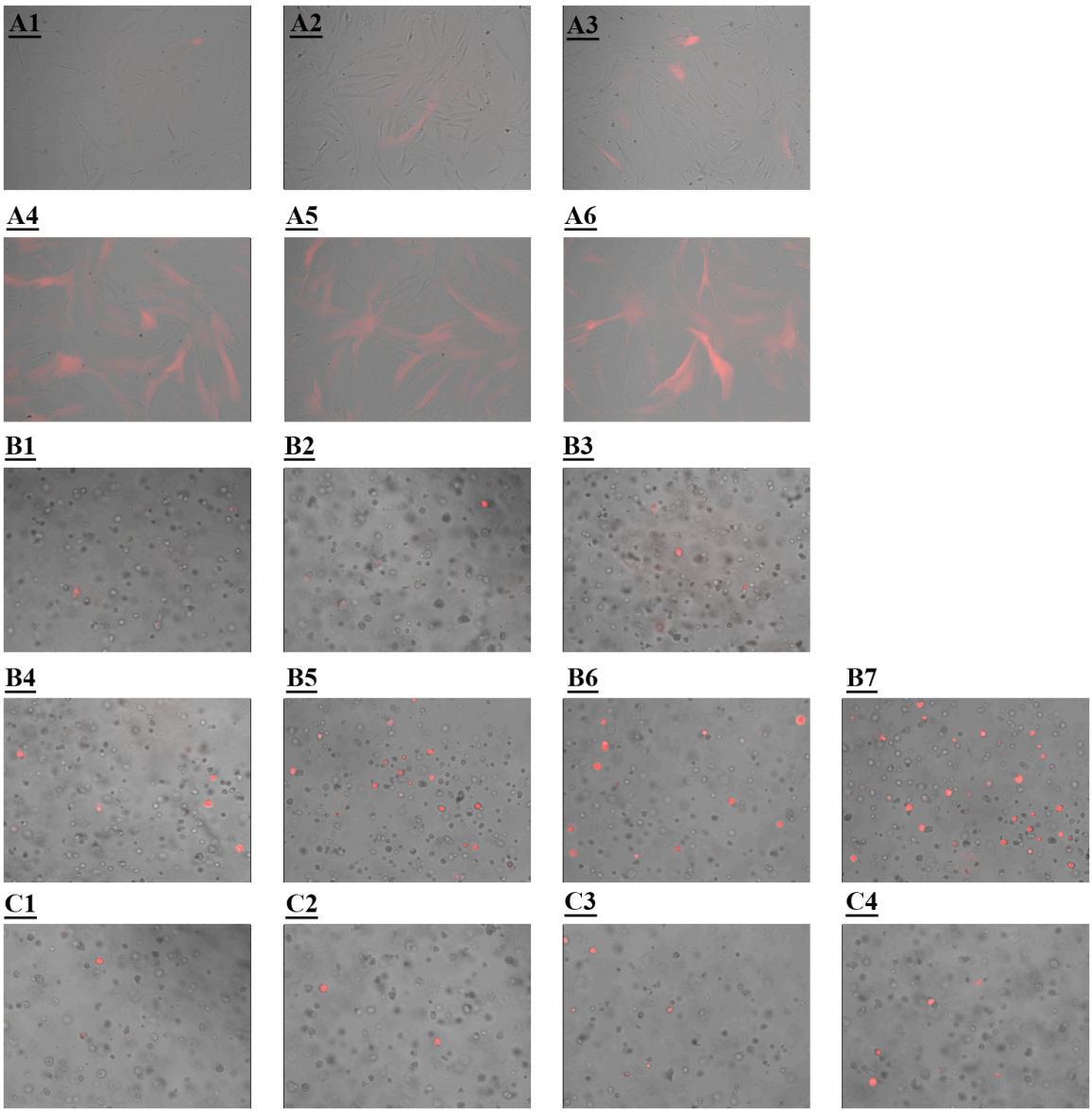

Figure 3.2: Hypoxia marker progression. (A1–A6) shows marker progression in 2D at 1%O_2 through 8, 12, 24, 48, 72, and 96 h, respectively. In 3D, onset of marker signal was first observed at 4 h (B1) and the prevalence of the signal increased over time, as shown in (B2–B7) corresponding to 8, 12, 24, 48, 72, and 96 h of culture, respectively. In 3D, signal was also observed in 20%O_2. These images (C1–C4) show marker progression at 24, 48, 72, and 96 h, respectively.

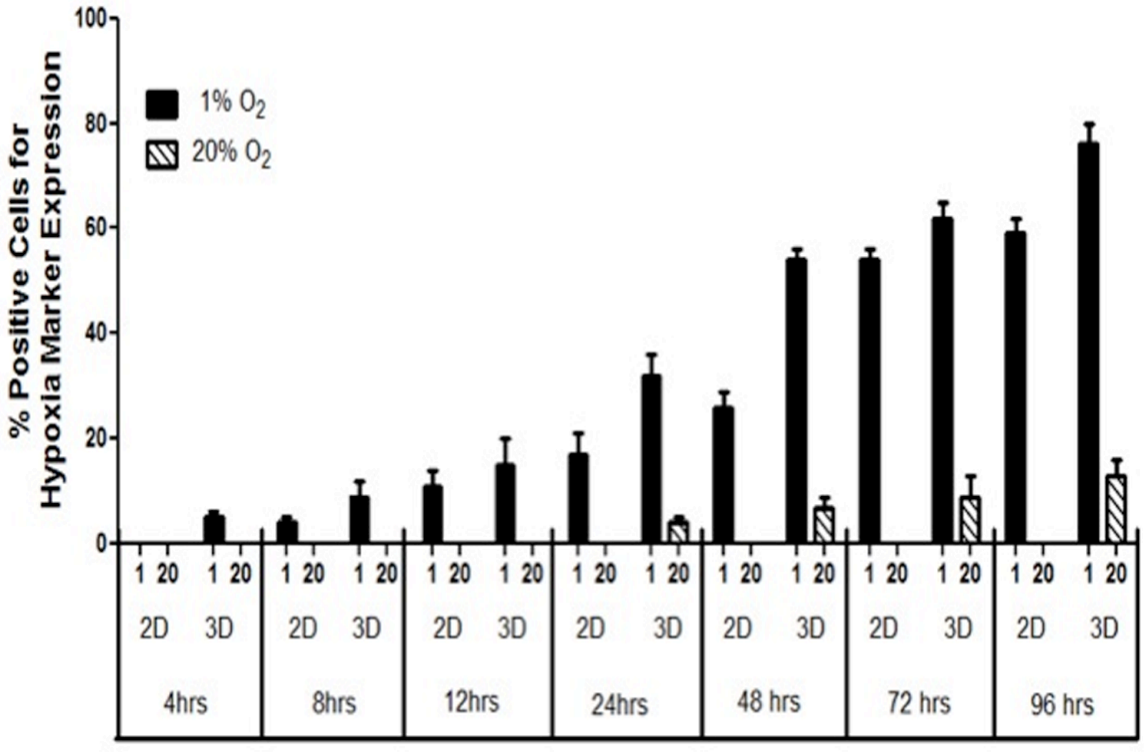

Figure 3.3: Quantification of cells positive for marker signal. The graph quantifies the percent positive cells expressing hypoxia marker signal in 2D and 3D conditions in both 1% and 20% O_2 conditions.

3.3.3 Quantification of HIF-1α protein

Western blotting was performed to quantify the amount of HIF-1α protein expressed in 2-D and 3-D culture conditions under 1% and 20% O_2. Figure 3.4A shows bands for HIF-1α protein in 1% O_2 in both 2-D and 3-D culture conditions. Quantification of these results using %IOD measurements and normalizing HIF-1α expression with β-actin expression showed an increase in HIF-1α expression over time. In 3-D at 1% O_2, we saw a %IOD fold difference of 6.01±0.42, 10.31±0.34, 11.31±0.453 and 11.39±0.31 at 24, 48, 72 and 96 hours respectively. In 2-D at 1% O_2, we observed a %IOD fold difference of 1.31±0.21, 2.52±0.34, 6.78±0.23 and 7.11±0.36 at 24, 48, 72 and 96 hours respectively. Figure 3.4B shows protein levels of HIF-1α examined at 20%

O_2 in both 2-D and 3-D. In 2-D, we observed no expression of HIF-1α throughout the study period. In 3-D the expression pattern was 0.61±0.246, 3.32±0.283, 3.98±0.183 and 4.01±0.15 %IOD fold difference at 24, 48, 72 and 96 hours respectively. The above results are summarized in Figure 3.4C.

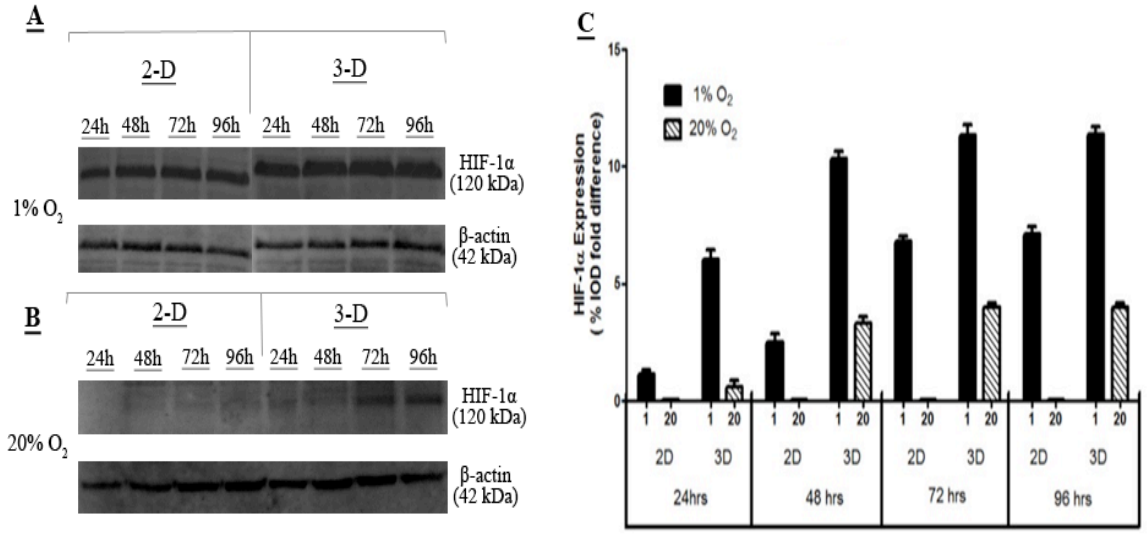

Figure 3.4: Western blot for HIF-1α and β-actin. Results are shown for ASCs cultured in 1% O_2 (A) and 20% O_2 (B). These results are quantified in (C).

3.3.4 ASC viability

Viability of ASCs in 2-D and 3-D culture at both 1% and 20% O_2 was observed every 24 hours for the time period of 4 days. In 2-D at 20% O_2, the % viability was 99±0.2%, 98±0.6%, 98±0.4% and 98±0.3%, at 24, 48, 72 and 96 hours respectively. At 1% O_2 incubation the % viability was observed at 99±0.4%, 99±.02%, 98±0.5% and 98±0.3% at 24, 48, 72 and 96 hours respectively. For 3-D cultures in 20% O_2, 99±0.4, 99±0.3, 98±0.6 and 97±0.4 % viability was observed at 24, 48, 72 and 96 hours respectively. Finally, for 3-D cultures in 1% O_2, 99±0.2, 98±0.4, 97±0.3, 97±0.4 % cell viability was observed at 24, 48, 72 and 96 hours respectively.

3.4 DISCUSSION

Immunostaining results in 2-D at 20% O_2 did not show any staining for HIF-1α at any of the time points, which correlates with our marker. At 1% O_2, signal was only observed at 72 and 96 hours which also correlated well with our marker. Interestingly in 3-D, we observed immunostaining and hypoxia marker signal (Figure 3.2: C1-C4) in both 1% and 20% O_2. The results in 20% oxygen show the impact of the PEG material on oxygen diffusion. The immunostaining in 3-D did not correlate as well with our marker, as a lower percentage of cells stained positive for HIF-1α (Figure 3.1F and Figure 3.3) than displayed the fluorescent marker signal under the same conditions.

The discrepancy could be due to limited diffusion of the primary and secondary antibodies through the scaffold. Crosslinked PEG hydrogels formed from macromers of mol. wt. 10kDa exhibit a mesh size of 7.78nm [Lin 2011]. The hydrodynamic radius of our antibodies should be below this size but the pore size is heterogeneous and diffusion may have been impeded. Limitations in protein diffusion were not observed in our western blotting experiments. The protein quantity yield of 400,000 cells lysed in 2-D culture was equivalent to that obtained when lysates were collected from gels containing 400,000 cells following 3-D culture. Quantification of HIF-1α by western blot displayed higher intensity bands in 3-D than 2-D at 1% O_2 at each of the time points (Figure 3.4A). At 20% O_2, there were no bands for HIF-1α in 2-D at any time points. Some HIF-1α was detected in 3-D cultures (Figure 3.4B). Figure 4C shows the % IOD fold difference in HIF-1α protein expression. Detection of HIF-1α by immunocytochemistry should not produce significantly different results from detection by western blotting and the two matched up quite well for 2-D studies. The lack of

correlation within the scaffold highlights the utility of the HRE Ds Red DR marker as it did not exhibit the same issues and matched the trend seen with the western blot results.

The cellular response to HIF-1 is not homogeneous across cell types, with degree of stabilization and upregulated target genes varying between and within tissues [Bracken 2006, Lendahl 2009]. In this respect, the amount of HIF-1α does not necessarily correlate with HIF-1 activity. If this was occurring with our ASCs, a difference would be expected between the signal from the marker and both methods used to detect HIF-1α quantity instead of just 3-D immunocytochemical results.

Extended exposure to hypoxia can affect the viability of cells. Our results showed that more than 95 percent of cells were viable at 1% O_2 in both 2-D and 3-D through 4 days of culture, suggesting that the low oxygen environment triggered HIF-1 activity but not a large drop in viability. This could be explained by the low metabolic activity of ASCs and that stabilization of HIF-1α protects cells against necrosis helping them to survive under acute or chronic hypoxia [Ginouves 2008].

As stated in the introduction, our goal was to establish whether the HRE Ds Red DR marker virus could be used to track HIF-1 activity in encapsulated ASCs and whether expression of the red fluorescent protein correlated with HIF-1α detected by traditional methods. The marker measures HIF activity rather than the amount of HIF-1α protein as measured with western blotting and immunocytochemical detection. A lag was expected between the stabilization of the transcription factor and expression of the fluorescent protein but it proved to be brief as the fluorescent signal was observed as early as 4 hr after exposure to hypoxic conditions. Our results show that detection of the signal is certainly possible and that image capture conditions can be established which

allow the observed signal to correlate with HIF-1α levels. These image capture conditions did not lead to background signal in cells when no HIF-1α was detected by other methods. We can monitor HIF activity in the same population of cells over time and this can be done in a 3-D culture environment without disruption of the scaffold.

The majority of cell culture studies have been performed on 2-D surfaces such as tissue culture plates/flasks because of the ease, convenience, and high cell viability of 2-D culture. These traditional 2-D cultures cannot be used to faithfully mimic the microenvironment of the particular tissue of interest. The combination of three-dimensional scaffolds and living cells is used to fill defect sites and support the transplanted cells. The material(s) selected for the scaffold and how it is synthesized influence the diffusion of oxygen and nutrients to the cells and this is a major limitation in tissue engineering [Volkmer 2008]. Gradients of oxygen concentration can form within materials and this will affect cellular differentiation or cell fate decisions [Malladi 2006, Grayson 2007, Mohyeldin 2010]. This marker system was developed to identify hypoxic signaling within these environments and to track this response at a cellular level without the need to disrupt the integrity of the scaffold or cells.

It is clear from previous studies that oxygen concentration and the cell response to the local oxygen tension are important parameters to track when devising novel, stem cell-based therapeutic systems. Our marker does not measure the oxygen concentration, but more importantly helps in the identification of a cellular response at low oxygen conditions. Several techniques have been applied to measure the spatial distribution of oxygen within tissues using blood-gas analyzers, dissolved oxygen probes and fluorescent/luminescent particles [Revsbech 1983, Krihak 1996, Zhao 2005, Butt

2007, Acosta 2009]. These systems offer high levels of sensitivity and specificity, but do not show how the cells respond to their local oxygen environment. The marker system described here can complement such techniques and offers great potential as a tool to track biological responses in tissue engineering studies.

Studies have shown that there may be a strong dependence of cellular metabolic activity and oxygen consumption rate on the scaffolding material and geometry, presumably due to altered cell-material interactions in the scaffold [Cukierman 2002, Malda 2004]. Therefore in the future, it would be interesting to evaluate the effect on the prevalence and onset of the marker signal within different scaffold materials for a range of cell densities. Due to the link between local oxygen levels and cell behavior, these gradients can cause heterogeneous differentiation of cells within tissue engineering scaffolds if steps are not taken to address the creation of these gradients. Future studies will take advantage of the versatility of our responsive hypoxia marker to show dynamic correlations between cell fate and function with oxygen concentration in engineered tissues in two-dimensional as well as three-dimensional environments.

CHAPTER 4

OSTEOGENIC DIFFERENTIATION OF ADIPOSE-DERIVED STEM CELLS IS HIF-1 INDEPENDENT

4.1 INTRODUCTION

Critical-size bone defects (CSDs), which can result from trauma, infection, genetic abnormalities and tumors, represent a challenge to the medical community. Tissue engineers seek to address this through implantation of cell-seeded scaffolds to fill these defects and accelerate formation of new bone [Chaikof 2002, Dupont 2010, Chimutengwende-Gordon 2012, Gamic 2012]. Adipose-derived, mesenchymal stem cells (ASCs) represent a potential source of cells for these strategies as they are more easily harvested than bone marrow-derived mesenchymal stem cells (BMSCs) and can differentiate into chondrocytes, osteoblasts and vascular cell phenotypes [Zuk 2002, Gimble 2003, Katz 2005].

The loss of vasculature at CSD sites creates a hypoxic environment with oxygen concentrations of approximately 0-3% [Heppenstall 1975, Schmitz and Hollinger 1986, Rodriguez-Merchan 2004, Kneser 2006]. Many stem cells are found in hypoxic environments in the body (defined as less than 5% oxygen) and HIF activity is critical in embryonic development [Dunwoodie 2009, Provot 2007, Ma 2009]. The important role HIF-1 plays in bone formation and repair has been discussed in a number of prior reviews [Tower 2008, Schipani 2009, Wan 2010].

Formation of new, vascularized bone to repair a CSD is a complex process involving numerous cell types and interplay of biochemical, mechanical and environmental stimuli. This contributes to the difficulty in interpreting results regarding the importance of hypoxia and HIF signaling in these processes. Studies conducted *in vivo* have shown the importance of HIF signaling on bone formation and repair but it is difficult to decouple osteogenesis from angiogenesis [Wan 2008, Zou 2011]. Hypoxic signaling is a major driving force for angiogenesis and VEGF is a critical target of HIF activity [Ferrara 2001, Dai 2007]. HIF-1 plays a key role in blood vessel formation and blocking HIF-1 activity will impair vascular growth and bone repair.

HIF-1 activity is also involved in chondrogenesis and maintenance of chondrocyte viability that are essential steps in endochondral bone formation [Malladi 2007, Pfander 2007, Araldi 2010]. The steps towards bone formation are difficult to track and isolate in *in vivo* and while HIF activity seems to be essential for bone formation in general, its impact on osteogenesis is less clear. The majority of the literature indicates an inhibitory role for hypoxia on osteogenesis of mesenchymal stem cells *in vitro* [Lennon 2001, D'Ippolito 2006, Malladi 2006, Fehrer 2007, Potier 2007, Holzwarth 2010]. A few studies, however, have shown the opposite effect [Grayson 2006, Ren 2006]. This could be due to varied cell sources, a range of oxygen conditions used to represent hypoxic conditions and the timing of hypoxic exposure [Volkmer 2010].

Bone formation strategies taking place ex vivo can occur in a wide range of possible oxygen concentrations and many utilize atmospheric conditions (20% oxygen). However, when differentiation takes place at a CSD, the environment will be hypoxic. Determination of whether HIF-1α represents a therapeutic target with respect to

osteogenesis would enhance bone tissue engineering efforts. Our studies were designed to provide information about the impact of hypoxia on osteogenesis of ASCs in both 2-D and 3-D culture conditions and whether blocking HIF-1 activity would alter this effect. VEGF secretion from ASCs in identical conditions was also monitored as coupling of osteogenesis and angiogenesis is essential to recreate endochondral bone formation.

4.2 Materials and Methods

4.2.1 Cell culture

Human ASCs were purchased from Invitrogen and cell culture was performed according to the supplier's specifications. Cells were cultured in proprietary MesenPRO RS^{TM} basal medium supplemented with MesenPRO RS^{TM} Growth Supplement, 1% penicillin/streptomycin (Mediatech, Manassas, VA) and 2 mM L-glutamine (MP Biomedicals, Irvine, CA, USA). Culture conditions for passaging were maintained at 95% air and 5% CO_2 at 37°C. For experiments, cells between passages 2 and 7 were used as recommended by the supplier.

4.2.2 Hypoxic culture conditions

Nitrogen-purged, programmable incubators were used to maintain a constant 1% or 2% oxygen level for hypoxic studies (Napco Series 8000 WJ, Thermo Electron). For 1% or 2% oxygen experiments, all media, buffered salt solutions, and fixatives to be used with cells were kept in vented tubes in the hypoxic incubator for 24 hours prior to use so as to equilibrate the solutions to the appropriate dissolved oxygen concentration. Previous studies in our lab have shown this period to be sufficient to

equilibrate the dissolved oxygen concentration [Skiles 2011]. Media changes and imaging procedures were kept under 10 minutes per day to limit exposure to atmospheric conditions. Dissolved oxygen concentration studies conducted in our lab showed that levels rose from 0.3 mg/L to 0.4 mg/L during a 10 minute atmospheric exposure (which correlates to a 1% oxygen to 1.5% oxygen environment). The 1% or 2% oxygen levels are reestablished within 10 minutes of return to the incubator.

4.2.3 Cell encapsulation for 3-D experiments

PEG with an average molecular weight of 10,000 Da (Sigma-Aldrich, St. Louis, MO) was functionalized by addition of methacrylate end groups resulting in PEGDM using a previously published method [Lin-Gibson 2004]. ASCs were trypsinized, counted using a hemocytometer and spun down in a microcentrifuge tube prior to removal of the media. Cells were then re-suspended in a solution of 10 wt% PEGDM and 0.025 wt% 2-hydoxy-1-[4-(2-hydroxyethoxy)-phenyl-2-methyl-1-propanone (Irgacure 2959) (Ciba, Tarrytown, NY) which is a photoinitiator in Hank's balanced salt solution (HBSS) (Mediatech Inc, Manassas, VA). ASCs were suspended in PEGDM to create a concentration of 10,000 cells/µl. For each gel, 40 µl of this ASC/PEGDM suspension was added to a 1 ml syringe and exposed to a 365 nm light source at an intensity of 7 mW cm^{-2} for 10 min under sterile conditions. The resulting gels were transferred to a 24 well plate, washed in HBSS and placed in 1 ml of media. The plates were cultured in the varied oxygen conditions on orbital shakers set to continuous rotation at 100 rpm. The encapsulation process is shown in a previously published video [Skiles 2011].

4.2.4 Osteogenic differentiation

Osteogenic differentiation was induced by culture in StemPro® Osteocyte/Chondrocyte Differentiation Basal Medium and StemPro® Osteogenesis Supplement (Invitrogen, USA). These experiments were carried out for ASCs in 2-D (100,000 ASCs seeded per well of 12-well culture plates) as well as 3-D environments (encapsulated ASCs as detailed in the previous section). The cells were monitored over a period of 28 days in 1%, 2% and 20% oxygen with the osteogenic medium replenished every 3 days.

4.2.5 HIF-1 inhibition

To inhibit the activity of HIF-1, a HIF-1 inhibitor [3-(2-(4-Adamantan-1-yl-phenoxy)-acetylamino)-4-hydroxybenzoic acid methyl ester)] (Calbiochem, USA) was used. It is a cell-permeable amidophenolic compound that inhibits hypoxia-induced HIF-1 transcription activity. The inhibitor selectively blocks the hypoxia-induced accumulation of cellular HIF-1α protein, while exhibiting no apparent effect on the cellular level of HIF-1α mRNA or that of HIF-1β protein. For both 1% and 2% O_2 samples, a concentration of 60μM of this inhibitor was sufficient to reduce accumulation of HIF-1α to levels below detection in western blotting. Toxicity tests showed no loss of viability of ASCs exposed to the inhibitor at concentrations up to 100μM (data not shown).

4.2.6 Alkaline phosphatase (ALP) activity and DNA quantification

Measurements of ALP activity in the media of ASCs were taken on days 7, 14, 21 and 28. The activity was determined using an ALP colorimetric assay kit (Abcam, USA) with p-nitrophenyl phosphate as substrate. The ALP activities were normalized to the cellular DNA content using a PicoGreen dsDNA quantitation kit (Molecular Probes, USA) according to the manufacturer's instructions. Alkaline phosphatase activity is quantified on days 7, 14, 21 and 28 and is expressed in μmol/ml/min/mg DNA. The values included represent the mean of three independent studies.

4.2.7 Alizarin Red staining for mineralization

Mineral deposition was quantified on days 14 and 28 using the Alizarin Red S staining procedure. The cells were rinsed with calcium and phosphate-free HBSS, and fixed with ice-cold 70% ethanol for 1 h. After a brief wash with HBSS, the cells were stained for 20 min with 40mM Alizarin Red solution (pH 4.2) at room temperature. The cells were rinsed two times for 15 min with HBSS (on an orbital shaker) to reduce nonspecific Alizarin Red staining. A 10% acetic acid was then added to the samples for 30 min on a shaker. Samples were collected by scraping (2-D) or vortex (3-D) and heated at 80°C for 10 min. The extracts are then centrifuged at 8000 rpm for 20 min and quantified spectrophotometrically with a microplate reader (Biotek, USA) at 570 nm. The calcium concentration was calculated from the standard curve generated from a serial dilution of a calcium standard solution and the values were normalized to DNA contents

(expressed in mg mineral/mg DNA). Values included represent the mean of three independent studies.

4.2.8 Protein expression

Total cell lysates were collected from the 2-D and 3-D samples with RIPA lysis buffer containing a protease and phosphatase inhibitor cocktail (Thermo Scientific, Rockford, IL), stirred on ice for 10 min and sonicated for 15 min. The mixtures were then centrifuged at 14000 rpm at 4°C for 15 min. The supernatants were collected and protein concentration was quantified using a Coomassie Plus Bradford Assay kit (Thermo Scientific, Rockford, IL) according to the manufacturers' instructions.

Western blotting was performed by SDS-PAGE with 50 µg of protein lysate loaded per lane of 4-20% gradient gels followed by transfer to PVDF membranes (Millipore, Billerica, MA). The membrane was first incubated in 5% dry milk, 1% bovine serum albumin (BSA) diluted in HBSS for 1 h at room temperature. The membrane was then washed twice for 10 min each in "wash 1" (0.1% Tween-20, 0.1% dry milk, 0.1% BSA in HBSS). The membrane was then incubated with rabbit anti-HIF-1α antibody (1 : 1000) (Santa Cruz Biotechnology, Santa Cruz, CA), rabbit anti-osteonectin/SPARC antibody (1 : 1000), anti-osteopontin (OPN) (1: 1000) or rabbit anti-β-actin antibody (1 : 1000) (Santa Cruz Biotechnology, Santa Cruz, CA) for 2 h at room temperature (RT). The membrane was then washed three times for 10 min each in "wash 1". Membranes were then incubated with peroxidase-conjugated, goat, anti-rabbit IgG (1 : 5000) (Rockland Immunochemicals, Gilbertsville, PA) for 2 h at RT. Membranes were then washed 3 times for 10 minutes each in "wash 2" (0.1% Tween-20 in HBSS). Protein

detection was achieved by 5 min incubation in a chemiluminescence reagent, SuperSignal West Pico Substrate (Thermo Scientific, Rockford, IL). Bands were then detected using ChemiDoc™ XRS$^+$ System with Image Lab™ image acquisition and analysis software (Bio-Rad, Hercules. CA). With densitometry analysis, the expression of proteins was normalized to β-actin and multiplied by 100 to generate a % IOD (intensity optical density) fold difference of protein expression. All incubation steps and washes were performed on an orbital shaker set to continuous rotation at 100 rpm. The statistics shown represent results obtained from three independent studies.

4.2.9 VEGF release

VEGF release was monitored in 2-D and 3-D samples with and without the HIF-1 inhibitor over 28 days. The supernatant was collected on Days 1, 4, 7 and 28 and VEGF levels were determined using a colorimetric VEGF ELISA kit according to manufacturer's instructions (Invitrogen, USA). The absorbance was measured at 450 nm and VEGF standards are used to calculate a VEGF concentration. These values are multiplied by the volume used during the release studies, normalized relative to the viable cell number and expressed as (fg/cell). The data represent three independent studies and release over a 24 hour period for all time points.

4.2.10 Viability of ASCs

A Live/Dead® staining kit (Invitrogen, USA) was used to test the viability of the samples over 28 days. Fluorescent dyes indicate esterase activity (observed as green signal in live cells) or loss of nuclear membrane integrity (observed as red signal in

dead cells). The 2-D and 3-D samples were kept in culture conditions identical to the previous experiments and the staining was performed in accordance with the manufacturer's guidelines. Results are given as a percentage of viable cells based on analysis of three independent studies.

4.2.11 Statistical analysis

Statistical analysis was performed using Graphpad Prism 4.01 (GraphPad Software Inc., San Diego, CA). Experimental results were expressed as the mean ± standard deviation. All the collected data were analyzed by two-way ANOVA for comparisons and p-values < 0.05 were defined as statistically significant differences.

4.3 RESULTS

4.3.1 ALP Activity

In 2-D, the ALP activity at 20% O_2 without the HIF inhibitor was 9.15± 0.93, 22.11± 3.14, 32.01±3.14 and 33.98± 2.34 µmol/ml/min/mg DNA on days 7, 14, 21 and 28 respectively. With the HIF inhibitor, the ALP levels were 8.43±2.76, 20.21±2.47, 28.73±2.31 and 31.79±3.12 µmol/ml/min/mg DNA on days 7, 14, 21 and 28 respectively. At 2% O_2, the ALP levels without the inhibitor were 9.42±0.72, 20.35±3.31, 21.82±3.32 and 23.21±1.68 µmol/ml/min/mg DNA on days 7, 14, 21 and 28 respectively. With the inhibitor, the ALP levels were 6.45±1.43, 18.75±2.36, 22.36±1.92 and 24.42±2.67 µmol/ml/min/mg DNA on days 7, 14, 21 and 28 respectively. At 1% O_2, ALP levels without the inhibitor were 8.11±0.91, 19.43±1.87, 23.13±1.21 and 23.89±1.62 µmol/ml/min/mg DNA on days 7, 14, 21 and 28 respectively. With the HIF inhibitor, the

ALP levels were 10.1±1.32, 16.23±2.42, 19.87±1.91 and 21.42±2.63 µmol/ml/min/mg DNA. These results are shown in Figure 4.1a.

In 3-D, ALP levels at 20% O_2 without the HIF inhibitor were 7.75±0.76, 19.11±1.34, 28.17±2.53 and 35.39±3.25 µmol/ml/min/mg DNA on days 7, 14, 21 and 28 respectively. With the inhibitor, the ALP levels were 8.91±1.65, 21.45±2.41, 27.81±3.11 and 38.21±3.22 µmol/ml/min/mg DNA on days 7, 14, 21 and 28 respectively. At 2% O_2, the ALP levels without the inhibitor were 7.51±0.75, 20.73±1.45, 23.26±3.62 and 24.32±2.33 µmol/ml/min/mg DNA on days 7, 14, 21 and 28 respectively. With the inhibitor, the ALP levels were 8.13±1.23, 17.53±2.62, 22.81±2.14 and 22.87±4.54 µmol/ml/min/mg DNA on days 7, 14, 21 and 28 respectively. At 1% O_2, the ALP levels without the inhibitor were 6.22±0.87, 16.95±1.52, 23.42±1.89 and 23.84±1.28 µmol/ml/min/mg DNA on days 7, 14, 21 and 28 respectively. With the inhibitor, the ALP levels were 9.65±1.54, 17.57±2.34, 21.42±3.73 and 22.13±2.51 µmol/ml/min/mg DNA on days 7, 14, 21 and 28 respectively. These results are shown in Figure 4.1b.

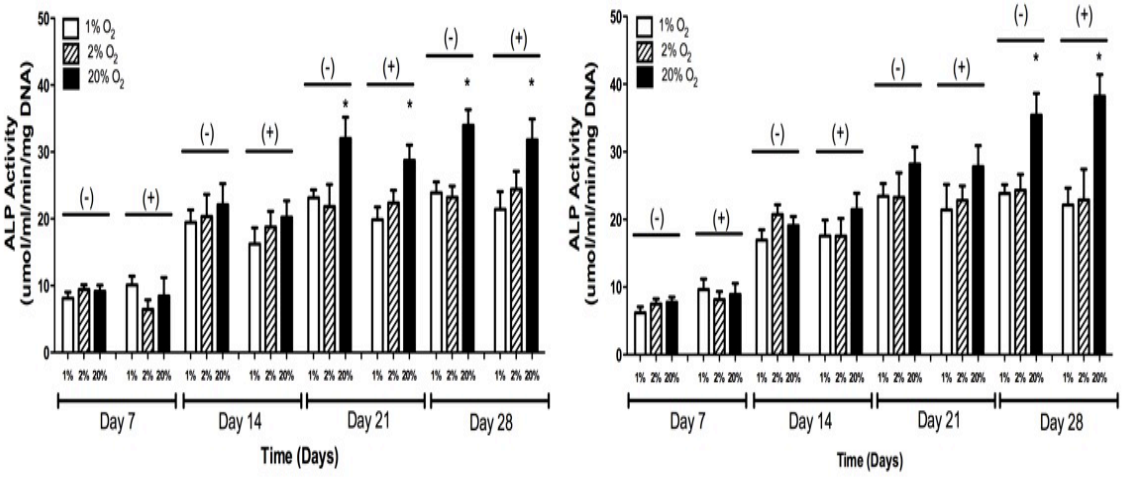

Figure 4.1: ALP activity of ASCs at 1%, 2% and 20% oxygen with and without the HIF-1 inhibitor in (A) 2-D and (B) 3-D culture conditions over a period of four weeks. The values have been normalized by total DNA and represent the mean±standard deviations.

4.3.2 Mineralization

In 2-D, at 20% O_2 and without the inhibitor, mineral deposition was observed to be 33.04±1.61 and 55.28±3.66 mg mineral/mg DNA on days 14 and 28 respectively. With the inhibitor, the mineral deposition levels were 31.13±1.52 and 54.21±3.54 mg mineral/mg DNA on days 14 and 28 respectively. At 2% O_2, the mineral deposition levels without the inhibitor were 11.34±1.34 and 34.87±2.76 mg mineral/mg DNA on days 14 and 28 respectively. With the HIF inhibitor, the mineral deposition levels were 9.83±3.16 and 32.45±2.710 mg mineral/mg DNA on days 14 and 28 respectively. At 1% O_2, the mineral deposition levels without the inhibitor were 8.85±0.63 and 32.04±2.04 mg mineral/mg DNA on days 14 and 28 respectively. Without the inhibitor, the mineral deposition levels were 12.26±2.17 and 31.52±2.64 mg mineral/mg DNA on days 14 and 28 respectively. These results are shown in Figure 4.2a.

In 3-D samples, at 20% O_2 and without the inhibitor, mineral deposition was observed to be 32.07±2.86 and 68.55±3.19 mg mineral/mg DNA on days 14 and 28. With the inhibitor the mineral deposition levels were 35.15±3.23 and 65.42±4.16 mg mineral/mg DNA on days 14 and 28 respectively. At 2% O_2, mineral deposition levels without the inhibitor were 28.56±3.72 and 54.23±4.28 mg mineral/mg DNA on days 14 and 28 respectively. With the inhibitor, the mineral deposition levels were 30.24±2.23 and 51.92±3.54 mg mineral/mg DNA on days 14 and 28 respectively. At 1% O_2, mineral deposition levels without the inhibitor were 33.04±1.52 and 51.77±1.36 mg mineral/mg DNA on days 14 and 28. With the inhibitor, the mineral deposition levels were 35.71±1.72 and 48.98±3.41 mg mineral/mg DNA on days 14 and 28 respectively. These results are shown in Figure 4.2b.

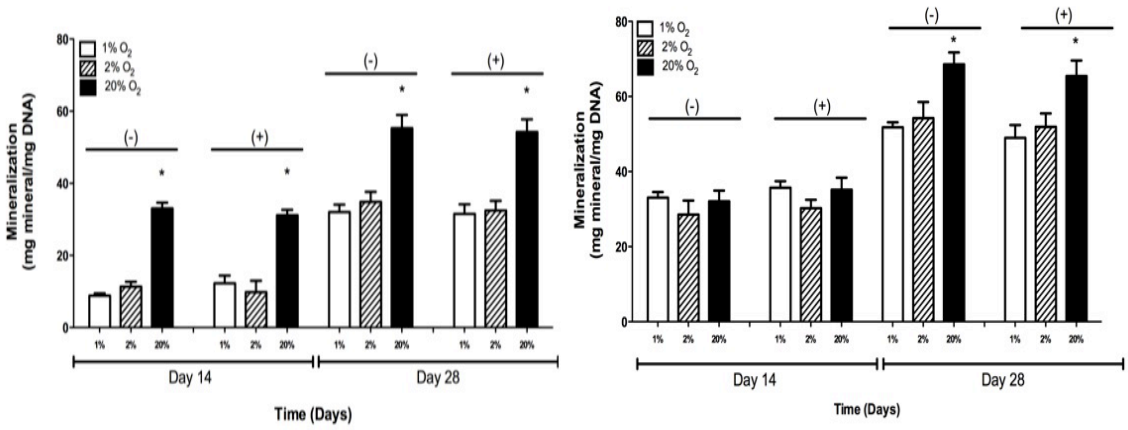

Figure 4.2: Quantification of Alizarin red staining of ASCs cultured in 1%, 2% and 20% oxygen with and without the HIF-1 inhibitor in (A) 2-D and (B) 3-D culture condition. The values have been normalized by total DNA and represent the mean± standard deviations. Statistically significant difference ($p<0.05$) is marked by (*) indicating higher absorbance at 20% oxygen in comparison to 1% and 2% oxygen.

4.3.3 HIF-1α protein expression

No HIF-1α protein was observed in 2-D studies when the inhibitor was present. In the absence of the inhibitor, no HIF-1α was observed at 20% oxygen. In the absence of the inhibitor, HIF-1α expression of 6.31±2.03 and 6.63±2.32 %IOD fold difference was observed in 2% and 1% oxygen environments respectively. A representative image of a gel and the collective results are shown in Figure 4.3 (A & B).

No HIF-1α protein was observed in 3-D studies when the inhibitor was present. In the absence of the inhibitor, HIF-1α expression of 1.14±0.34, 5.12±1.63 and 6.47±1.91 %IOD fold difference was observed in 20%, 2% and 1% oxygen environments respectively. A representative image of a gel and the collective results are shown in Figure 4.4 (A & B).

4.3.4 OPN protein expression

For 2-D studies in the absence of the inhibitor, OPN expression of 6.38±0.73, 1.82±0.72 and 1.92±0.61 %IOD fold difference was observed in 20%, 2% and 1% oxygen environments respectively. When the inhibitor was present, OPN expression of 7.21±1.37, 1.71±0.57 and 2.15±0.43 %IOD fold difference was observed in 20%, 2% and 1% oxygen environments respectively. A representative image of a gel and the collective results are shown in Figure 4.3 (A & C).

For 3-D studies in the absence of the inhibitor, OPN expression of 8.16±1.12, 2.15±0.83 and 1.79±0.82 %IOD fold difference was observed in 20%, 2% and 1% oxygen environments respectively. When the inhibitor was present, OPN expression of 9.34±0.54, 1.43±0.61 and 1.23±0.25 %IOD fold difference was observed in 20%, 2% and 1% oxygen environments respectively. A representative image of a gel and the collective results are shown in Figure 4.4 (A & C).

4.3.5 ON protein expression

For 2-D studies in the absence of the inhibitor, ON expression of 5.97±0.81, 2.13±1.01 and 3.23±1.27 %IOD fold difference was observed in 20%, 2% and 1% oxygen environments respectively. When the inhibitor was present, ON expression of 5.41±1.13, 2.67±1.34 and 2.93±1.09 %IOD fold difference was observed in 20%, 2% and 1% oxygen environments respectively. A representative image of a gel and the collective results are shown in Figure 4.3 (A & D).

For 3-D studies in the absence of the inhibitor, ON expression of 6.88±0.34, 2.33±1.03 and 3.41±1.65 %IOD fold difference was observed in 20%, 2% and

1% oxygen environments respectively. When the inhibitor was present, ON expression of 7.21±0.87, 3.67±1.24 and 2.45±1.19 %IOD fold difference was observed in 20%, 2% and 1% oxygen environments respectively. A representative image of a gel and the collective results are shown in Figure 4.4 (A & D).

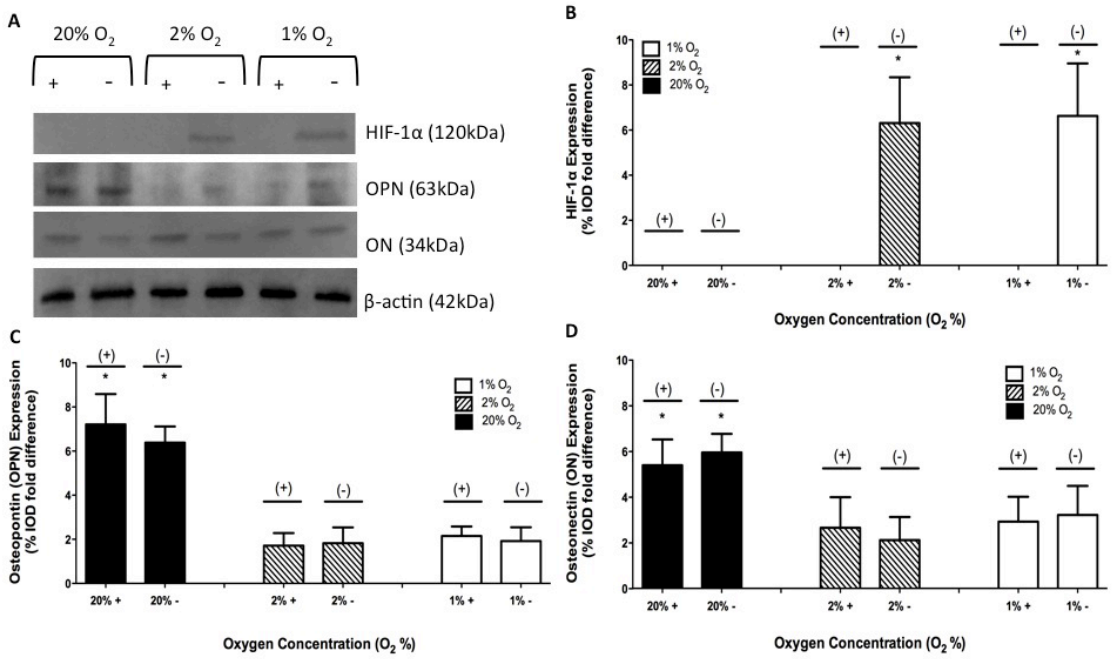

Figure 4.3: Protein expression of HIF-1α, Osteopontin (OPN) and Osteonectin (ON) on day 28 at 1%, 2% and 20% oxygen with and without the HIF-1 inhibitor in 2-D culture. A representative gel is shown in (A). Results of three independent studies are quantified in (B) HIF-1α, (C) OPN and (D) ON. The values have been normalized to β-actin and represent the mean±standard deviations. When a statistically significant difference ($p<0.05$) is observed between 20% oxygen in comparison to 1% and 2% oxygen it is marked (*).

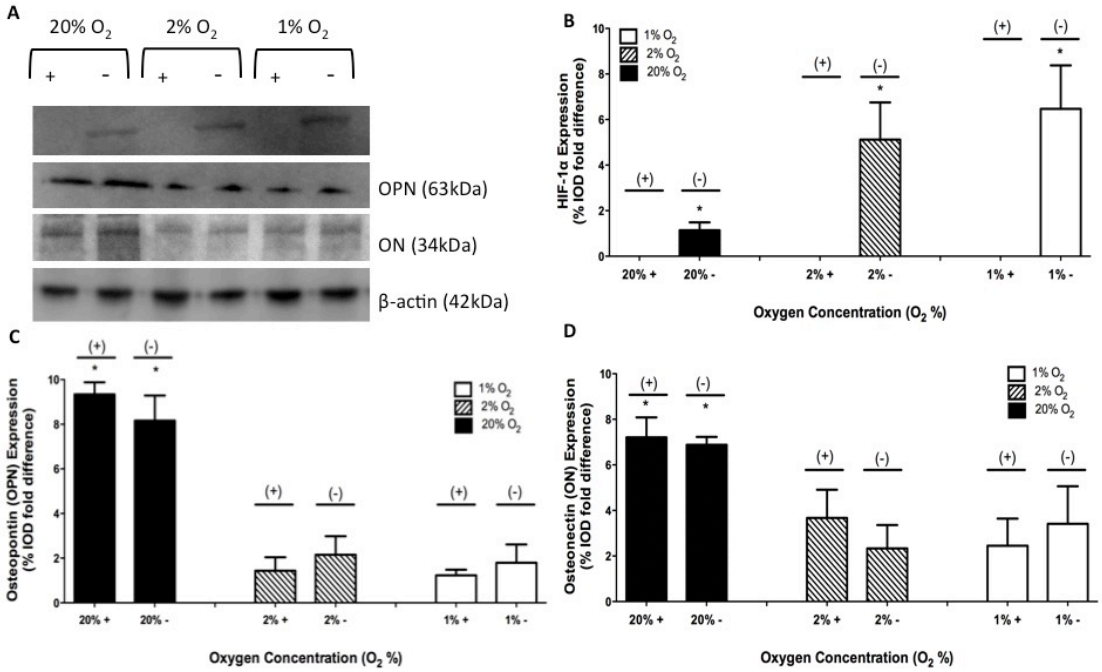

Figure 4.4: Protein expression of HIF-1α, Osteopontin (OPN) and Osteonectin (ON) on day 28 at 1%, 2% and 20% oxygen with and without the HIF-1 inhibitor in 3-D culture. A representative gel is shown in (A). Results of three independent studies are quantified in (B) HIF-1α, (C) OPN and (D) ON. The values have been normalized to β-actin and represent the mean±standard deviations. When a statistically significant difference ($p<0.05$) is observed between 20% oxygen in comparison to 1% and 2% oxygen it is marked (*).

4.3.6 VEGF release

For 2-D studies at 20% O_2 in the absence of the inhibitor, VEGF secretion was 1.52±0.21, 1.39±0.12, 1.63±0.16 and 1.78±0.23 fg/cell on days 1, 4, 7 and 28 respectively. With the HIF inhibitor, VEGF secretion was 1.81±0.55, 1.09±0.30, 1.61±0.25 and 2.08±0.15 fg/cell on days 1, 4, 7 and 28 respectively. At 2% O_2 in the absence of the inhibitor, VEGF secretion was 23.51±2.13, 15.07±1.29, 12.82±0.84 and 5.21±0.94 fg/cell on days 1, 4, 7 and 28 respectively. With the HIF inhibitor, VEGF secretion was 4.51±1.38, 1.77±0.28, 1.64±0.08 and 1.88±0.30 fg/cell on days 1, 4, 7 and 28 respectively. At 1% O_2 in the absence of the inhibitor, VEGF secretion was

31.26±1.24, 15.14±1.13, 12.55±0.92 and 7.57±0.48 fg/cell on days 1, 4, 7 and 28 respectively. With the HIF inhibitor, VEGF secretion was 5.78±0.82, 2.30±0.31, 2.48±0.47 and 1.67±0.25 fg/cell on days 1, 4, 7 and 28 respectively. The results are shown in Figure 4.5a.

For 3-D studies at 20% O_2 in the absence of the inhibitor, VEGF secretion was 0.80±0.33, 0.40±0.23, 0.41±0.10 and 0.51±0.22 fg/cell on days 1, 4, 7 and 28 respectively. With the HIF inhibitor, VEGF secretion was 1.2±0.18, 0.68±0.10, 0.60±0.08, and 0.54±0.12 fg/cell on days 1, 4, 7 and 28 respectively. At 2% O_2 in the absence of the inhibitor, VEGF secretion was 14.86±0.71, 6.91±0.46, 7.18±0.36 and 4.82±0.23 fg/cell on days 1, 4, 7 and 28 respectively. With the HIF inhibitor, VEGF secretion was 1.61±0.11, 0.74±0.065, 0.61±0.23 and 1.19±0.06 fg/cell on days 1, 4, 7 and 28 respectively. At 1% O_2 in the absence of the inhibitor, VEGF secretion was 15.43±0.41, 8.32±0.26, 7.00±0.41 and 4.42±0.28 fg/cell on days 1, 4, 7 and 28 respectively. With the HIF inhibitor, VEGF secretion was 1.80±0.15, 1.04±0.16, 0.71±0.08 and 1.13±0.20 fg/cell on days 1, 4, 7 and 28 respectively. The results are shown in Figure 4.5b

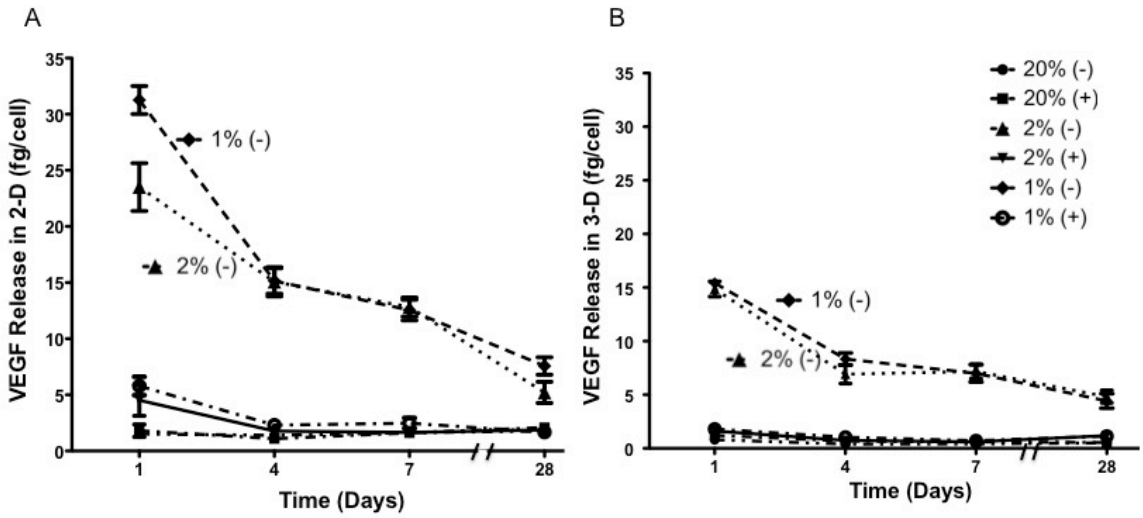

Figure 4.5: VEGF release of ASCs at 1%, 2% and 20% oxygen with and without the HIF-1 inhibitor in (A) 2-D and (B) 3-D culture conditions over a period of four weeks. The values have been normalized by viable cell number and represent the mean±standard deviation.

4.3.7 ASC viability

In 2-D, at 20% O_2 and without the inhibitor, the percent viability was 99±1%, 97±1%, 91±2%, 84±4% and 81±6% on days 1, 7, 14, 21, 28 respectively. With the HIF inhibitor, the percent viability was 99±1%, 98±1%, 93±2%, 85±6% and 78±4% on days 1, 7, 14, 21, 28 respectively. At 2% O_2, the percent viability without the inhibitor were 99±1%, 96±2%, 84±5%, 72±3% and 64±5% on days 1, 7, 14, 21, 28 respectively. With the inhibitor, the percent viability was 99±1%, 98±1%, 82±3%, 64±7% and 59±5% with the inhibitor on days 1, 7, 14, 21, 28 respectively. At 1% O_2, percent viability with the inhibitor was 99±1%, 96±2%, 84±3%, 69±4% and 66±4% on days 1, 7, 14, 21, 28 respectively. With the inhibitor, the percent viability was 99±1%, 98±1%, 85±7%, 73±5% and 61±7% on days 1, 7, 14, 21, 28 respectively. These results are shown in Figure 4.6a.

In 3-D culture, at 20% O_2 and without the inhibitor, percent viability was

99±1%, 94±4, 75±4%, 61±4% and 47±6% on days 1, 7, 14, 21, 28 respectively. With the HIF inhibitor, the percent viability was 99±1%, 89±6, 76±7%, 58±6% and 44±3% on days 1, 7, 14, 21, 28 respectively. At 2% O_2, percent viability without the inhibitor was 99±1%, 92±4%, 66±5%, 46±3% and 33±5% on days 1, 7, 14, 21, 28 respectively. With the inhibitor, the percent viability was 99±1%, 89±3%, 71±4%, 43±7% and 36±6% with the inhibitor on days 1, 7, 14, 21, 28 respectively. At 1% O_2, percent viability without the inhibitor was 99±1%, 88±5%, 63±6%, 42±3% and 29±5% on days 1, 7, 14, 21, 28 respectively. With the inhibitor, the percent viability was 99±1%, 92±3%, 55±4%, 38±6% and 27±3% on days 1, 7, 14, 21, 28 respectively. These results are shown in Figure 4.6b.

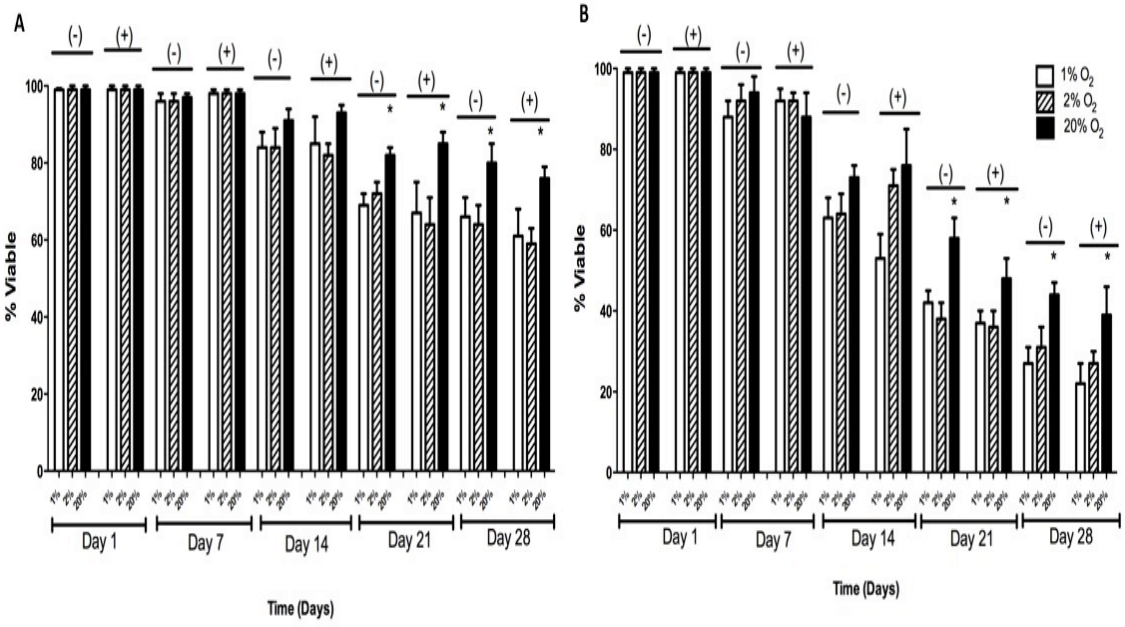

Figure 4.6: Viability of ASCs in 1%, 2% and 20% oxygen with and without the HIF-1 inhibitor in (A) 2-D and (B) 3-D culture conditions over a period of four weeks. The values shown represent the mean±standard deviations from three independent experiments. When a statistically significant difference ($p<0.05$) is observed between 20% oxygen in comparison to 1% and 2% oxygen it is marked (*) for both 2-D and 3-D studies.

4.4 DISCUSSION

Our results demonstrate a reduced capacity for ASCs to differentiate into osteoblasts in hypoxic conditions when compared with atmospheric conditions. ASCs in 1 and 2% oxygen environments displayed reduced ALP activity, mineralization and expression of ON and OPN in 2-D and 3-D culture geometries compared with ASCs in 20% oxygen environments. HIF-1 activity does not appear to be an essential component of the varied response of ASCs in hypoxic conditions. For all oxygen concentrations and in both 2-D and 3-D cultures, pharmacologically-induced inhibition of HIF-1α had no impact on any of these markers of osteogenesis.

Viability of ASCs dropped over the course of our differentiation experiment but our data are normalized to total DNA or β-actin to account for this. The viability decrease in 3-D was more pronounced than for 2-D cultures and this was probably a result of using an unmodified PEG gel. Previous work has shown that integrating integrin-binding sequences into the scaffold or genetic modification of cells can extend survival of MSCs in these materials by preventing anoikis [Benoit 2007]. We utilized a blank PEG gel to remove the impact of peptide modification on osteogenic differentiation but future studies could evaluate peptide-modified PEG gels in combination with varied oxygen concentration.

As mentioned earlier, the literature shows mixed results concerning the impact of hypoxic conditions on osteogenesis and healing of CSDs. Given the large number of variables in play, this is not surprising. Different research groups utilize a range of cell types and hypoxic conditions vary across the entire range from below 1% up to 5% oxygen. When 3-D studies are conducted, oxygen levels and the state of hypoxic

signaling can vary widely for cells depending on experimental conditions (size of scaffolds, scaffold material(s) and cell density within scaffolds for example). All of these factors make it difficult to draw definitive conclusions regarding the impact of hypoxia on bone formation that will hold regardless of cell type employed and oxygen concentration used.

Previous studies that have examined the role of HIF-1 through genetic engineering, have demonstrated how changes in experimental procedure can impact the results. Three factors stand out in addition to those mentioned above. First, the role of HIF-1 may be impacted by whether the studies are investigating intramembranous or endochondral bone formation. Our studies are an *in vitro* model of intramembranous bone formation as mesenchymal stem cells are directly differentiated into osteoblasts. Our results are in agreement with a previous study that showed no impact on HIF-1α deletion on osteogenic differentiation of ASCs [Malladi 2007]. Mice lacking HIF-1α showed impaired formation of long bones (endochondral) but no impact on bone formation in the skull (intramembranous) [Wan 2008]. HIF-1 activity has been linked to chondrogenesis so whether this step is necessary could explain the varied results [Schipani 2005, Pfander 2007].

Second, HIF-1 activity has also been shown to impact angiogenesis [Tower 2008, Schipani 2009]. Our *in vitro* work included studies to look at VEGF release, which correlated with the oxygen concentrations. Inhibition of HIF-1 also inhibited the release profile of VEGF. Release of VEGF at 1 and 2% oxygen was significantly higher than at 20% or when the inhibitor was used for all time points ($p<0.01$). Our studies are in agreement with previous studies that have shown that VEGF

is HIF-1 regulated [Ferrara 2001, Dai 2007, Brahimi-Horn 2005, Schipani 2009, Tang 2004, Carroll 2006, Yamazaki 2003]. Our *in vitro* analysis does not include studies looking at the role of HIF-1 in vascularizing bone but this is a critical process that would need to occur *in vivo*. Blocking vascular growth and maturation will lead to formation of thin, weak bone and this has been demonstrated by previous studies [Wan 2008, Zou 2011]. Bone formation *in vivo* requires a coupling of osteogenesis and angiogenesis, making it difficult to evaluate the impact of HIF-1 on each process individually.

Finally, the timing of hypoxic exposure to cells plays a role in this process. A recent study showed the impact of conditioning human MSCs in 2% oxygen prior to osteogenic differentiation in such an environment [Volkmer 2010]. The inhibitory effect of low oxygen on osteogenic differentiation (relative to culture in 20% oxygen) was mitigated when the cells were conditioned to this environment prior to differentiation.

Our results indicate that low oxygen culture reduces osteogenic differentiation of ASCs compared with atmospheric conditions in a HIF-1 independent manner. However, differentiation will never occur in atmospheric conditions if this event is to take place *in vivo*. Efforts to accelerate bone formation at CSD sites could potentially look at HIF-1 as a therapeutic target but for modification of processes other than osteogenic differentiation of ASCs. There are numerous strategies to track HIF-1 activity at the cellular level [Zhou 2011, Sahai 2012]. These systems show how the cells respond to their local oxygen environment and can guide future work that targets HIF-1. In general, HIF-1 activity should be beneficial for repair of CSDs but this effect is not necessarily observed for all processes involved in bone formation.

CHAPTER 5

VARIED ISCHEMIC PRECONDITIONING PROTOCOLS TO ENHANCE ENGRAFTMENT AND DIFFERENTIATION OF ADIPOSE-DERIVED STEM CELLS

5.1 INTRODUCTION

Stem cell therapy is one of the most promising techniques to treat a defect in an organ. Massive cell death occurs after transplantation which significantly lowers the efficiency and efficacy of the therapy [Martin 1998, Sortwell 2000, Manoonkitiwongsa 2001, Thum 2005]. Hence it is imperative to reinforce the donor cells to withstand the rigors of the microenvironment of the injury site from ischemia, inflammatory response, and pro-apoptotic factors in order to develop cell therapy into an effective therapeutic modality.

Several anti-death strategies have been explored to promote the survival of transplanted cells. These strategies include continous infusion of neurotrophic factors, genetic manipulation by overexpressing anti-apoptotic and growth factor genes, and knocking down pro-apoptotic genes [Zawada 1998, Park 2003, Wei 2005]. However, there are multiple limitations with each of these current approaches, including safety issues associated with permanent gene alterations, and in addition to being clinically unfeasible. Ischemic preconditioning (IPC) which is a transient phenomenon induced by brief episodes of sublethal hypoxia that activates endogeneous trophic signals, has been suggested as a strategy to improve ischemic tolerance [Samoilov 2003, Sharp 2004].

The beneficial effects of IPC have been most widely studied in cardiac tissue with the first demonstration over 25 years ago [Murry 1986]. Its application was further tested on cells transplanted into ischemic limb and ischemic brain [Akita 2003, Rosova 2008, Theus 2008]. IPC alters gene expression and activates different intracellular signaling pathways in a time dependent manner. These findings have also been correlated with improved functional recovery of the ischemic tissues.

In the previous chapter we observed that the osteogenic differentiation of ASCs is impaired in hypoxic environments and how to accelerate the process will address a critical barrier in the field. An important recent study showed that MSCs cultured in 2% oxygen showed superior, subsequent osteogenic differentiation in 2% oxygen [Volkmer 2010]. The central hypothesis is that IPC can be used to create ASCs more resistant to apoptosis and display increased osteogenic potential in physiological oxygen levels. Studies on cardiac tissue have shown two phases of protection resulting from IPC. The first occurs within minutes and lasts for a few hours. A second window apprears upto 24 hours later and lasts approximately 48 hours. This second protective window is thought to result from changes in gene expression possibly mediated by HIF-1 activity [Cai 2003, Hausenloy 2010]. Mechanistic evaluation of the cytoprotective effect of IPC suggests the expression of pAKT and the ratio of Bcl-2/Bax (anti-apoptotic/ pro-apoptotic) should be increased following IPC, and this will serve as our success criteria, and this will be one of our success criteria.

IPC protocols have not been closely studied or optimized. HIF-1α is an important transcription factor that may play a role in mediating its effect. In this study, we aim to test different IPC protocols wherein we place the ASCs at specific higher

(Step-down IPC) or lower oxygen concentrations (Step-down IPC) in-vitro as compared the levels present at the transplantation site, which would stimulate expression of proteins that would prevent hypoxia and cytokine-induced apoptosis at the tissue injury site. The IPC protocol can then be optimized on the basis of time duration, oxygen concentration and HIF-1α levels for the use of hypoxia as a stimulus based on the levels of pro-apoptotic and anti-apoptotic proteins released. The success criteria of our IPC protocols will be based on the expression levels of pAKT (atleast 10 fold higher expression over control) and ratio of Bcl-2/Bax (atleast 3-fold over control). The time point that will meet our success criteria will be used to precondition the ASCs to examine its effects on osteogenic differentiation.

The experiments are designed in way to give us insights on do oxygen concentration and duration affect HIF-1α stability and expression of genes regulating apoptosis, and the impact of IPC IPC on stemness of ASCs and osteogenic differentiation.

5.2 Materials and Methods

5.2.1 Cell culture

Human ASCs were purchased from Invitrogen and cell culture was performed according to the supplier's specifications. Cells were cultured in proprietary MesenPRO RSTM basal medium supplemented with MesenPRO RSTM Growth Supplement, 1% penicillin/streptomycin (Mediatech, Manassas, VA) and 2 mM L-glutamine (MP Biomedicals, Irvine, CA, USA). Culture conditions for passaging were

maintained at 95% air and 5% CO2 at 37°C. For experiments, cells between passages 2 and 4 were used as recommended by the supplier.

5.2.2. HIF-1 inhibition

To inhibit the activity of HIF-1, a HIF-1 inhibitor [3-(2-(4-Adamantan-1-yl-phenoxy)-acetylamino)-4-hydroxybenzoic acid methyl ester)] (Calbiochem, USA) was used. It is a cell-permeable amidophenolic compound that inhibits hypoxia-induced HIF-1 transcription activity. The inhibitor selectively blocks the hypoxia-induced accumulation of cellular HIF-1α protein, while exhibiting no apparent effect on the cellular level of HIF-1α mRNA or that of HIF-1β protein. For both 1% and 2% O_2 samples, a concentration of 60μM of this inhibitor was sufficient to reduce accumulation of HIF-1α to levels below detection in western blotting. Toxicity tests showed no loss of viability of ASCs exposed to the inhibitor at concentrations up to 100μM [Sahai 2013].

5.2.3 Ischemic Preconditioning

Nitrogen-purged, programmable incubators were used to maintain a constant 1%, 2% and 4% oxygen level for hypoxic studies (Napco Series 8000 WJ, Thermo Electron). Cells are seeded into a 6-well plate (5,000 cells/cm^2) and placed in atmospheric oxygen levels for 12 hours to allow attachment. After this period, the plates are moved to 1, 2 or 4% oxygen environments for ischemic exposure or left in atmospheric conditions. Every 24 hours, a new set of plates is moved from atmospheric conditions to ischemic conditions. This continues until 108 hours after plating and creates conditions where cells are exposed to 1, 2 or 4% oxygen between 24 and 96 hours. All

media, buffered salt solutions, and fixatives to be used with cells were kept in vented tubes in the hypoxic incubator for 24 hours prior to use so as to equilibrate the solutions to the appropriate dissolved oxygen concentration. Previous studies in our lab have shown this period to be sufficient to equilibrate the dissolved oxygen concentration [Skiles 2011]. Media changes and imaging procedures were kept under 10 mins per day to limit exposure to atmospheric conditions. Dissolved oxygen concentration studies conducted in our lab showed that levels rose from 0.3 mg/L to 0.4 mg/L during a 10 minute exposure (which correlates to a 1% oxygen to 1.5% oxygen environment). The oxygen levels are reestablished within 10 minutes of return to the incubator.

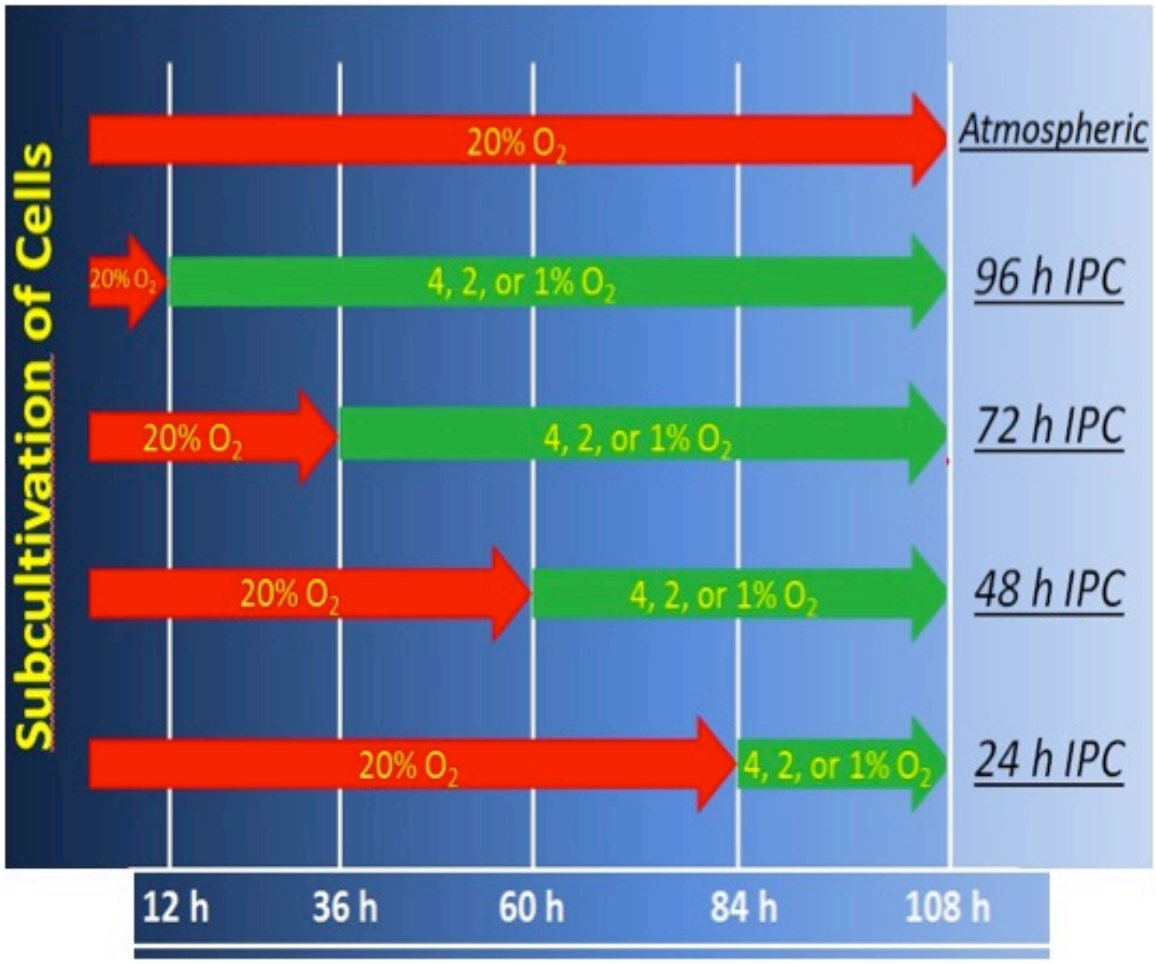

Figure 5.1: Overview of Ischemic Preconditioning (IPC)

5.2.4 Analysis of ASCs Stemness and Apoptosis by Flow Cytometry

To assess stemness of ASCs, cells were trypsinized and washed using a wash buffer. Cells are counted using a hemocytometer and 200,000 cells are added to each polystyrene flow cytometry tubes on ice. Cells were analyzed by staining with FITC conjugated CD44, PE conjugated CD105 and a combination of both. Both antibodies were purchased from BD Biosciences (San Diego, CA, USA). To assess apoptosis of ASCs, DeadEnd^{TM} Fluorometric TUNEL System was used according to the manufacturer's instructions (Promega, USA). Labeled cells were analyzed by Beckman Coulter- Cytomics FC 500 and CXP Analysis software.

5.2.5 Protein extraction and western blotting for pAkt, Bcl-2, Bax, Caspase-3, HIF-1α, ON, OPN

Total cell lysates were collected from samples with RIPA lysis buffer (Thermo Scientific, Rockford, IL) containing a protease and phosphatase inhibitor cocktail (Thermo Scientific, Rockford, IL), stirred on ice for 10 min and sonicated for 15 min. The mixtures were then centrifuged at 14000 rpm at 4°C for 15 min. The supernatants were collected and protein concentration was quantified using a Coomassie Plus Bradford Assay kit (Thermo Scientific, Rockford, IL) according to the manufacturers' instructions.

Western blotting was performed by SDS-PAGE with 50 µg of protein lysate loaded per lane of 4-20% gradient gels followed by transfer to PVDF membranes (Millipore, Billerica, MA). The membrane was first incubated in 5% dry milk, 1% bovine serum albumin (BSA) diluted in HBSS for 1 h at room temperature. The membrane was

then washed twice for 10 min each in "wash 1" (0.1% Tween-20, 0.1% dry milk, 0.1% BSA in HBSS). The membrane was then incubated with rabbit anti-HIF-1α antibody (1 : 1000) (Santa Cruz Biotechnology, Santa Cruz, CA), rabbit anti-bcl-2 antibody (1 : 1000), rabbit anti-pAkt (1 : 1000), rabbit anti-bax (1:1000), rabbit anti-active caspase-3 (1:1000), rabbit anti-osteonectin/SPARC antibody (1 : 1000), anti-osteopontin (OPN) (1: 1000) or rabbit anti-b-actin antibody (1 : 1000) (Santa Cruz Biotechnology, Santa Cruz, CA) for 2 h at room temperature (RT). The membrane was then washed three times for 10 min each in "wash 1". Membranes were then incubated with peroxidase-conjugated, goat, anti-rabbit IgG (1 : 5000) (Rockland Immunochemicals, Gilbertsville, PA) for 2 h at RT. Membranes were then washed 3 times for 10 minutes each in "wash 2" (0.1% Tween-20 in HBSS). Protein detection was achieved by 5 min incubation in a chemiluminescence reagent, SuperSignal West Pico Substrate (Thermo Scientific, Rockford, IL). Bands were then detected using ChemiDoc™ XRS+ System with Image Lab™ image acquisition and analysis software (Bio-Rad, Hercules. CA). With densitometry analysis, the expression of proteins was normalized to β-actin to account for % IOD (intensity optical density) and expressed as fold difference of protein expression compared to 20% oxygen. All incubation steps and washes were performed on an orbital shaker set to continuous rotation at 100 rpm. The statistics shown represent results obtained from three independent studies.

5.2.6 Osteogenic differentiation

Osteogenic differentiation was induced by culture in StemPro® Osteocyte/Chondrocyte Differentiation Basal Medium and StemPro® Osteogenesis

Supplement (Invitrogen, USA). The cells were monitored over a period of 28 days at 2% O_2 with the osteogenic medium replenished every 3 days. All preconditioned cells and one set of cells cultured in 20% oxygen will be differentiated in 2% oxygen.

5.2.7 Alkaline phosphatase (ALP) activity and DNA quantification

Measurements of ALP activity in the media of ASCs were taken on days 7, 14, 21 and 28. The activity was determined using an ALP colorimetric assay kit (Abcam, USA) with p-nitrophenyl phosphate as substrate. The ALP activities were normalized to the cellular DNA content using a PicoGreen dsDNA quantitation kit (Molecular Probes, USA) according to the manufacturer's instructions. Alkaline phosphatase activity is quantified on days 7, 14, 21 and 28 and is expressed in μmol/ml/min/mg DNA. The values included represent the mean of 3 independent studies.

5.2.8 Alizarin Red staining for mineralization

Mineral deposition was quantified on days 14 and 28 using the Alizarin Red S staining procedure. The cells were rinsed with calcium and phosphate-free HBSS, and fixed with ice-cold 70% ethanol for 1 h. After a brief wash with HBSS, the cells were stained for 20 min with 40mM Alizarin Red solution (pH 4.2) at room temperature. The cells were rinsed two times for 15 min with HBSS (on an orbital shaker) to reduce nonspecific Alizarin Red staining. A 10% acetic acid was then added to the samples for 30 min on a shaker. Samples were collected by scraping and heated at 80°C for 10 min. The extracts are then centrifuged at 8000 rpm for 20 min and quantified spectrophotometrically with a microplate reader (Biotek, USA) at 570 nm. The calcium

concentration was calculated from the standard curve generated from a serial dilution of a calcium standard solution and the values were normalized to DNA contents (expressed in mg mineral/mg DNA). Values included represent the mean of three independent studies.

5.2.9 Statistical analysis

Statistical analysis was performed using Graphpad Prism 4.01 (GraphPad Software Inc., San Diego, CA). Experimental results were expressed as the mean ± standard deviation. All the collected data were analyzed by two-way ANOVA for comparisons and p-values < 0.05 were defined as statistically significant differences.

5.3 RESULTS

5.3.1 Stemness Markers

As shown in Figure 5.2, the percentages of ASC population after preconditioning for 96 hours in 1%, 2%, 4% and 20% O_2 were 99.5±0.05 %, 99% ±1%, 98.8%±1% and 99% ±0.8%, respectively.

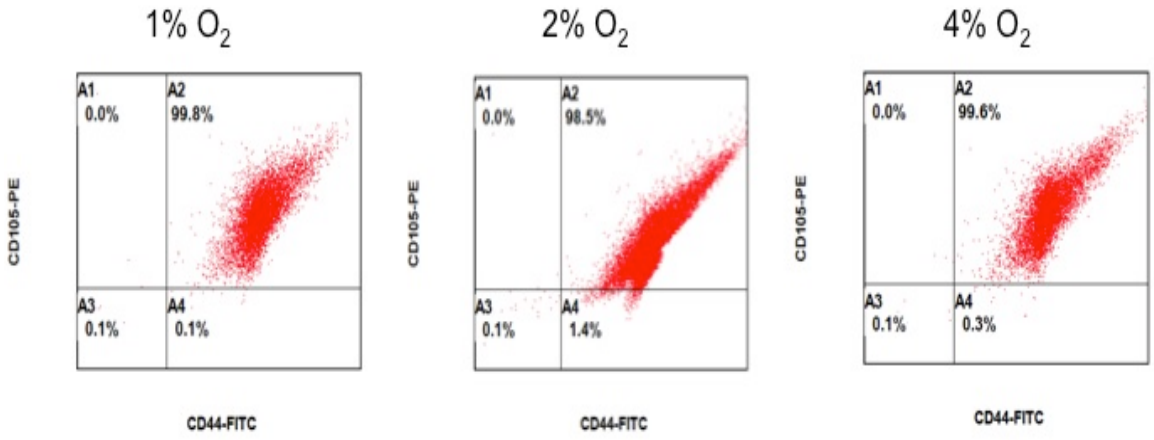

Figure 5.2: Stemness markers after 96 hrs IPC at 1%, 2% and 4% oxygen environment.

5.3.2 pAkt Expression

In the absence of HIF-1 inhibitor, At 1% oxygen condition, the pAkt expression was 7.61±0.43, 8.52±0.61, 12.16±0.56 and 14.13±0.71 %IOD fold difference against the samples in 20% oxygen at 24, 48, 72 and 96 hours respectively. In 2% oxygen condition, pAkt expression was 6.82±0.32, 10.24.52±0.73, 12.37±0.36 and 12.56±0.66 %IOD fold difference against the samples in 20% oxygen at 24, 48, 72 and 96 hours respectively. In 4% oxygen condition, pAkt expression was 2.31±0.21, 4.61±1.21, 5.62±1.43 and 7.42±0.97 %IOD fold difference against the samples in 20% oxygen at 24, 48, 72 and 96 hours respectively. A representative image of a gel and the collective results are shown in Figure 5.3.

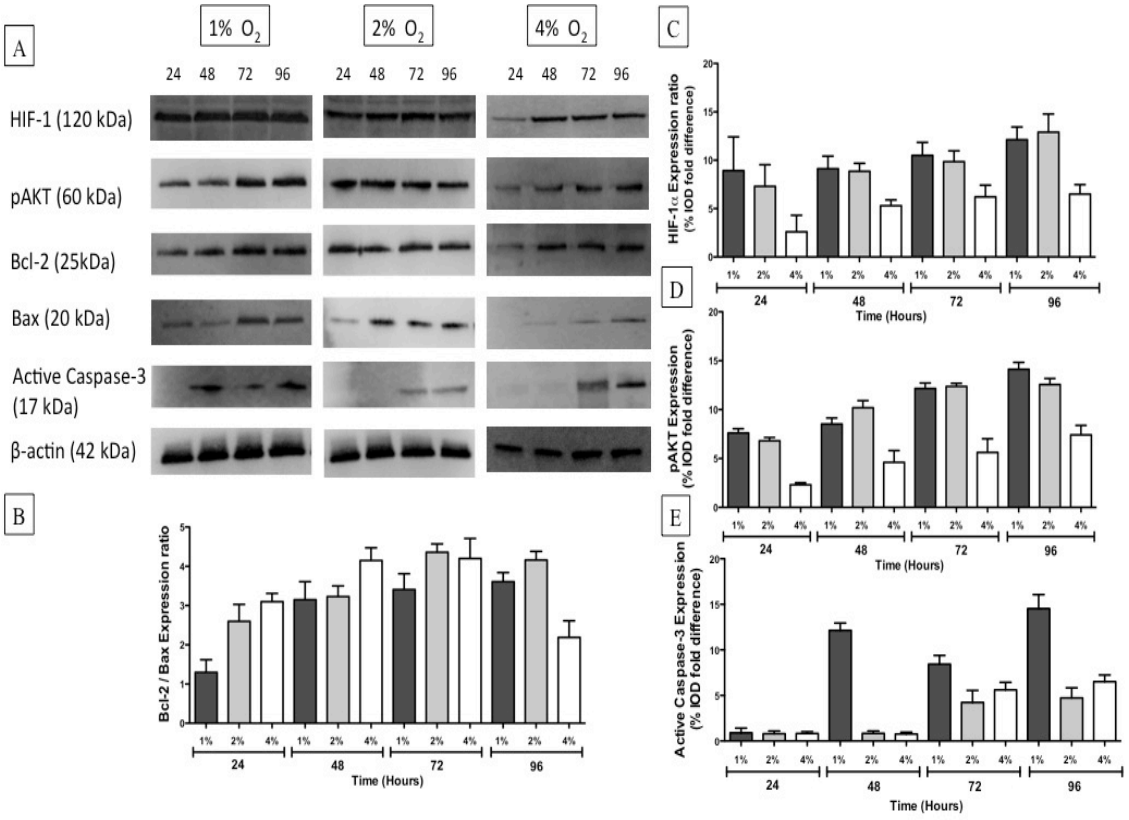

Figure 5.3: Apoptotic Markers in the absence of HIF-1 inhibitor.

In the presence of HIF-1 inhibitor, At 1% oxygen condition, the pAkt expression was 5.73±0.78, 8.34±0.76, 10.83±0.34 and 11.23±1.31 %IOD fold difference against the samples in 20% oxygen at 24, 48, 72 and 96 hours respectively. In 2% oxygen condition, pAkt expression was 6.24±0.41, 9.15±1.04, 10.13±0.51 and 11.51±1.27 %IOD fold difference against the samples in 20% oxygen at 24, 48, 72 and 96 hours respectively. In 4% oxygen condition, pAkt expression was 1.72±0.35, 2.21±0.73, 6.04±0.59 and 8.28±1.14 %IOD fold difference against the samples in 20% oxygen at 24, 48, 72 and 96 hours respectively. A representative image of a gel and the collective results are shown in Figure 5.4.

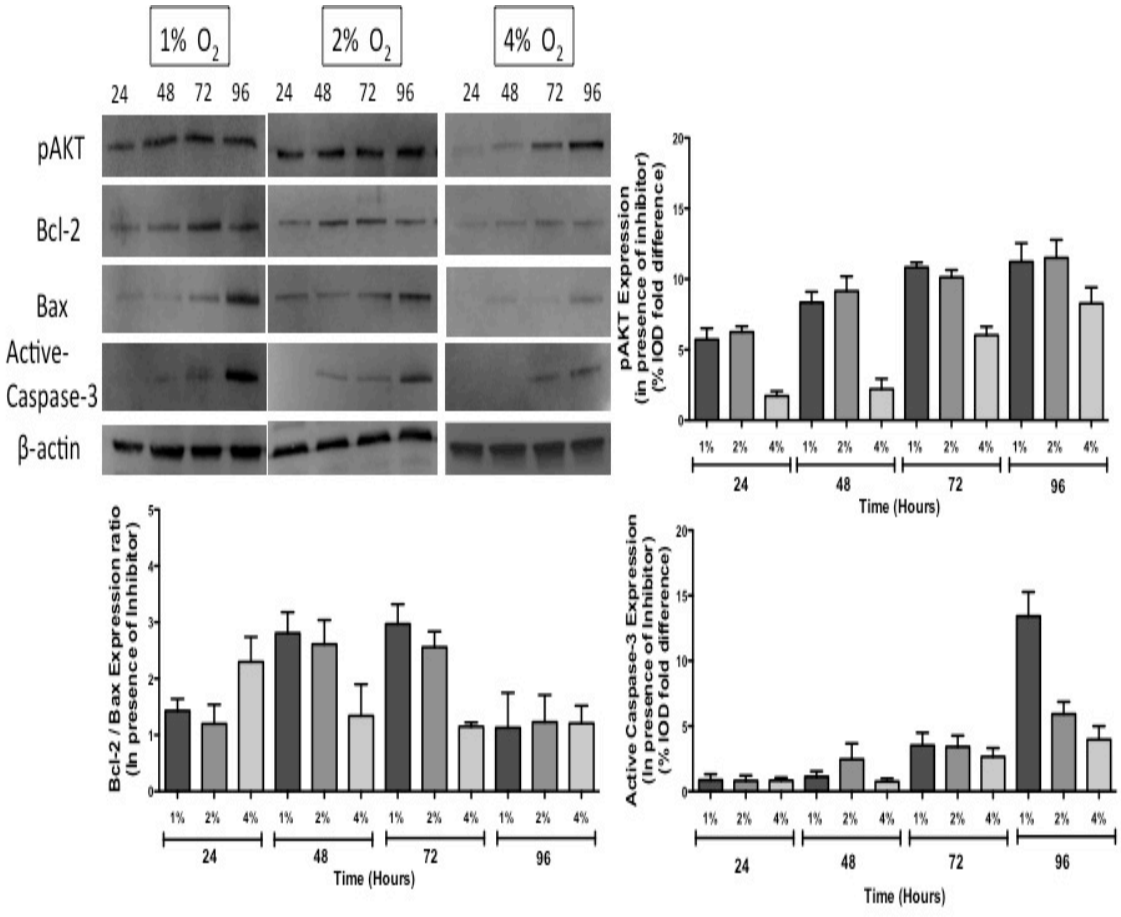

Figure 5.4: Apoptotic Markers in the presence of HIF-1 inhibitor.

5.3.3 Active Caspase-3 Expression

In the absence of the HIF inhibitor, At 1% oxygen condition, the active caspase-3 expression was 0.91±0.52, 12.14±0.81, 8.43±0.96 and 14.54±1.53 %IOD fold difference against the samples in 20% oxygen at 24, 48, 72 and 96 hours respectively. In 2% oxygen condition, active caspase-3 expression was 0.83±0.31, 0.85±0.24, 4.23±1.32 and 4.73±1.12 %IOD fold difference against the samples in 20% oxygen at 24, 48, 72 and 96 hours respectively. In 4% oxygen condition, active caspase-3 expression was 0.84±0.22, 0.76±0.21, 5.61±0.84 and 6.51±0.73 %IOD fold difference against the samples in 20% oxygen at 24, 48, 72 and 96 hours respectively. A representative image of a gel and the collective results are shown in Figure 5.3.

In the presence of the HIF inhibitor, At 1% oxygen condition, the active caspase-3 expression was 0.87±0.44, 1.12±0.43, 3.53±1.06 and 13.42±1.86 %IOD fold difference against the samples in 20% oxygen at 24, 48, 72 and 96 hours respectively. In 2% oxygen condition, active caspase-3 expression was 0.81±0.42, 2.46±1.30, 3.41±0.86 and 5.92±0.94 %IOD fold difference against the samples in 20% oxygen at 24, 48, 72 and 96 hours respectively. In 4% oxygen condition, active caspase-3 expression was 0.83±0.23, 0.77±0.15, 2.65±0.67 and 3.97±1.02 %IOD fold difference against the samples in 20% oxygen at 24, 48, 72 and 96 hours respectively. A representative image of a gel and the collective results are shown in Figure 5.4.

5.3.4 Bcl-2/Bax ratio expression

In the absence of the HIF inhibitor, At 1% oxygen condition, the Bcl-2/Bax ratio expression was 1.34±0.31, 3.15±0.36, 3.41±0.46 and 3.53±0.23 %IOD fold

difference against the samples in 20% oxygen at 24, 48, 72 and 96 hours respectively. In 2% oxygen condition, the Bcl-2/Bax ratio expression was 2.62±0.43, 3.23±0.27, 4.36±0.21 and 4.16±0.35 %IOD fold difference against the samples in 20% oxygen at 24, 48, 72 and 96 hours respectively. In 4% oxygen condition, the Bcl-2/Bax ratio expression was 3.10±0.21, 4.15±0.32, 4.26±0.55 and 2.18±0.42 %IOD fold difference against the samples in 20% oxygen at 24, 48, 72 and 96 hours respectively. A representative image of a gel and the collective results are shown in Figure 5.3.

In 1% oxygen condition, the Bcl-2/Bax ratio expression was 1.45±0.27, 2.81±0.41, 2.98±0.35 and 1.14±0.62 %IOD fold difference against the samples in 20% oxygen at 24, 48, 72 and 96 hours respectively. In 2% oxygen condition, the Bcl-2/Bax ratio expression was 1.24±0.51, 2.63±0.43, 2.59±0.31 and 1.23±0.48 %IOD fold difference against the samples in 20% oxygen at 24, 48, 72 and 96 hours respectively. In 4% oxygen condition, the Bcl-2/Bax ratio expression was 2.33±0.65, 1.34±0.58, 1.15±0.07 and 1.22±0.41 %IOD fold difference against the samples in 20% oxygen at 24, 48, 72 and 96 hours respectively. A representative image of a gel and the collective results are shown in Figure 5.4.

5.3.5 HIF-1α expression

In 1% oxygen condition, the HIF-1α expression was 8.92±2.51, 9.12±1.23, 10.52±1.34 and 14.12±1.46 %IOD fold difference against the samples in 20% oxygen at 24, 48, 72 and 96 hours respectively. In 2% oxygen condition, the HIF-1α expression was 7.31±1.31, 8.76±0.83, 9.85±1.25 and 14.9±1.37 %IOD fold difference against the samples in 20% oxygen at 24, 48, 72 and 96 hours respectively. A

representative image of a gel and the collective results are shown in Figure 5.3.

Table 5.1: Comparison of Apoptotic markers with and without the HIF-1 inhibitor at 1% O_2 (** ($p<0.01$), *$p<0.05$).

At 1% O_2	**24h**	**48h**	**72h**	**96h**
HIF-1α	**	**	**	**
pAKT	**		**	
Bcl-2/Bax				*
Caspase-3		*	*	

Table 5.2: Comparison of Apoptotic markers with and without the HIF-1 inhibitor at 2% O_2 (** ($p<0.01$), *$p<0.05$).

At 2% O_2	**24h**	**48h**	**72h**	**96h**
HIF-1α	**	**	**	**
pAKT			**	
Bcl-2/Bax	**		**	*
Caspase-3				

Table 5.3: Comparison of Apoptotic markers with and without the HIF-1 inhibitor at 4% O_2 (** ($p<0.01$), *$p<0.05$).

At 4% O_2	**24h**	**48h**	**72h**	**96h**
HIF-1α	**	**	**	**
pAKT		**		**
Bcl-2/Bax		*	*	
Caspase-3			*	*

5.3.6 ALP Activity

In 2% oxygen condition, the ALP activity of samples not preconditioned, step-up (1% O_2) preconditioned, standard preconditioned (2% O_2) and step-down preconditioned (4% O_2) was 19.31± 1.23, 24.21± 4.11, 28.21±1.9 and 29.32± 3.14 µmol/ml/min/mg DNA on day 28 as seen in Figure 5.5.

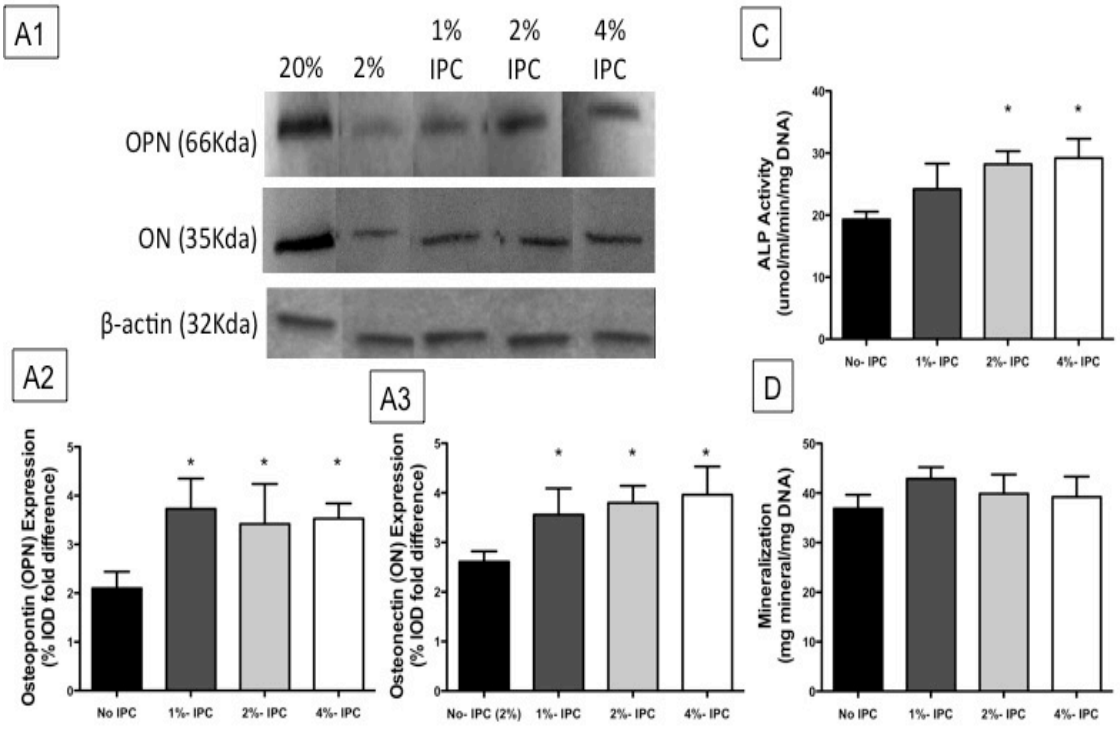

Figure 5.5: Osteogenic Markers after 72hr IPC.

5.3.7 Mineralization

In 2% oxygen condition, the mineral deposition of samples not preconditioned, step-up (1% O_2) preconditioned, standard preconditioned (2% O_2) and step-down preconditioned (4% O_2) was 36.87± 2.76, 42.81± 2.36, 39.72±3.91 and 39.22± 4.12 mg mineral/mg DNA on day 28 as seen in Figure 5.5.

5.3.8 ON Expression

In 2% oxygen condition, the ON expression of samples not preconditioned, step-up (1% O_2) preconditioned, standard preconditioned (2% O_2) and step-down preconditioned (4% O_2) was 2.61±0.21, 3.56±0.53, 3.81±0.34 and 3.96±0.57 %IOD fold difference was observed on day 28 respectively as seen in Figure 5.5.

5.3.9 OPN Expression

In 2% oxygen condition, the OPN expression of samples not preconditioned, step-up (1% O_2) preconditioned, standard preconditioned (2% O_2) and step-down preconditioned (4% O_2) was 2.11±0.34, 3.73±0.62, 3.42±0.82 and 3.53±0.31 %IOD fold difference was observed on day 28 respectively as seen in Figure 5.5.

5.4 DISCUSSION

The study shows a various ischemic preconditioning strategy that can be used to enhance the ability of ASCs to survive under pathological conditions and promote their therapeutic effects. The results show that IPC maintained their stemness after 96 hours of exposure to 1%, 2% and 4% oxygen concentrations. It regulated the anti-apoptotic and pro-apoptotic markers in a time and oxygen concentration dependent manner. In our study we model the CSD environment with a 2% oxygen level and used different protocols of IPC (step-up, standard and step-down) to examine the effect on osteogenic differentiation of ASCs. The standard and the step-down IPC resulted in significantly higher ALP activity, ON and OPN expression but not on mineralization compared to the control. The step-up IPC did not have a significant effect on ALP

activity and mineralization, but did have a significantly higher expression of ON and OPN expression.

Accounting the underlying mechanism, most of the previous studies using IPC have reported that HIF-1α serves as the master regulator of genes responsible for survival signaling [Hu 2008, Nanduri 2008, Yuan 2008]. The PI3 kinase pathway, similar to HIF-1α, is activated in response to hypoxia [Datta 1999]. Upregulation of pAKT in response to PI3 kinase activation also promotes cell survival by either directly targeting proteins involved in apoptosis or by modulating cell metabolism when under stress [Datta 1999]. Our first goal of the study was to examine the effect of IPC on gene expression and monitor the role of HIF-1 in the process. HIF-1 expression varied for cells cultured in 1%, 2% and 4% oxygen. If the cells will be transplanted into a 2% oxygen environment within the body, the transition from atmospheric conditions coud trigger oxidative stress and apoptosis. Exposure to 4% oxygen conditions (step-down) lead to low levels of HIF-1 expression to blunt the damage of a subsequent transition to 2% oxygen and may not trigger apoptosis. ASCs cultured in 1% oxygen conditions (step-up) triggered higher HIF-1 expression, potentially providing an increased protective effect in 2% oxygen. We observed increased levels of pAKT upon ischemic preconditioning with and without the HIF-1 inhibitor compared to the control (20%). We only observed significant different expression levels at 72hr (1%), 72hr (2%), and at 48hr and 96hr (4%) in the presence of HIF-1α inhibition (Table 2-4). The ratio of Bcl-2/Bax ratio is also upregulated in in preconditioned cells and we saw a peak of expression at 72 hours for 1%, 2% and 4% with or without the HIF-1 inhibitor. The 10-fold increase in the pAKT levels and the 3-

fold increase in expression of Bcl-2/Bax ratio at 72 hours in 1%, 2% and 4% oxygen met our success criteria as the best candidates to resist apoptosis.

The 72 hours of exposure for step-up, standard and step-down IPC accelerated the expression of osteogenic markers at 2% oxygen when compared to the non-IPC ASCs. These results helped us to answer the questions that motivated us to examine the different IPC protocols and examine its effects to resist apoptosis and osteogenic potential at physiological levels. In conclusion, the IPC protocols represent a clinically feasible manipulation of cell preparation for an effective transplantation therapy.

CHAPTER 6

SCIENTIFIC CONTRIBUTIONS OF THIS STUDY

The results detailed in the previous chapters provide insight and methods to detect several factors affecting key developmental characteristics of hASCs. Our first goal was to establish whether the HRE DsRed-DR marker virus could be used to track HIF-1 activity in encapsulated ADSCs and whether expression of the red fluorescent protein correlated with HIF-1α detected by traditional methods. Our results show that detection of the signal is certainly possible and that image capture conditions can be established that allow the observed signal to correlate with HIF-1α levels. The marker measures HIF activity rather than the amount of HIF-1α protein as measured with western blotting and immunocytochemical detection. The combination of 3D scaffolds and living cells is used to fill defect sites and support the transplanted cells. The material(s) selected for the scaffold and how it is synthesized influence the diffusion of oxygen and nutrients to the cells and this is a major limitation in tissue engineering. Gradients of oxygen concentration can form within materials and this will affect cellular differentiation or cell fate decisions. We can monitor HIF activity in the same population of cells over time and this can be done in a 3D culture environment without disruption of the scaffold. The tissue engineering community can take advantage of the versatility of our responsive hypoxia marker to show dynamic correlations between cell fate and function with oxygen concentration in engineered tissues in 2D as well as 3D environments.

The second goal of our study was to examine the role of hypoxia on the osteogenic differentiation of hASCs and establish the role of HIF-1 in mediating that effect. Our results demonstrate a reduced capacity for ADSCs to differentiate into osteoblasts in hypoxic conditions when compared with atmospheric conditions. HIF-1 activity does not appear to be an essential component of the varied response of ADSCs in hypoxic conditions. Bone formation *in vivo* requires a coupling of osteogenesis and angiogenesis, making it difficult to evaluate the impact of HIF-1 on each process individually. Our *in vitro* analysis does not include studies looking at the role of HIF-1 in vascularizing bone but this is a critical process that would need to occur *in vivo*. Our studies are an *in vitro* model of intramembranous bone formation as mesenchymal stem cells are directly differentiated into osteoblasts. However, differentiation will never occur in atmospheric conditions if this event is to take place *in vivo*. Efforts to accelerate bone formation at CSD sites could potentially look at HIF-1 as a therapeutic target but for modification of processes other than osteogenic differentiation of ADSCs.

The third goal was to examine different IPC protocols and its effect on ASCs phenotype. The characteristic stem cell markers were maintained in all conditions and the three IPC protocols (Step-up IPC, Standard IPC, Step-down IPC) introduced, led to oxygen and time dependent expression of apoptotic markers. Also, the IPC of ASCs led to accelerated osteogenesis in physiological oxygen environment. Thus, IPC seems to be a promising strategy and clinically feasible for cell preparation for more effective transplantation therapy.

REFERENCES

Abdollahi, H., Harris, L.J., Zhang, P., McIlhenny, S., Srinivas, V., Tulenko, T., and DiMuzio, P.J. The role of hypoxia in stem cell differentiation and therapeutics. J Surg Res 165, 112, 2011.

Acker, H. Cellular oxygen sensors, Ann. NY Acad Sci 718, 3, 1994.

Acker, H. PO2 chemoreception in arterial chemoreceptors. Ann Rev Phys 51, 835, 1989.

Acosta, M.A., Leki, P.Y., Kostov, Y.V., and Leach, J. B. Fluorescent microparticles for sensing cell microenvironment oxygen levels within 3D scaffolds. Biomaterials 30, 3068, 2009.

Aebischer, P., N.A. Pochon, B. Heyd, N. Deglon, J.M. Joseph, A.D. Zurn, E.E. Baetge, J.P. Hammang, M. Goddard, M. Lysaght, F. Kaplan, A.C. Kato, M. Schluep, L. Hirt, F. Regli, F. Porchet, and N. De Tribolet. Gene therapy for amyotrophic lateral sclerosis (ALS) using a polymer encapsulated xenogenic cell line engineered to secrete hCNTF. Hum Gene Ther 7, 851, 1996.

Agani, F.H., Pichiule, P., Chavez, J.C., LaManna, J.C. The role of mitochondria in the regulation of hypoxia-inducible factor 1 expression during hypoxia. J Biol Chem 275, 35863, 2000.

Albrektsson, T. In: Black JHG, editor. Hard tissue response. London, UK: Chapman & Hall; 1998.

Allison, M.R, Poulsom, R., Forbes, S., Wright, J.N.A. An introduction to stem cells. Pathol 197, 419, 2002.

Alsberg, E., Anderson, K.W., Albeiruti, A., Rowley, J.A., Mooney, D.J.: Engineering growing tissues. Proc Natl Acad Sci USA 99, 12025, 2002.

Antonio, C., Spaggiari, B., Ravanetti, F., Martini, F.M., Borghetti, P., Gabbi, C. The critical sized bone defect: morphological study of bone healing. Ann. Fac. Medic. Vet. Di Parma 97, 2006.

Antoniou, E.S., Sund, S., Homsi, E.N. A theoretical simulation of hematopoietic stem cells during oxygen fluctuations: prediction of bone marrow responses during hemorrhagic shock. Shock 22, 415, 2004.

Araldi, E., and Schipani, E. Hypoxia, HIFs and bone development. Bone 47, 190, 2010.

Asahara, T., Takahashi, T., Masuda, H., Kalka, C., Chen, D., Iwaguro, H., Inai, Y., Silver, M., and Isner, J.M. VEGF contributes to postnatal neovascularization by mobilizing bone marrow-derived endothelial progenitor cells. EMBO J 18, 3964, 1999.

Ashjian, P.H., Elbarbary, A.S., Edmonds, B., DeUgarte, D., Zhu, M., Zuk, P.A., Lorenz, H.P., Benhaim, P., Hedrick, M.H. In vitro differentiation of human processed lipoaspirate cells into early neural progenitors. Plast Reconstr Surg 111, 1922, 2003.

Augstein, A., Poitz, D.M., Braun-Dullaeus, R.C., Strasser, R.H., Schmeisser, A. Cell-specific and hypoxia-dependent regulation of human HIF-3α: inhibition of the expression of HIF target genes in vascular cells. Cell Mol Life Sci. 68, 2627, 2011.

Aust, L., Devlin, B., Foster, S.J., Halvorsen, Y.D., Hicok, K., du, L.T., Sen, A., Willingmyre, G.D., Gimble, J.M. Yield of human adiposederived adult stem cells from liposuction aspirates. Cytotherapy 6, 7, 2004.

Baht, G.S., Hunter, G.K., Goldberg, H.A. Bone sialoprotein-collagen interaction promotes hydroxyapatite nucleation. Matrix Biol 27, 600, 2008.

Barry, F.P., Murphy, J.M. Mesenchymal stem cells: clinical applications and biological characterization. Int J Biochem Cell Biol. 36, 568, 2004.

Bassett, C., and Herrmann, I. Influence of oxygen concentration and mechanical factors on differentiation of connective tissues in vitro. Nature 190, 460, 1961.

Benoit, D.S.W., Collins, S.D., and Anseth, K.S. Multifunctional Hydrogels that Promote Osteogenic Human Mesenchymal Stem Cell Differentiation Through Stimulation and Sequestering of Bone Morphogenic Protein 2. Advanced Functional Materials 17, 2085, 2007.

Benoit, D.S.W., Durney, A.R., and Anseth, K.S. The Effects of Heparin-functionalized PEG Hydrogels on Three-dimensional Human Mesenchymal Stem Cell Osteogenic Differentiation. Biomaterials 28, 66, 2007.

Benton, J.A., Fairbanks, B.D., and Anseth KS. Characterization of valvular interstitial cell function in three dimensional matrix metalloproteinase degradable PEG hydrogels. Biomaterials 30, 6593, 2009.

Betre, H., Ong, S.R., Guilak, F., Chilkoti, A., Fermor, B., Setton, L.A. Chondrocytic differentiation of human adipose-derived adult stem cells in elastin-like polypeptide. Biomaterials. 27, 91, 2006.

Bhang, S.H., Cho, S.W., La, W.G., Lee, T.J., Yang, H.S., Sun, A.Y., Baek, S.H., Rhie, J.W., and Kim, B.S. Angiogenesis in ischemic tissue produced by spheroid grafting of human adipose-derived stromal cells. Biomaterials 32, 2734, 2011.

Bielby, R.C., Boccaccini, A.R., Polak, J.M., Buttery, L.D. In vitro differentiation and in vivo mineralization of osteogenic cells derived from human embryonic stem cells. Tissue Eng 10, 1518, 2004.

Black, J. Orthopaedic biomaterials in research and practice. New York, USA. Churchill Livingstone, 1988.

Blau, H.M, Brazelton, T.R., Weimann, J.M. The evolving concept of a stem cell: Entity or function?. Cell 105, 829, 2001.

Borner, C., Diminished cell proliferation associated with the death-protective activity of Bcl-2. J Biol Chem, 271, 22, 12695, 1996.

Bracken, C.P., Fedele, A.O., Linke, S., Balrak, W., Lisy, K., Whitelaw, M.L., and Peet, D.J. Cell-specific regulation of hypoxia-inducible factor (HIF)-1alpha and HIF-2alpha stabilization and transactivation in a graded oxygen environment. J Biol Chem 281, 22575, 2006.

Brahimi-Horn, M.C., Pouysségur, J. The hypoxia-inducible factor and tumor progression along the angiogenic pathway. Int Rev Cytol. 242, 157, 2005.

Bruder, S. P., and Fox, B. S. Tissue engineering of bone. Cell based strategies. Clin Orthop Relat Res, S68, 1999.

Bruder, S.P., Kraus, K.H., Goldberg, V.M., Kadiyala, S. The effect of implants loaded with autologous mesenchymal stem cells on the healing of canine segmental bone defects. J Bone Joint Surg Am 80, 985, 1998.

Bruder, S.P., Kurth, A.A., Shea, M., Hayes, W.C., Jaiswal, N., Kadiyala, S. Bone regeneration by implantation of purified, culture-expanded human mesenchymal stem cells; J Orthop Res 16, 155, 1998.

Bruick, R.K. & McKnight,S.L. Transcription. Oxygen sensing gets a second wind. Science 295, 807, 2002.

Bryant, S.J. and Anseth, K.S. Hydrogel properties influence ECM production by chondrocytes photoencapsulated in poly(ethylene glycol) hydrogels. Journal of Biomedical Materials Research 59, 63, 2002.

Bryant, S.J., Nuttelman, C.R., and Anseth, K.S. Cytocompatibility ofUV and visible light photoinitiating systems on cultured NIH/3T3 fibroblasts in vitro. Journal of Biomaterial Science Polymer Edition 11, 439, 2000.

Bunn, H.F., Poyton, R.O. Oxygen sensing and molecular adaptation to hypoxia, Phys Rev 76, 839, 1996.

Bunnell, B.A., Flaat, M., Gagliardi, C., Patel, B., and Ripoll, C. Adipose-derived stem cells: isolation, expansion and differentiation. Methods 45, 115, 2008.

Buravkova, L.B., Anokhina, E.B. Effect of hypoxia on stromal precursors from rat bone marrow at the early stage of culturing. Bull Exp Biol Med 143, 411, 2007.

Burdick, J.A. and Anseth, K.S. Photoencapsulation of osteoblasts in injectable RGD modified hydrogels for bone tissue engineering. Biomaterials 23, 4315, 2002.

Butt, O.I., Carruth, R., Kutala, V.K., Kuppusamy, P., and Moldovan, N.I. Stimulation of peri-implant vascularisation with bone marrow-derived progenitor cells: monitoring by in vivo EPR oximetry. Tissue Eng 13, 2053, 2007.

Buxton, A.N., Zhu, J., Marchant, R., West, J.L., Yoo, J.U., and Johnstone, B. Design and characterization of poly(ethylene glycol) photopolymerizable semi-interpenetrating networks for chondrogenesis of human mesenchymal stem cells. Tissue Eng 13, 2549, 2007.

Cadenas, E. Biochemistry of Oxygen Toxicity. Ann Rev Biochem 58, 79, 1989.

Cai, Z., Manalo, D.J., Wei, G., Rodriguez, E.R., Fox-Talbot, K., Lu, H., Zweier, J.L., Semenza, G.L. Hearts from rodents exposed to intermittent hypoxia or erythropoietin are protected against ischemia-reperfusion injury. Circulation. 108, 79, 2003.

Carmeliet, P., Dor, Y., Herbert, J., Fukumura, D., Brusselmans, K., Dewerchin, M., Neeman, M., Bono, F., Abramovitch, R., Maxwell, P., Koch, C.J., Ratcliffe, P., Moons, L., Jain, R.K., Collen, D., Keshet, E. Role of HIF-1 in hypoxia-mediated apoptosis, cell proliferation and tumor angiogenesis, Nature 394, 485, 1998.

Carrancio, S., Lopez-Holgado, N., Sanchez-Guijo, F.M., Villaron, E., Barbado, V., Tabera, S. et al. Optimization of mesenchymal stem cell expansion procedures by cell separation and culture conditions modification; Exp Hematol 36, 1014, 2008.

Carroll, V.A., Ashcroft, M. Role of hypoxia-inducible factor (HIF)-1alpha versus HIF-2alpha in the regulation of HIF target genes in response to hypoxia, insulin-like growth factor-I, or loss of von Hippel-Lindau function: implications for targeting the HIF pathway. Cancer Res. 66, 6264, 2006.

Carter, D.R. and Hayes, W.C. The compressive behavior of bone as a two-phase porous structure. J Bone Joint Surg Am 59, 954, 1977.

Catt, J.W., Henman, M. Toxic effects of oxygen on human embryo development. Hum Reprod 15, 199, 2000.

Ceradin, D.J., Kulkarni, A.R., Callaghan, M.J., Tepper, O.M., Bastidas, N., Kleinman, M.E., Capla, J.M., Galiano, R.D., Levine, J.P., and Gurtner, G.C. Progenitor cell trafficking is regulated by hypoxic gradients through HIF-1 induction of SDF-1. Nat Med 10, 858, 2004.

Chaikof, E.L., Matthew, H., Kohn, J., Mikos, A.G., Prestwich, G.D., and Yip, C.M. Biomaterials and scaffolds in reparative medicine. Ann N Y Acad Sci 961, 96, 2002.

Chandel, N.S., D.S. McClintock, C.E. Feliciano, T.M. Wood, J.A. Melendez, A.M. Rodriguez, and P.T. Schumacker, Reactive oxygen species generated at mitochondrial complex III stabilize hypoxia-inducible factor-1 alpha during hypoxia - A mechanism of O2 sensing. Journal of Biological Chemistry 275, 33, 25130, 2000.

Chandel, N.S., Maltepe, E., Goldwasser, E., Mathieu, C.E., Simon, M.C., Schumacker, P.T. Mitochondrial reactive oxygen species trigger hypoxia-induced transcription, Proc Natl Acad Sci 95, 11715, 1998.

Chen, L., Fink, T., Ebbesen, P., and Zachar, V. Optimized chondrogenesis of ATCD5 cells through sequential regulation of oxygen conditions. Tissue Eng 12, 559, 2006.

Chimutengwende-Gordon, M., and Khan, W.S. Advances in the use of stem cells and tissue engineering applications in bone repair. Curr Stem Cell Res Ther 7, 122, 2012.

Cho, S.W., Kim, S.S., Rhie, J.W., Cho, H.M., Choi, C.Y., Kim, B.S. Engineering of volume-stable adipose tissues. Biomaterials 26, 3577, 2005.

Chow, D.C., Wenning, L.A., Miller, W.M, and Papoutsakis, E.T., 2001. Modeling pO(2) distributions in bone marrow hematopoietic compartment. I. Krogh's model. Biophys J 81, 675, 2001.

Chung, D.J., Hayashi, K., Toupadakis, C.A., Wong, A., Yellowley, C.E. Osteogenic proliferation and differentiation of canine bone marrow and adipose tissue derived mesenchymal stromal cells and the influence of hypoxia.Res Vet Sci. 92,66, 2012.

Chung, U.I., Kawaguchi, H., Takato, T., and Nakamura, K. Distinct osteogenic mechanisms of bones of distinct origins. J Orthop Sci 9, 410, 2004.

Cipolleschi, M.G., Dellosbarba, P., Olivotto, M. The role of hypoxia in the maintenance of hematopoietic stem-cells. Blood 82, 2031, 1993.

Clemens, T.L. The hypoxia inducible factor alpha pathway couples angiogenesis to osteogenesis during skeletal development. J Clin Invest 117, 1616, 2007.

Cochran, D.M., Fukumura, D., Ancukiewicz, M., Carmeliet, P., and Jain, R.K. Evolution of oxygen and glucose concentration profiles in a tissue-mimetic culture system of embryonic stem cells. Ann Biomed Eng 34, 1247, 2006.

Cockman, M.E., Masson, N., Mole, D.R., Jaakkola, P., Chang, G., Clifford, S.C., Maher, E.R., Pugh, C.W., Ratcliffe, P.J., Maxwell, P.H. Hypoxia-inducible factor-α Binding and Ubiquitylation by the von Hippel-Lindau Tumor Suppression Protein. J Biol Chem 275, 25733, 2000.

Cohen, M.M. Jr. The new bone biology: pathologic, molecular, and clinical correlates; Am J Med Genet A 140, 2646, 2006.

Compernolle, V., Brusselmans, K., Acker, T., Hoet, P., Tjwa, M., Beck, H., Plaisance, S., Dor, Y., Keshet, E., Lupu, F., Nemery, B., Dewerchin, M., Van Veldhoven, P., Plate, K., Moons, L., Collen, D., Carmeliet, P. Loss of HIF-2α and inhibition of VEGF impair fetal lung maturation, whereas treatment with VEGF prevents fatal respiratory distress in premature mice. Nat Med 8, 702, 2002.

Cruise, G.M., Scharp, D.S., and Hubbell, J.A. Characterization of permeability and network structure of interfacially photopolymerized poly(ethylene glycol) diacrylate hydrogels. Biomaterials 19, 1287, 1998.

Cukierman, E., Pankov, R., and Yamada, K.M. Cell interactions with three-dimensional matrices. Curr Opin Cell Biol 14, 633, 2002.

D'Ippolito, G., Diabira, S., Howard, G.A., Roos, B.A., and Schiller, P.C. Low oxygen tension inhibits osteogenic differentiation and enhances stemness of human MIAMI cells. Bone 39, 513, 2006.

Dai, Y., Xu, M., Wang, Y., Pasha, Z., Li, T. and Ashraf, M. HIF-1 alpha induced-VEGF overexpression in bone marrow stem cells protects cardiomyocytes against ischemia. J Mol Cell Cardiol. 42, 1036. 2007.

Damien, C.J., and Parsons, J.R. Bone graft and bone graft substitutes: a review of current technology and applications. J Appl Biomater 2, 187, 1991.

Das, R., Jahr, H., van Osch, G.J., and Farrell, E. The role of hypoxia in bone marrow-derived mesenchymal stem cells: considerations for regenerative medicine approaches. Tissue Eng 16, 159, 2010.

de Oliveira, P.T., Nanci, A. Nanotexturing of titanium-based surfaces upregulates expression of bone sialoprotein and osteopontin by cultured osteogenic cells. Biomaterials 25, 403, 2004.

Dee, K.C., Andersen, T.T., Bizios, R. Osteoblast migration characteristics on substrates modified with immobilized adhesive peptides. Biomaterials 20, 221, 1999.

Derubeis, A. R., and Cancedda, R. Bone marrow stromal cells (BMSCs) in bone engineering: limitations and recent advances. Ann Biomed Eng 32, 160, 2004.

Desplat, V., Faucher, J., Mahon, F.X., Sbarba, P.D., Praloran, V., Ivanovic, Z. Hypoxia Modifies Proliferation and Differentiation of CD34+ CML Cells. Stem Cells 20 347, 2002.

Domm, C., Schunke, M., Christesen, K., and Kurz, B. Redifferentiation of dedifferentiated bovine articular chondrocytes in alginate culture under low oxygen tension. Osteoarthritis Cartilage 10, 13, 2002.

Drosse, I., Volkmer, E., Capanna, R., De Biase, P., Mutschler, W., Schieker, M. Tissue engineering for bone defect healing: an update on a multi-component approach. Injury 39, 9, 2008.

Ducy, P., Geoffroy, V., Karsenty, G. Study of osteoblast-specific expression of one mouse osteocalcin gene: characterization of the factor binding to OSE2. Connect Tissue Res 35, 7, 1996.

Dunwoodie, S.L. The role of hypoxia in development of the Mammalian embryo. Dev Cell 17, 755, 2009.

Dupont, K.M., Sharma, K., Stevens, H.Y., Boerckel, J.D., García, A.J., and Guldberg, R.E. Human stem cell delivery for treatment of large segmental bone defects. Proc Natl Acad Sci U S A 107, 3305, 2010.

Ebert, B.L., Firth, J.D., Ratcliffe, P.J. Hypoxia and Mitochondrial Inhibitors Regulate Expression of Glucose Transporter-1 via Distinct Cis-acting Sequences. J Biol Chem 270, 29083, 1995.

Einhorn, T.A. Enhancement of fracture-healing. J Bone Joint Surg Am 77, 940, 1995.
El-Amin, S.F., Kofron, M.D., Attawia, M.A., Lu, H.H., Tuan, R.S., Laurencin, C.T. Molecular regulation of osteoblasts for tissue engineered bone repair. Clin Orthop Relat Res 220, 2004.

Fandrey, J., Frede, S., Jelkmann, W. Role of hydrogen peroxide in hypoxia-induced erythropoietin production, Biochem J 303, 507, 1994.

Fandrey, J., Seydel, F.P., Siegers, C.P., Jelkmann, W. Role of Cytochrome P450 in the Control of the Production of Erythropoietin. Life Sci 47, 127, 1990.

Fedele, A.O., Whitelaw, M.L., Peet, D.J. Regulation of gene expression by the hypoxia inducible factors, Mol Interven 2, 229, 2002.

Fehrer, C., Brunauer, R., Laschober, G., Unterluggauer, H., Reitinger, S., Kloss, F., Gully, C., Gassner, R., Lepperdinger, G. Reduced oxygen tension attenuates differentiation capacity of human mesenchymal stem cells and prolongs their lifespan. Aging Cell 6, 745, 2007.

Ferrara, N. and Gerber, H.P. The role of vascular endothelial growth factor in angiogenesis. Acta Haematol. 106,148. 2001.

Fink, T., Rasmussen, J.G., Lund, P., Pilgaard, L., Soballe, K., Zachar, V. Isolation and expansion of adipose-derived stem cells for tissue engineering. Front Biosci. 3, 256, 2011.

Ford, M.C., Bertram, J.P., Hynes, S.R., Michaud, M., Li, Q., Young, M., Segal, S.S., Madri, J.A., and Lavik, E.B. A macroporous hydrogel for the coculture of neural progenitor and endothelial cells to form functional vascular networks in vivo. Proc Natl Acad Sci U S A 103, 2512, 2006.

Forsyth, N.R., Musio, A., Vezzoni, P., Simpson, A., Noble, B.S., McWhir, J. Physiologic oxygen enhances human embryonic stem cell clonal recovery and reduces chromosomal abnormalities. Cloning Stem Cell 8, 16, 2006.

Forsythe, J.A., Jiang, B.H., Iyer, N.V., Agani, F., Leung, S.W., Koos, R.D., and Semenza, G.L. Activation of vascular endothelial growth factor gene transcription by hypoxiainducible factor 1. Mol Cell Biol 16, 4604, 1996.

Fraser, J.K., Wulur, I., Alfonso, Z., and Hedrick, M.H. Fat tissue: an underappreciated source of stem cells for biotechnology. Trends Biotechnol 24, 150, 2006.

Friedenstein, A.J., Piatetzky-Shapiro, I.I., Petrakova, K.V. Osteogenesis in transplants of bone marrow cells. J Embryol Exp Morphol 16, 381, 1966.

Gamie, Z., Tran, G.T., Vyzas, G., Korres, N., Heliotis, M., Mantalaris, A., and Tsiridis, E. Stem cells combined with bone graft substitutes in skeletal tissue engineering. Expert Opin Biol Ther 12, 713, 2012.

Giannoudis, P.V., Einhorn, T.A., Marsh, D. Fracture healing: the diamond concept. Injury 38, 3, 2007.

Gibson, L.J. The mechanical behaviour of cancellous bone. J Biomech 18, 317, 1985.

Gierse, H., Donath, K. Reactions and complications after the implantation of Endobon including morphological examination of explants. Arch Orthop Trauma Surg 119, 349, 1999.

Gimble, J., and Guilak, F. Adipose-derived adult stem cells: isolation, characterization, and differentiation potential. Cytotherapy 5, 362, 2003.

Ginouves, A., Ilc, K., Macias, N., Pouyssegur, J., and Berra, E. PHDs overactivation during chronic hypoxia ‘‘desensitizes desensitizes’’ HIF alpha and protects cells from necrosis. Proc Natl Acad Sci U S A 105, 4745, 2008.

Gleadle, J.M., Ebert, B.L., Firth, J.D., Ratcliffe, P.J. Regulation of angiogenic growth factor expression by hypoxia, transition metals and chelating agents. Am J Phys 268, 1362, 1995a.

Gleadle, J.M., Ebert, B.L., Ratcliffe, P.J. Diphenylene iodonium inhibits the induction of erythropoietin and other mammalian genes by hypoxia. Eur J Biochem 234, 92, 1995b.

Goldberg, M.A., Dunning, S.P., Bunn, H.F. Regulation of the erythropoietin gene: evidence that the oxygen sensor is a heme protein. Science 242, 1412, 1988.

Goldberg, M.A., Schneider, T.J. Similarities between the oxygen-sensing mechanisms. J Biol Chem. 269, 4355, 1994.

Görlach, A., Fandrey, J., Holtermann, G., Acker, H. Effects of cobalt on haem proteins of erythropoietin-producing HepG2 cells in multicellular spheroid culture. FEBS Letters 348, 216, 1994.

Görlach, A., Holtermann, G., Jelkmann, W., Hancock, J.T., Jones, S.A., Jones, O.T.G., Acker, H. Photometric characteristics of haem proteins in erythropoietin-producing hepatoma cells (HepG2). Biochem J 290, 771, 1993.

Granero-Molto, F., Weis, J.A., Longobardi, L., Spagnoli, A. Role of mesenchymal stem cells in regenerative medicine: application to bone and cartilage repair. Expert Opin Biol Ther 8, 255, 2008.

Grant, M.B., May, W.S., Caballero, S., Brown, G.A., Guthrie, S.M., Mames, R.N., Byrne, B.J., Vaught, T., Spoerri, P.E., Peck, A.B., and Scott, E.W. Adult hematopoietic stem cells provide functional hemangioblast activity during retinal neovascularization. Nat Med 8, 607, 2002.

Grayson, W.L., Zhao, F., Bunnell, B., and Ma, T. Hypoxia enhances proliferation and tissue formation of human mesenchymal stem cells. Biochem Biophys Res Commun 358, 948-953. 2007.

Grayson, W.L., Zhao, F., Izadpanah, R., Bunnell, B., and Ma T. Effects of hypoxia on human mesenchymal stem cell expansion and plasticity in 3D constructs. J Cell Physiol 207, 331, 2006.

Green, W.T. Jr. Articular cartilage repair: behavior of rabbit chondrocytes during tissue culture and subsequent allografting. Clin Orthop 124, 237, 1977.

Gronthos, S., Franklin, D.M., Leddy, H.A., Robey, P.G., Storms, R.W., Gimble, J.M. Surface protein characterization of human adipose tissue-derived stromal cells. J Cell Physiol. 189, 54, 2001.

Guilak, F., Lott, K.E., Awad, H.A., Cao, Q., Hicok, K.C., Fermor, B., Gimble, J.M. Clonal analysis of the differentiation potential of human adiposederived adult stem cells. J Cell Physiol 206, 229, 2006.

Haase, V.H. Regulation of erythropoiesis by hypoxia-inducible factors. Blood Rev. 27, 41, 2013.

Haase, V.H. The VHL tumor suppressor in development and disease: functional studies in mice by conditional gene targeting. Semin Cell Dev Biol 16, 564, 2005.

Haddad, J.J.E., R.E. Olver, and S.C. Land, Antioxidant/pro-oxidant equilibrium regulates HIF-1 alpha and NF-kappa B redox sensitivity - Evidence for inhibition by glutathione oxidation in alveolar epithelial cells. Journal of Biological Chemistry 275, 28, 21130, 2000.

Harvey, A.J., Kind, K.L., Pantaleon, M., Armstrong, D.T., Thompson, J.G. Oxygen-regulated gene expression in bovine blastocysts. Biol Reprod 71, 1108, 2004.

Hausenloy, D.J., Yellon, D.M. The second window of preconditioning (SWOP) where are we now? Cardiovasc Drugs Ther. 24, 235, 2010.

Hench, L.L. Biomaterials; Science 208, 826, 1980.

Hench, L.L. Bioactive materials: the potential for tissue regeneration. J Biomed Mater Res 41, 511, 1998.

Hench, L.L., Polak, J.M. Third-generation biomedical materials. Science 295, 1014, 2002.

Heppenstall, R.B., Grislis, G., and Hunt, T.K. Tissue Gas Tensions and Oxygen Consumption in Healing Bone Defects. Clin Orthop Relat Res 106, 357, 1975.

Hertel, R., Strebel, N., and Ganz, R. Amputation versus reconstruction in traumatic defects of the leg: outcome and costs. J Orthop Trauma 10, 223, 1996.

Hirao, M., Tamai, N., Tsumaki, N., Yoshikawa, H., and Myoui, A. Oxygen tension regulates chondrocyte differentiation and function during endochondral ossification. J Biol Chem 281, 31079, 2006.

Hollinger, J., McAllister, B. In: Wilson, J., Hench, L.L., Greenspon, D., editors. Bone and its repair. FL, USA: Pergamon Press, 1995.

Holzwarth, C., Vaegler, M., Gieseke, F., Pfister, S.M., Handgretinger, R., and Kerst, G., Müller, I. Low physiologic oxygen tensions reduce proliferation and differentiation of human multipotent mesenchymal stromal cells. BMC Cell Biol 11, 11, 2010.

Horiguchi, H., Teranishi, H., Niiya, K., Aoshima, K., Katoh, T., Sakuragawa, N. & Kasuya, M. Hypoproduction of erythropoietin contributes to anemia in chronic cadmium intoxication: clinical study on Itai-itai disease in Japan. Arch Toxicol 68, 632, 1994.

Hu, C.J., Iyer, S., Sataur, A., Covello, K.L., Chodosh, L.A., Simon, M.C. Differential regulation of the transcriptional activities of hypoxia-inducible factor 1 alpha (HIF-1 alpha) and HIF-2alpha in stem cells. Mol Cell Biol. 26, 3514, 2006.

Huang, D.C., J.M. Adams, and S. Cory, The conserved N-terminal BH4 domain of Bcl-2 homologues is essential for inhibition of apoptosis and interaction with CED-4. Embo J 17, 1029, 1998.

Huang, J., Deng, F., Wang, L., Xiang, X.R., Zhou, W.W., Hu, N., Xu, L. Hypoxia induces osteogenesis-related activities and expression of core binding factor α1 in mesenchymal stem cells. Tohoku J Exp Med. 224, 7, 2011.

Huang, L.E., Arany, Z., Livingston, D.M., Bunn, H.F. Activation of hypoxia inducible transcription factor depends primarily upon redox-sensitive stabilization of its α subunit. J Biol Chem 271, 32253, 1996.

Huang, L.E., Gu, J., Schau, M., Bunn, H.F. Regulation of hypoxia inducible factor 1α is mediated by an O2-dependent degradation domain via the ubiquitin proteasome pathway, Proc Natl Acad Sci 95, 7987, 1998.

Hulth, A. Current concepts of fracture healing. Clin Orthop 249, 265, 1989.

Hung, S.P., Ho, J.H., Shih, Y.R., Lo, T., Lee, O.K. Hypoxia promotes proliferation and osteogenic differentiation potentials of human mesenchymal stem cells. J Orthop Res. 30, 260, 2012.

Hunter, J.J., B.L. Bond, and T.G. Parslow, Functional dissection of the human Bc12 protein: sequence requirements for inhibition of apoptosis. Mol Cell Biol 16, 877, 1996.

Hwang, J.M., Weng, Y.J., Lin, J.A., Bau, D.T., Ko, F.Y., Tsai, F.J., Tsai, C.H., Wu, C.H., Lin, P.C., Huang, C.Y., and Kuo, W.W. Hypoxia-induced compensatory effect as related to Shh and HIF-1 alpha in ischemia embryo rat heart. Mol Cell Biochem 311, 179, 2008.

Hwang, N.S., Kim, M.S., Sampattavanich, S., Baek, J.H., Zhang, Z., and Elisseeff, J. Effects of three-dimensional culture and growth factors on the chondrogenic differentiation of murine embryonic stem cells. Stem Cells 24, 284, 2006.

Iida, T., Mine, S., Fujimoto, H., Suzuki, K., Minami, Y., Tanaka, Y. Hypoxia-inducible factor-1α induces cell cycle arrest of endothelial cells. Genes Cells 7, 143, 2002.

Ivan, M., Kondo, K., Yang, H., Kim, W., Valiando, J., Ohh, M., Salic, A., Asara, J.M., Lane, W.S., Kaelin, Jr. W.G. HIF-α targeted for VHL-mediated destruction by proline hydroxylation: Implications for O2 Sensing. Science 292, 464, 2001.

Ivanovic, Z. Hypoxia or in situ normoxia: The stem cell paradigm. The Journal of Cellular Physiology 219, 271, 2009.

Iyer, N.V., Kotch, L.E., Agani, F., Leung, S.W., Laughner, E., Wenger, R.H., Gassmann, M., Gearhart, J.D., Lawler, A.M., Yu, A.Y., Semenza, G.L. Cellular and developmental control of O2 homeostasis by hypoxia-inducible factor 1α. Genes Dev 12, 149, 1998.

Jaakkola, P., Mole, D.R., Tian, Y.M., Wilson, M., Gielbert, J., Gaskell, S.J., von Kriegshem, A., Hebestreit, H.F., Mukherji, M., Schoffield, C.J., Maxwell, P.H., Pugh, C.W., Ratcliffe, P.J. Targeting of HIF-α to the von Hippel-Lindau Ubiquitylation Complex by O2-Regulated Prolyl Hydroxylation. Science 292, 468, 2001.

Jeschke, B., Meyer, J., Jonczyk, A., Kessler, H., Adamietz, P., Meenen, N.M., Kantlehner, M., Goepfert, C., Nies, B. RGD-peptides for tissue engineering of articular cartilage. Biomaterials 23, 3455, 2002.

Jiang, B.H., Rue, E., Wang, G.L., Roe, R., and Semenza, G.L. Dimerization, DNA binding, and transactivation properties of hypoxia-inducible factor 1. J Biol Chem 271, 17771, 1996.

Jiang, B.H., Semenza, G.L., Bauer, C., Marti, H.H. Hypoxia-inducible factor 1 levels vary exponentially over a physiologically relevant range of O2 tension. Am J Phys 271, 1172, 1996.

Jiang, B.H., Zheng, Z.H., Leung, S.W., Roe, R., Semenza, G.L. Transactivation and inhibitory domains of hypoxia-inducible factor 1 alpha. Modulation of transcriptional activity by oxygen tension. J Biol Chem 272, 19253, 1997.

Jilka, R.L., Weinstein, R.S., Bellido, T., Parfitt, A.M., Manolagas, S.C. Osteoblast programmed cell death (apoptosis): modulation by growth factors and cytokines. J Bone Miner Res 13, 793, 1998.

Jorgensen, N.R., Henriksen, Z., Brot, C.,. Human osteoblastic cells propagateintercellular calcium signals by two different mechanisms. J Bone Miner Res 15, 1024, 2000.

Kallio, P.J., Okamoto, K., O'Brien, S., Carrero, P., Makin, Y., Tanaka, H., Poellinger, L. Signal Transduction in Hypoxic Cells: Inducible Nuclear Translocation and Recruitment of the CBP/p300 Coactivator by the Hypoxia Inducible Factor-1α. EMBO J 17, 6573, 1998.

Kane, D.J., T. Ord, R. Anton, and D.E. Bredesen, Expression of bcl-2 inhibits necrotic neural cell death. J Neurosci Res 40, 269, 1995.

Kantz, B.S. Erythropoietin. Blood 77, 419, 1991.

Karner, E., Unger, C., Sloan, A.J., Ahrlund-Richter, L., Sugars, R.V., Wendel, M. Bone matrix formation in osteogenic cultures derived from human embryonic stem cells in vitro. Stem Cells Dev 16, 39, 2007.

Katz, A.J., Tholpady, A., Tholpady, S.S., Shang, H., and Ogle, R.C. Cell surface and transcriptional characterization of human adipose-derived adherent stromal (hADAS) cells. Stem Cells 23, 412, 2005.

Ke, Q., Costa, M. Hypoxia-inducible factor-1 (HIF-1). Mol Pharmacol 70, 1469, 2006.

Kellner, K., Liebsch, G., Klimant, I., Wolfbeis, O.S., Blunk, T., Schulz, M.B., and Gopferich, A. Determination of oxygen gradients in engineered tissue using a fluorescent sensor. Biotechnol Bioeng 80, 73, 2002.

Kelly, B.D., Hackett, S.F., Hirota, K., Oshima, Y., Cai, Z., Berg-Dixon, S., Rowan, A., Yan, Z., Campochiaro, P.A., and Semenza, G.L. Cell type-specific regulation of angiogenic growth factor gene expression and induction of angiogenesis in nonischemic tissue by a constitutively active form of hypoxia-inducible factor 1. Circ Res 93, 1074, 2003.

Kewley, R.J., Whitelaw, M.L., and Chapman-Smith, A. The mammalian basic helixloophelix/ PAS family of transcriptional regulators. The International Journal of Biochemistry & Cell Biology 36, 189, 2004.

Khan, W.S., Adesida, A.B., Hardingham, T.E. Hypoxic conditions increase hypoxia-inducible transcription factor 2 alpha and enhance chondrogenesis in stem cells from the infrapatellar fat pad of osteoarthritis patients. Arthritis Res Ther 9, 55, 2007.

Kinnaird, T., Stabile, E., Burnett, M.S., Lee, C.W., Barr, S., Fuchs, S., and Epstein, S.E. Marrow-derived stromal cells express genes encoding a broad spectrum of arteriogenic cytokines and promote in vitro and in vivo arteriogenesis through paracrine mechanisms. Circ Res 94, 678, 2004.

Kinnaird, T., Stabile, E., Burnett, M.S., Lee, C.W., Barr, S., Fuchs, S., and Epstein, S.E. Local delivery of marrowderived stromal cells augments collateral perfusion through paracrine mechanisms. Circulation 109, 1543, 2004.

Kneser, U., D. J. Schaefer, B. Munder, C. Klemt, C. Andree, G. B. Stark. Tissue engineering of bone. Min Invas Ther Allied Technol 11, 107, 2002.

Kneser, U., Schaefer, D.J., Polykandriotis, E., and Horch, R.E. Tissue engineering of bone: the reconstructive surgeon's point of view. J Cell Mol Med 10, 7, 2006.

Knippenberg, M., Helder, M.N., Doulabi, B.Z., Semeins, C.M., Wuisman, P.I., Klein-Nulend, J. Adipose tissue-derived mesenchymal stem cells acquire bone cell-like responsiveness to fluid shear stress on osteogenic stimulation. Tissue Eng 11, 1780, 2005.

Kofoed, H., Sjontoft, E., Siemssen, S.O., Olesen, H.P. Bone-marrow circulation after osteotomy—blood-flow, pO2, pCO2, and pressure studied in dogs. Acta Orthop Scand 56, 400, 1985.

Kozak, K.R., Abbott, B., Hankison, O. ARNT-Deficient mice and placental differentiation, Dev Biol 191, 297, 1997.

Krihak, M.K., and Shahriari, M.R. Highly sensitive, all solid state fibre optic oxygen sensor based on the sol-gel coating technique. Electron Lett 32, 240, 1996.

Ladoux, A., Frelin, C. Hypoxia is a strong Inducer of Vascular Endothelial Growth Factor mRNA Expression in the Heart. Biochem Bioph Res Co 195, 1005, 1993.

Lando, D., Peet, D.J., Gorman, J.J., Whelan, D.A., Whitelaw, M.L., Bruick, R.K. FIH-1 is an asparaginyl hydroxylase enzyme that regulates the transcriptional activity of hypoxia inducible factor. Genes Dev.16, 1466, 2002.

Langer, R., Vacanti, J.P. Tissue engineering. Science 260, 920, 1993.

Langlois, G., Dusseault, J., Bilodeau, S., Tam, S.K., Magassouba, D., and Hallé, J.P. Direct effect of alginate purification on the survival of islets immobilized in alginate-based microcapsules. Acta Biomaterialia 5, 3433, 2009.

Lash, G.E., Fitzpatrick, T.E., Graham, C.H. Effect of Hypoxia on Cellular Adhesion to Vitronectin and Fibronectin. Biochem Bioph Res Co 287, 622, 2001.

Laurencin, C.T., Ambrosio, A. M. A., Borden, M. D., Cooper, J. A. Tissue Engineering: Orthopedic Applications. Annu Rev Biomed Eng 1, 19, 1999.

Lee, E.Y., Xia, Y., Kim, W.S., Kim, M.H., Kim, T.H., Kim, K.J., Park, B.S., Sung, J.H. Hypoxia enhanced wound-healing function of adipose-derived stem cells: increase in stem cell proliferation and up-regulation of VEGF and bFGF. Wound Repair Regen.17, 540, 2009.

Lee, J.H., and Kemp, D.M. Human adipose-derived stem cells display myogenic potential and perturbed function in hypoxic conditions. Biochem Biophys Res Commun 341, 882, 2006.

Lendahl, U., Lee, K.L., Yang, H., and Poellinger, L. Generating specificity and diversity in the transcriptional response to hypoxia. Nat Rev Genet 10, 821, 2009.

Lennon, D.P., Edmison, J.M., and Caplan, A.I. Cultivation of rat marrow-derived mesenchymal stem cells in reduced oxygen tension: effects on in vitro and in vivo osteochondrogenesis. J Cell Physiol 187, 345, 2001.

Lewis, G. and Nyman, J.S. The use of nanoindentation for characterizing the properties of mineralized hard tissues: state-of-the art review. J Biomed Mater Re. B Appl Biomater 87, 286, 2008.

Li, J.M., Foote, R.H. Culture of rabbit zygotes into blastocysts in protein-free medium with one to 20 per cent oxygen. J Reprod Fertil 98, 163, 1993.

Li, P., Ye, X., Kangasniemi, I., De Blieck-Hogervost, J.M.A., Klein, C.P.A.T., De Groot, K. In vivo calcium phosphate formation induced by sol-gel prepared silica. J Biomed Mater Res 29, 325, 1995.

Lin-Gibson, S., Bencherif, S., Cooper, J.A., Wetzel, S.J., Antonucci, J.M., Vogel, B.M., Horkay, F., and Washburn, N.R. Synthesis and characterization of PEG dimethacrylates and their hydrogels. Biomacromolecules 5, 1280, 2004.

Lin, Q., Kim, Y., Alarcon, R.M., and Yun, Z. Oxygen and cell fate decisions. Gene Regul Syst Bio 2, 43, 2008.

Lin, S., Sangaj, N., Razafiarison, T., Zhang, C., and Varghese, S. Influence of physical properties of biomaterials on cellular behavior. Pharm Res 28, 1422, 2011.

Lin, T.M., Tsai, J.L., Lin, S.D., Lai, C.S., Chang, C.C. Accelerated growth and prolonged lifespan of adipose tissue-derived human mesenchymal stem cells in a medium using reduced calcium and antioxidants. Stem Cells Dev 14, 92, 2005.

Liu, G., Cheng, Y., Guo, S., Feng, Y., Li, Q., Jia, H., Wang, Y., Tong, L., and Tong, X. Transplantation of adipose-derived stem cells for peripheral nerve repair. Int J Mol Med 28, 565, 2011.

Liu, X.Y., Nothias, J.M., Scavone, A., Garfinkel, M., and Millis, J.M. Biocompatibility investigation of polyethylene glycol and alginate-poly-L-lysine for islet encapsulation. American Society for Artificial Internal Organs Journal 56, 241, 2010.

Loboda, A., Jozkowicz, A., Dulak, J. HIF-1 and HIF-2 transcription factors--similar but not identical. Mol Cells. 29, 435, 2010.

Luria, E. A., Owen, M. E., Friedenstein, A. J., Morris, J. F., and Kuznetsow, S. A. Bone formation in organ cultures of bone marrow. Cell Tissue Res 248, 449, 1987.

Ma, T., Grayson, W.L., Frohlich, M., and Vunjak-Novakovic, G. Hypoxia and stem cell-based engineering of mesenchymal tissue. Biotechnol Prog 25, 32, 2009.

MacKenzie, E. J., Jones, A. S., Bosse, M. J., Castillo, R. C., Pollak, A. N., Webb, L. X., Swiontkowski, M. F., Kellam, J. F., Smith, D. G., Sanders, R. W. Health-care costs associated with amputation or reconstruction of a limb-threatening injury. J Bone Joint Surg Am 89, 1685, 2007.

Mackie, E.J. Osteoblasts: novel roles in orchestration of skeletal architecture. Int J Biochem Cell Biol 35, 1301, 2003.

Malda, J., Klein, T.J., and Upton, Z. The roles of hypoxia in the in vitro engineering of tissues. Tissue Eng 13, 2153, 2007.

Malda, J., Martens, D.E., Tramper, J., van Blitterswijk, C.A., and Riesle, J. Cartilage tissue engineering: controversy in the effect of oxygen. Crit Rev Biotechnol 23, 175, 2003.

Malda, J., Rouwkema, J., Martens, D.E., Le, E.P., Kooy, F.K., Tramper, J., van Blitterswijk, C.A., and Riesle, J. Oxygen gradients in tissue-engineered PEGT/PBT cartilaginous constructs: measurement and modeling. Biotechnol Bioeng 86, 9, 2004.

Malda, J., Van Blitterswijk, C.A., Van Geffen, M., Martens, D.E., Tramper, J., and Riesle, J. Low oxygen tension stimulates the redifferentiation of dedifferentiated adult human nasal chondrocytes. Osteoarthritis Cartilage 12, 306, 2004.

Malladi, P., Xu, Y., Chiou, M., Giaccia, A.J., and Longaker, M.T. Effect of reduced oxygen tension on chondrogenesis and osteogenesis in adipose-derived mesenchymal cells. Am J Physiol Cell Physiol 290, C1139, 2006.

Malladi, P., Xu, Y., Chiou, M., Giaccia, A.J., and Longaker, M.T. Hypoxia inducible factor-1alpha deficiency affects chondrogenesis of adipose-derived adult stromal cells. Tissue Eng 13, 1159, 2007.

Manalo, D.J., Rowan, A., Lavoie, T., Natarajan, L., Kelly, B.D., Ye, S.Q., Garcia, J.G., and Semenza, G.L. Transcriptional regulation of vascular endothelial cell responses to

Mankani, M. H., Kuznetsov, S. A., Fowler, B., Kingman, A., and Robey, P. G. In vivo bone formation by human bone marrow stromal cells: effect of carrier particle size and shape. Biotechnol Bioeng 72, 96, 2001.

Marcacci, M., Kon, E., Moukhachev, V., Lavroukov, A., Kutepov, S., Quarto, R. et al. Stem cells associated with macroporous bioceramics for long bone repair: 6-to 7-year outcome of a pilot clinical study. Tissue Eng 13, 947, 2007.

Martin-Rendon, E., Hale, S.J.M., Ryan, D., Baban, D., Forde, S.P., Roubelakis, M., Sweeney, D., Moukayed, M., Harris, A.L., Davies, K., Watt, S.M. Transcriptional profiling of human cord blood CD133 and cultured bone marrow mesenchymal stem cells in response to hypoxia. Stem Cell 25, 1003, 2007.

Matsumoto, A., Matsumoto, S., Sowers, A.L., Koscielniak, J.W., Trigg, N.J., Kuppusamy, P., Mitchell, J.B., Subramanian, S., Krishna, M.C., Matsumoto, K. Absolute oxygen tension (pO2) muscle tissue as determined by in murine fatty and EPR. Magn Reson Med 54, 1530, 2005.

Maurer, P., Hohenester, E., Engel, J. Extracellular calcium-binding proteins. Curr Opin Cell Biol 8, 609, 1996.

Maxwell, P.H., Pugh, C.W., Ratcliffe, P.J. Inducible operation of the erythropoietin 3' enhancer in multiple cell lines: evidence for a widespread oxygen-sensing mechanism. Proc Natl Acad Sci U S A. 90, 2423, 1993.

Maynard, M.A., Evans, A.J., Shi, W., Kim, W.Y., Liu, F.F., Ohh, M. Dominant-negative HIF-3 alpha 4 suppresses VHL-null renal cell carcinoma progression. Cell Cycle. 6, 2810, 2007.

McFarland, C.D., Mayer, S., Scotchford, C., Dalton, B.A., Steele, J.G., Downes, S. Attachment of cultured human bone cells to novel polymers. J Biomed Mater Res 44, 1, 1999.

McKee, M.D., Nanci, A. Osteopontin: an interfacial extracellular matrix protein in mineralized tissues. Connect Tissue Res 35, 197, 1996.

Meinel, L., Fajardo, R., Hofmann, S., Langer, R., Chen, J., Snyder, B., et al. Silk implants for the healing of critical size bone defects. Bone 37, 688, 2005.

Merceron, C., Vinatier, C., Portron, S., Masson, M., Amiaud, J., Guigand, L., Chérel, Y., Weiss, P., Guicheux, J. Differential effects of hypoxia on osteochondrogenic potential of human adipose-derived stem cells. Am J Physiol Cell Physiol. 298, 355, 2010.

Minchenko, A., Salceda, S., Bauer, T., Caro, J. Hypoxia Regulatory Elements of the Human Vascular Endothelial Growth Factor Gene. Cell Mol Biol Res 40, 35, 1994.

Minguell, J.J., Erices, A., Conget, P. Mesenchymal stem cells. Exp Biol Med 226, 507, 2011.

Mizuno, S., and Glowacki, J. Low oxygen tension enhances chondroinduction by demineralized bone matrix in human dermal fibroblasts in vitro. Cells Tissues Organs 180, 151, 2005.

Mohyeldin, A., Garzon-Muvdi, T., and Hinojosa, A.Q. Oxygen in stem cell biology: a critical component of the stem cell niche. Cell Stem Cell 7, 150, 2010.

Moore, K.A., and Lemischka, I.R. Stem cells and their niches. Science 311, 1880, 2006.

Muhonen, A., Haaparanta, M., Gronroos, T., Bergman, J., Knuuti, J., Hinkka, S., Happonen, R.P. Osteoblastic activity and neoangiogenesis in distracted bone of irradiated rabbit mandible with or without hyperbaric oxygen treatment. Int J Oral Maxillofac Surg 33, 173, 2004.

Murphy, C., and Sambanis, A. Effect of oxygen tension and alginate encapsulation on restoration of the differentiated phenotype of passaged chondrocytes. Tissue Eng 7, 791, 2001.

Murphy, C.L., and Polak, J.M. Control of human articular chondrocyte differentiation by reduced oxygen tension. J Cell Physiol 199, 451, 2004.

Murphy, W.L., Simmons, C.A., Kaigler, D., Mooney, D.J. Bone regeneration via a mineral substrate and induced angiogenesis. J Dent Res 83, 204, 2004.

Murry, C.E., Jennings, R.B., Reimer, K.A. Preconditioning with ischemia: a delay of lethal cell injury in ischemic myocardium.Circulation. 74, 1124, 1986.

Muschler, G. F., and Midura, R. J. Connective tissue progenitors: practical concepts for clinical applications. Clin Orthop Relat Res 66, 2002.

Muschler, G.F., Nakamoto, C., Griffith, L.G. Engineering principles of clinical cell-based tissue engineering. J Bone Joint Surg Am 86, 1541, 2004.

Nakao, H., Nakatsuji, N. Effects of coculture, medium components and gas-phase on in vitro culture of in vitro matured and in vitro fertilized bovine embryos. Theriogenology 33, 591, 1990.

Nakashima, K., de Crombrugghe, B. Transcriptional mechanisms in osteoblast differentiation and bone formation. Trends Genet 19, 458, 2003.

Nguyen, L.K., Cavadas, M.A., Scholz, C.C., Fitzpatrick, S.F., Bruning, U., Cummins, E.P., Tambuwala, M.M., Manresa, M.C., Kholodenko, B.N., Taylor, C.T., Cheong, A. A dynamic model of the hypoxia-inducible factor 1-alpha (HIF-1α) network. J Cell Sci. Feb 6, 2013.

Ninikoski, J., and Hunt, T.K. Oxygen Tension in Healing Bone Surgical Gynecology and Obstetrics 134, 746, 1972.

Nuttelman, C.R., Tripodi, M.C., and Anseth, K.S. In vitro osteogenic differentiation of human mesenchymal stem cells photoencapsulated in PEG hydrogels. J Biomed Mater Res A 68, 773, 2004.

Olivier, V., Faucheux, N., Hardouin, P. Biomaterial challenges and approaches to stem cell use in bone reconstructive surgery. Drug Discov Today 9, 803, 2004.

Otto, W.R., Rao, J. Tomorrow's skeleton staff: mesenchymal stem cells and the repair of bone and cartilage. Cell Prolif 37, 97, 2004.

Owen, M. Histogenesis of bone cells. Calcif Tissue Res 25, 205, 1978.

Owen, M., and Friedenstein, A. J. Stromal stem cells: marrow-derived osteogenic precursors. Ciba Found Symp 136, 42, 1988.

Park, J.H., Park, B.H., Kim, H.K., Park, T.S., Baek, H.S. Hypoxia decreases Runx2/Cbfa1 expression in human osteoblast-like cells. Mol Cell Endocrinol 192, 197, 2002.

Park, J.H., Park, B.H., Kim, H.K., Park, T.S., Baek, H.S. Hypoxia decreases Runx2/ Cbfa1 expression in human osteoblast-like cells. Mol Cell Endocrinol 192, 2002.

Parmar, K., Mauch, P., Vergilio, J.A., Sackstein, R., Down, J.D. Distribution of hematopoietic stem cells in the bone marrow according to regional hypoxia. Proc Natl Acad Sci USA 104, 5431, 2007.

Parrinello, S., Samper, E., Krtolica, A., Goldstein, J., Melov, S., Campisi, J. Oxygen sensitivity severely limits the replicative lifespan of murine fibroblasts. nat cell biol 5, 741, 2003.

Peng, J., Zhang, L., Drysdale, L., Fong, G.H. The transcription factor HIF-2α plays an important role in vascular remodeling, Proc Natl Acad Sci 97, 8386, 2000.

Peterson, B., Zhang, J., Iglesias, R., Kabo, M., Hedrick, M., Benhaim, P., Lieberman, J.R. Healing of critically sized femoral defects, using genetically modified mesenchymal stem cells from human adipose tissue. Tissue Eng 11, 120, 2005.

Pfander, D., and Gelse, K. Hypoxia and osteoarthritis: how chondrocytes survive hypoxic environments. Curr Opin Rheumatol 19, 457, 2007.

Pietak, A.M., Sayer, M. Functional atomic force microscopy investigation of osteopontin affinity for silicon stabilized tricalcium phosphate bioceramic surfaces. Biomaterials 27, 3, 2006.

Pittenger, M.F., Mackay, A.M., Beck, S.C., Jaiswal, R.K., Douglas, R., Mosca, J.D., Moorman, M.A., Simonetti, D.W., Craig, S., Marshak, D.R. Multilineage potential of adult human mesenchymal stem cells. Science 284 143, 1999.

Polykandriotis, E., Arkudas, A., Euler, S., Beier, J.P., Horch, R.E., Kneser, U. Prevascularisation strategies in tissue engineering. Handchir Mikrochir Plast Chir 38, 217, 2006.

Potier, E., Ferreira, E., Andriamanalijaona, R., Pujol, J.P., Oudina, K., Logeart-Avramoglou, D., and Petite, H. Hypoxia affects mesenchymal stromal cell osteogenic differentiation and angiogenic factor expression. Bone 40, 1078, 2007.

Prabhakar, N.R. sensing hypoxia: physiology, genetics and epigenetics. J Physiol. 2013 [Epub ahead of print]

Presnell S.C, Petersen, B., Heidaran, M. Stem cells in adult tissues. Semin Cell Dev Biol 13, 369, 2002.

Preston S.L, M. R. Alison, S. J. Forbes, N. C. Direkze, R. Poulsom, N. A. Wright, J. The new stem cell biology: something for everyone. Clin Pathol Molec Pathol 56, 86, 2003.

Prockop, D.J. Marrow stromal cells as stem cells for nonhematopoietic tissues; Science 276, 71, 1997.

Provot, S., and Schipani, E. Fetal growth plate: a developmental model of cellular adaptation to hypoxia. Ann N Y Acad Sci 1117, 26, 2007.

Puleo, D.A., Nanci, A. Understanding and controlling the boneimplant interface. Biomaterials 20, 2311, 1999.

Quarto, R., Mastrogiacomo, M., Cancedda, R., Kutepov, S.M., Mukhachev, V., Lavroukov, A., Kon, E., Marcacci, M. Repair of large bone defects with the use of autologous bone marrow stromal cells; N Engl J Med 344, 385, 2001.

Radin, S.R., Ducheyne, P. The effect of calcium phosphate ceramic composition and structure on in vitro behavior. II. Precipitation. J Biomed Mater Res 27, 35, 1993.

Radisic, M., Malda, J., Epping, E., Geng, W., Langer, R., and Vunjak-Novakovic, G. Oxygen gradients correlate with cell density and cell viability in engineered cardiac tissue. Biotechnol Bioeng 93, 332, 2006.

Ramírez-Bergeron, D.L., Runge, A., Dahl, K.D., Fehling, H.J., Keller, G., Simon, M.C. Hypoxia affects mesoderm and enhances hemangioblast specification during early development. Development 131, 4623, 2004.

Ramirez-Bergeron, D.L., Simon, M.C. Hypoxia-inducible factor and the development of stem cells of the cardiovascular system. Stem Cells 19, 279, 2001.

Rankin, E.B., Biju, M.P., Liu, Q., Unger, T.L., Rha, J., Johnson, R.S., Simon, M.C., Keith, B., Haase, V.H. Hypoxia-inducible factor-2 (HIF-2) regulates hepatic erythropoietin in vivo. J Clin Invest. 117, 1068, 2007.

Rasmussen, J.G., Frøbert, O., Pilgaard, L., Kastrup, J., Simonsen, U., Zachar, V., Fink, T. Prolonged hypoxic culture and trypsinization increase the pro-angiogenic potential of human adipose tissue-derived stem cells. Cytotherapy.13, 318, 2011.

Ratner, B.D., Bryant, S.J. Biomaterials: where we have been and where we are going; Annu Rev Biomed Eng 6, 41, 2004.

Ren, H., Cao, Y., Zhao, Q., Li, J., Zhou, C., Liao, L., Jia, M., Zhao, Q., Cai, H., Han, Z.C., Yang, R., Chen, G., and Zhao, R.C. Proliferation and differentiation of bone marrow stromal cells under hypoxic conditions. Biochem Biophys Res Commun 347, 12, 2006.

Revsbech, N.P., and Ward, D.M. Oxygen microelectrode that is insensitive to medium chemical composition: use in an acid microbial mat dominated by cyanidium caldarium. Appl Environ Microbiol.45, 755, 1983.

Rezania, A., Healy, K.E. Biomimetic peptide surfaces that regulate adhesion, spreading, cytoskeletal organization, and mineralization of the matrix deposited by osteoblast-like cells. Biotechnol Prog 15, 19, 1999.

Rezwan, K., Chen, Q.Z., Blaker, J.J., Boccaccini, A.R. Biodegradable and bioactive porous polymer/inorganic composite scaffolds for bone tissue engineering; Biomaterials 27, 3413, 2006.

Rho, J.Y., Kuhn-Spearing, L. & Zioupos, P. Mechanical properties and the hierarchical structure of bone. Med. Eng Phys. 20, 92, 1998.

Rice, M.A. and Anseth, K.S. Encapsulating chondrocytes in copolymer gels: Bimodal degradation kinetics influence cell phenotype ad extracellular matrix development. Journal of Biomedical Materials Research Part A 70, 560, 2004.

Ritchie, R.O. How does human bone resist fracture? Ann. N Y Acad Sci 1192, 72, 2010.

Robins, J.C., Akeno, N., Mukherjee, A., Dalal, R.R., Aronow, B.J., Koopman, P., and Clemens, T.L. Hypoxia induces chondrocyte-specific gene expression in mesenchymal cells in association with transcriptional activation of Sox9. Bone 37, 313, 2005.

Rodriguez-Merchan, E.C., and Forriol, F. Nonunion: general principles and experimental data. Clin Orthop Relat Res 419, 4, 2004.

Rosova, I., Dao, M., Capoccia, B., Link, D., Nolta, J.A. Hypoxic preconditioning results in increased motility and improved therapeutic potential of human mesenchymal stem cells. Stem Cells 26, 2173, 2008.

Safadi, F.F., Xu, J., Smock, S.L., Kanaan, R.A., Selim, A.H., Odgren, P.R., Marks, S.C., Jr, Owen, T.A., Popoff, S.N. Expression of connective tissue growth factor in bone: its role in osteoblast proliferation and differentiation in vitro and bone formation in vivo. J Cell Physiol 196, 51, 2003.

Sahai, S., McFarland, R., Skiles, M.L., Sullivan, D., Williams, A., and Blanchette, J.O. Tracking Hypoxic Signaling in Encapsulated Stem Cells. Tissue Eng, 18, 557, 2012.

Saini, S., and Wick, T.M. Effect of low oxygen tension on tissue-engineered cartilage construct development in the concentric cylinder bioreactor. Tissue Eng 10, 825, 2004.

Salceda, S., Caro, J. Hypoxia-inducible factor-1α (HIF-1α) protein is rapidly degraded by the ubiquitin-proteasome system under normoxic conditions. J Biol Chem 272, 22642, 1997.

Salim, A., Nacamuli, R.P., Morgan, E.F., Giaccia, A.J., Longaker, M.T. Transient changes in oxygen tension inhibit osteogenic differentiation and Runx2 expression in osteoblasts; J Biol Chem 279, 40007, 2004.

Salinas, C.N., Cole, B.B., Kasko, A.M., and Anseth, K.S. Chondrogenic differentiation potential of human mesenchymal stem cells photoencapsulated within poly(ethylene glycol)-arginine-glycine-aspartic acid-serine thiol-methacrylate mixed-mode networks. Tissue Eng 13, 1025, 2007.

Schaffler, A., and Buchler, C. Concise review: adipose tissuederived stromal cells-basic and clinical implications for novel cell-based therapies. Stem Cells 25, 818, 2007.

Schipani, E. Hypoxia and HIF-1 alpha in chondrogenesis. Semin Cell Dev Biol 16, 539, 2005.

Schipani, E., Maes, C., Carmeliet, G., and Semenza, G.L. Regulation of osteogenesis-angiogenesis coupling by HIFs and VEGF. J Bone Miner Res 24, 1347, 2009.

Schmitz, J.P., and Hollinger, J.O. The critical size defect as an experimental model for craniomandibulofacial nonunions. Clin Orthop Relat Res 205, 299, 1986.

Schofield, R. The relationship between the spleen colony-forming cell and the haemopoietic stem cell. Blood Cells 4, 7, 1978.

Scotchford, C.A., Cooper, E., Leggett, G.J., Downes, S. Growth of human osteoblast-like cells on alkanethiol on gold self assembled monolayers: the effect of surface chemistry. J Biomed Mater Res 41, 431, 1998.

Seeman, E., Delmas, P.D. Bone quality--the material and structural basis of bone strength and fragility. N Engl J Med 354, 2250, 2006.

Semenza, G.L. Expression of hypoxia-inducible factor 1: mechanisms and consequences. Biochem Pharmacol 59, 47, 2000.

Semenza, G.L. Hypoxia-inducible factor 1: master regulator of O2 homeostasis. Curr Opin Genet Dev 8, 588, 1998.

Semenza, G.L. Oxygen homeostasis. Syst Biol Med 2, 336, 2010.

Semenza, G.L. Perspectives on oxygen sensing. Cell 98, 281, 1999.

Semenza, G.L. Regulation of mammalian O2 homeostasis by hypoxiainducible factor 1. Annu. Rev Cell Dev Biol 15, 551, 1999.

Semenza, G.L. Signal transduction to hypoxia-inducible factor 1. Biochem Pharmacol 64, 993, 2002.

Sengers, B.G., Taylor, M., Please, C.P., and Oreffo, R.O.C. Computational modeling of cell spreading and tissue regeneration in porous scaffolds. Biomaterials 13, 1926, 2007.

Sharp, F.R., and Bernaudin, M. HIF-1 and oxygen sensing in the brain. Nat Rev Neurosci 5, 437, 2004.

Shimizu, S., Eguchi, Y., Kamiike, W., Itoh, Y., Hasegawa, J., Yamabe, K., Otsuki, Y., Matsuda, H., and Tsujimoto, Y. Induction of apoptosis as well as necrosis by hypoxia and predominant prevention of apoptosis by Bcl-2 and Bcl-XL. Cancer Res 56, 2161, 1996.

Shimizu, S., Y. Eguchi, H. Kosaka, W. Kamiike, H. Matsuda, and Y. Tsujimoto, Prevention of hypoxia-induced cell death by Bcl-2 and Bcl-xL. Nature 374, 811, 1995.

Shimizu, S., Y. Eguchi, W. Kamiike, S. Waguri, Y. Uchiyama, H. Matsuda, and Y. Tsujimoto, Retardation of chemical hypoxia-induced necrotic cell death by Bcl-2 and ICE inhibitors: possible involvement of common mediators in apoptotic and necrotic signal transductions. Oncogene 12, 2045, 1996.

Shors, E.C. Coralline bone graft substitutes. Orthop Clin North Am 30, 599, 1999.

Simon, M.C., and Keith, B. The role of oxygen availability in embryonic development and stem cell function. Nat Rev Mol Cell Biol 9, 285, 2008.

Simon, M.P., Tournaire, R., and Pouyssegur, J. The angiopoietin-2 gene of endothelial cells is up-regulated in hypoxia by a HIF binding site located in its first intron and by the central factors GATA-2 and Ets-1. J Cell Physiol 217, 809, 2008.

Skiles, M. L., Sahai, S., and Blanchette, J. O. Tracking Hypoxic Signaling within Encapsulated Cell Aggregates. J Vis Exp 58, e3521, 2011.

Skiles, M.L., Fancy, R., Topiwala, P., Sahai, S., and Blanchette, J.O. Correlating hypoxia with insulin secretion using a fluorescent hypoxia detection system. J Biomed Mater Res B Appl Biomater 97, 148, 2011.

Slater, B.J., Kwan, M.D., Gupta, D.M., Panetta, N.J., Longaker, M.T. Mesenchymal cells for skeletal tissue engineering; Expert Opin Biol Ther 8, 885, 2008.

Spraddling, A., Barbosa, D., Kai, T. Stem cells find their niche. Nature 414, 98, 2001.

Stains, J.P., Civitelli, R. Cell-cell interactions in regulating osteogenesis and osteoblast function. Birth Defects Res C Embryo Today 75, 72, 2005.

Stains, J.P., Civitelli, R. Cell-to-cell interactions in bone. Biochem Biophys Res Commun 328, 721, 2005.

Stanford, C.M., Jacobson, P.A., Eanes, E.D., Lembke, L.A., Midura, R.J. Rapidly forming apatitic mineral in an osteoblastic cell line (UMR 106-01 BSP). J Biol Chem 270, 9420, 1995.

Stosich, M.S., Bastian, B., Marion, N.W., Clark, P.A., Reilly, G., and Mao, J.J. Vascularized adipose tissue grafts from human mesenchymal stem cells with bioactive cues and microchannel conduits. Tissue Eng 13, 2881, 2007.

Strem, B.M., Hicok, K.C., Zhu, M., Wulur, I., Alfonso, Z., Schreiber, R.E., Fraser, J.K., Hedrick, M.H. Multipotential differentiation of adipose tissue-derived stem cells. Keio J Med 54, 132, 2005.

Tang, N., Wang, L., Esko, J., Giordano, F.J., Huang, Y., Gerber, H.P., Ferrara, N., Johnson, R.S. Loss of HIF-1 alpha in endothelial cells disrupts a hypoxia-driven VEGF autocrine loop necessary for tumorigenesis. Cancer Cell. 6, 485, 2004.

Thompson, J.G.E., Simpson, A.C., Pugh, P.A., Donnelly, P.E., Tervit, H.R. Effect of oxygen concentration on in vitro development of preimplantation sheep and cattle embryos. J Reprod Fertil 89, 573, 1990.

Thurner, P.J. Atomic force microscopy and indentation force measurement of bone. Wiley Interdiscip Rev Nanomed Nanobiotechnol 1, 624, 2009.

Togawa, D., Bauer, T.W., Lieberman, I.H., and Sakai, H. Lumbar intervertebral body fusion cages: histological evaluation of clinically failed cages retrieved from humans. J Bone Joint Surg Am 86, 70, 2004.

Tower, D.A. The osteogenic-angiogenic interface: novel insights into the biology of bone formation and fracture repair. Curr Osteoporos Rep 6, 67, 2008.

Towler, D.A. Vascular biology and bone formation: hints from HIF. J Clin Invest 117, 1477, 2007.

Tremoleda, J.L., Forsyth, N.R., Khan, N.S., Wojtacha, D., Christodoulou, I., Tye, B.J. Bone tissue formation from human embryonic stem cells in vivo. Cloning Stem Cells 10, 119, 2008.

Tsujimoto, Y., Stress-resistance conferred by high level of bcl-2 alpha protein in human B lymphoblastoid cell. Oncogene, 4, 11, 1331, 1989.

Umaoka, Y., Noda, Y., Narimoto, K., Mori, T. Effects of oxygentoxicity on early development of mouse embryos. Mol Reprod Dev 31, 28, 1992.

Utting, J.C., Robins, S.P., Brandao-Burch, A., Orriss, I.R., Behar, J., and Arnett, T.R. Hypoxia inhibits the growth, differentiation and bone-forming capacity of rat osteoblasts. Exp Cell Res 312, 1693, 2006.

Valorani, M.G., Montelatici, E., Germani, A., Biddle, A., D'Alessandro, D., Strollo, R., Patrizi, M.P., Lazzari, L., Nye, E., Otto, W.R., Pozzilli, P., Alison, M.R. Pre-culturing human adipose tissue mesenchymal stem cells under hypoxia increases their adipogenic and osteogenic differentiation potentials. Cell Prolif. 45, 225, 2012.

Vaux, D.L., S. Cory, and J.M. Adams, Bcl-2 gene promotes haemopoietic cell survival and cooperates with c-myc to immortalize pre-B cells. Nature 335, 6189, 440, 1988.

Volkmer, E., Drosse, I., Otto, S., Stangelmayer, A., Stengele, M., Kallukalam, B.C., Mutschler, W., and Schieker, M. Hypoxia in static and dynamic 3-D culture systems for tissue engineering of bone. Tissue Eng Part A 14, 1331, 2008.

Volkmer, E., Kallukalam, B.C., Maertz, J., Otto, S., Drosse, I., Polzer, H., Bocker, W., Stengele, M., Docheva, D., Mutschler, W., and Schieker, M. Hypoxic preconditioning of human mesenchymal stem cells overcomes hypoxia-induced inhibition of osteogenic differentiation. Tissue Eng 16, 153, 2010.

Vunjak-Novakovic, G., Martin, I., Obradovic, B., Treppo, S., Grodzinsky, A.J., Langer, R. Bioreactor cultivation conditions modulate the composition and mechanical properties of tissue-engineered cartilage. J Orthop Res 17, 130, 1999.

Wagegg, M., Gaber, T., Lohanatha, F.L., Hahne, M., Strehl, C., Fangradt, M., Tran, C.L., Schönbeck, K., Hoff, P., Ode, A., Perka, C., Duda, G.N., Buttgereit, F. Hypoxia promotes osteogenesis but suppresses adipogenesis of human mesenchymal stromal cells in a hypoxia-inducible factor-1 dependent manner. PLoS One. 7, e46483, 2012.

Wan, C., Gilbert, S.R., Wang, Y., Cao, X., Shen, X., Ramaswamy, G., Jacobsen, K.A., Alaql, Z.S., Eberhardt, A.W., Gerstenfeld, L.C., Einhorn, T.A., Deng, L., and Clemens, T.L. Activation of the hypoxia-inducible factor-1alpha pathway accelerates bone regeneration. Proc Natl Acad Sci U S A 105, 686, 2008.

Wan, C., Shao, J., Gilbert, S.R., Riddle, R.C., Long, F., Johnson, R.S., Schipani, E., and Clemens, T.L. Role of HIF-1 alpha in skeletal development. Ann N Y Acad Sci 1192, 322, 2010.

Wang, D.W., Fermor, B., Gimble, J.M., Awad, H.A., Guilak, F. Influence of oxygen on the proliferation and metabolism of adipose derived adult stem cells. J Cell Physiol 204, 184, 2005.

Wang, F.N., Thirumangalathu, S., Loeken, M.R. Establishment of new mouse embryonic stem cell lines is improved by physiological glucose and oxygen. Cloning Stem Cell 8, 108, 2006.

Wang, G.L., Semenza, G.L. Desferrioxamine induces erythropoietin gene expression and hypoxia inducible factor 1 DNA binding activity: implications for models of hypoxia signal transduction. Blood 82, 3610, 1993.

Wang, J.A., Chen, T.L., Jiang, J., Shi, H., Gui, C., Luo, R.H. et al. Hypoxic preconditioning attenuates hypoxia/reoxygenation-induced apoptosis in mesenchymal stem cells. Acta Pharmacol Sin 29, 74, 2008.

Wang, J.C., Alanay, A., Mark, D., Kanim, L.E., Campbell, P.A., Dawson, E.G. A comparison of commercially available demineralized bone matrix for spinal fusion. Eur Spine J 16, 1233, 2007.

Wang, X.D., Liu, C.X., Wu, Y.L., Chen, J. Hypoxia and its simulant CoCl(2) down regulates Foxp3 expression independent from HIF-1αlpha. 17, 533, 2009.

Wang, Y., Wan, C., Deng, L., Liu, X., Cao, X., Gilbert, S.R., Bouxsein, M.L., Faugere, M.C., Guldberg, R.E., Gerstenfeld, L.C., Haase, V.H., Johnson, R.S., Schipani, E., and. The hypoxia inducible factor alpha pathway couples angiogenesis to osteogenesis during skeletal development. J Clin Invest 117, 1616, 2007.

Warren, S.M., Steinbrech, D.S., Mehrara, B.J., Saadeh, P.B., Greenwald, J.A., Spector, J.A. Hypoxia regulates osteoblast gene expression. J Surg Res 99, 147, 2001.

Watt, F.M., Hogan, B.L.M. Out of Eden: stem cells and their niches. Science 287, 1427, 2000.

Weber, L.M., He, J., Bradley, B., Haskins, K., and Anseth, K.S. PEG-based hydrogels as an in vitro encapsulation platform for testing controlled β-cell microenvironments. Acta Biomaterialia 2, 1, 2006.

Weber, L.M., Lopez, C.G., and Anseth, K.S. Effects of PEG hydrogel crosslinking density on protein diffusion and encapsulated islet survival and function. Journal of Biomedical Materials Research Part A 90, 720, 2009.

Weiner, C.M., Booth, G., Semenza, G.L. In vivo expression of mRNAs encoding hypoxia inducible factor 1. Biochem Bioph Res Co 225, 485, 1996.

Weiss, L. Hematopoietic microenvironment of bone-marrow ultrastructural-study of stroma in rats. Anat Rec 186, 161, 1976.

Wenger, R.H. Mammalian Oxygen Sensing, Signalling and Gene Regulation. J Exp Biol 203, 1253, 2000.

Williams, M. O. Long-term cost comparison of major limb salvage using the Ilizarov method versus amputation. Clin Orthop Relat Res, 156, 1994.

Xiao, S.J., Textor, M., Spencer, N.D., Sigrist, H. Covalent attachment of cell-adhesive, (Arg-Gly-Asp)-containing peptides to titanium surfaces. Langmuir 14, 5507, 1998.

Yamamuro, T., Hench, L., Wilson, J. editors. CRC handbook of bioactive ceramics, vol 2 Boca Raton, FL: CRC Press 235, 1992.

Yamazaki, Y., Egawa, K., Nose, K., Kunimoto, S., Takeuchi, T. HIF-1 dependent VEGF reporter gene assay by a stable transformant of CHO cells. Biol Pharm Bull. 26, 417, 2003.

Yang-Sook Chun, Eunjoo Choi, Gi-Tae Kim, Hong Choi, Chan-Hyung Kim, Min-Jae Lee, Myung-Suk Kim and Jong-Wan Park Cadmium blocks hypoxia-inducible factor (HIF)-1-mediated response to hypoxia by stimulating the proteasome-dependent degradation of HIF-1α. Eur J Biochem 267, 4198, 2000.

Yaszemski, M.J., Oldham, J.B., Lu, I., and Currier, B.L. Bone Engineering. Toronto: Em Squared 541, 1994.

Yaszemski, M.J., Payne, R.G., Hayes, W.C., Langer, R., Mikos, A.G. Evolution of bone transplantation: molecular cellular and tissue strategies to engineer human bone. Biomaterials 17, 175, 1996.

Yoo, J. U., and Johnstone, B. The role of osteochondral progenitor cells in fracture repair. Clin Orthop Relat Res, 73, 1998.

Young, M.F., Kerr, J.M., Ibaraki, K., Heegaard, A.M., Robey, P.G. Structure, expression, and regulation of the major noncollagenous matrix proteins of bone. Clin Orthop Relat Res 281, 275, 1992.

Yu, A.Y., Frid, M.G., Shimoda, L.A., Weiner, C.M., Stenmark, K., Semenza, G.L. Temporal, Spatial, and Oxygen-regulated expression of hypoxia-inducible factor-1 in the lung, Am J Phys 275, 818, 1998.

Yuan, Y., Hilliard, G., Ferguson, T., Millhorn, D.E. Cobalt inhibits the interaction between hypoxia-inducible factor-alpha and von Hippel- Lindau protein by direct binding to hypoxia-inducible factor-alpha. J Biol Chem 278, 15911, 2003.

Zachar, V., Duroux, M., Emmersen, J., Rasmussen, J.G., Pennisi, C.P., Yang, S., Fink, T. Hypoxia and adipose-derived stem cell-based tissue regeneration and engineering. Expert Opin Biol Ther. 11, 775, 2011.

Zhang, M., Xuan, S., Bouxsein, M.L. et al. Osteoblast-specific knockout of the insulin-like growth factor (IGF) receptor gene reveals an essential role of IGF signaling in bone matrix mineralization. J Biol Chem 277, 44005, 2002.

Zhao, F., Pathi, P., Grayson, W., Xing, Q., Locke, B.R., and Ma, T. Effects of oxygen transport on 3-D human mesenchymal stem cell metabolic activity in perfusion and static cultures: experiments and mathematical model. Biotechnol Prog 21, 1269, 2005.

Zhou, W., Dosey, T.L., Biechele, T., Moon, R.T., Horwitz, M.S., and Ruohola-Baker, H. Assessment of hypoxia inducible factor levels in cancer cell lines upon hypoxic induction using a novel reporter construct. PLoS One 6, e27460, 2011.

Zhou, Y., Guan, X., Wang, H., Zhu, Z., Li, C., Wu, S., Yu, H. Hypoxia induces osteogenic/angiogenic responses of bone marrow-derived mesenchymal stromal cells seeded on bone-derived scaffolds via ERK1/2 and p38 pathways. Biotechnol Bioeng. Jan 7, 2013 [Epub ahead of print]

Zhu, H. and Bunn, H.F. Signal transduction. How do cells sense oxygen?. Science 292, 449, 2001.

Zimmermann, W.H., Eschenhagen, T. Cardiac tissue engineering for replacement therapy, Heart Fail Rev 8, 259, 65, 2003.

Zou, D., Zhang, Z., Ye, D., Tang, A., Deng, L., Han, W., Zhao, J., Wang, S., Zhang, W., Zhu, C., Zhou, J., He, J., Wang, Y., Xu, F., Huang, Y., and Jiang, X. Repair of critical-sized rat calvarial defects using genetically engineered bone marrow-derived mesenchymal stem cells overexpressing hypoxia-inducible factor-1α. Stem Cells 29, 1380, 2011.

Zuk, P.A., Zhu, M., Ashjian, P., De Ugarte, D.A., Huang, J.I., Mizuno, H., Alfonso, Z.C., Fraser, J.K., Benhaim, P., and Hedrick, M.H. Human adipose tissue is a source of multipotent stem cells. Mol Biol Cell 13, 4279, 2002.

Zuk, P.A., Zhu, M., Mizuno, H., Huang, J., Futrell, J.W., Katz, A.J., Benhaim, P., Lorenz, H.P., and Hedrick, M.H. Multilineage cells from human adipose tissue: implications for cell based therapies. Tissue Eng 7, 211, 2001.